CYCLIC LOADING RESPONSE OF FRASER RIVER SAND FOR VALIDATION OF NUMERICAL MODELS SIMULATING CENTRIFUGE TESTS

by

SOMASUNDARAM SRISKANDAKUMAR

B.Sc.Eng., University of Peradeniya, Sri Lanka, 2000

A THESIS SUBMITTED IN PARTIAL FULFILLMENT OF
THE REQUIREMENTS FOR THE DEGREE OF
MASTER OF APPLIED SCIENCE

in

THE FACULTY OF GRADUATE STUDIES
DEPARTMENT OF CIVIL ENGINEERING

We accept this thesis as conforming
to the required standard

THE UNIVERSITY OF BRITISH COLUMBIA

March, 2004

Library Authorization

In presenting this thesis in partial fulfillment of the requirements for an advanced degree at the University of British Columbia, I agree that the Library shall make it freely available for reference and study. I further agree that permission for extensive copying of this thesis for scholarly purposes may be granted by the head of my department or by his or her representatives. It is understood that copying or publication of this thesis for financial gain shall not be allowed without my written permission.

SOMASUNDARAM SRISKANDAKUMAR
Name of Author *(please print)*

25/03/2004
Date (dd/mm/yyyy)

Title of Thesis: CYCLIC LOADING RESPONSE OF FRASER RIVER SAND FOR VALIDATION OF NUMERICAL MODELS SIMULATING CENTRIFUGE TESTS.

Degree: M.A.Sc Year: 2004

Department of CIVIL ENGINEERING.
The University of British Columbia
Vancouver, BC Canada

ABSTRACT

Cyclic loading response of Fraser River sand was investigated using the UBC direct simple shear (DSS) device as input to numerical simulation of centrifuge physical models. A simple air-pluviation method was developed to reconstitute laboratory sand samples replicating the soil fabric anticipated in centrifuge specimens. Constant-volume (undrained) tests were conducted with and without initial static shear stress condition at loose and dense density states. While the observed trends in mechanical response were similar, the loose air-pluviated samples were more susceptible to liquefaction under cyclic loading than their water-pluviated counterparts. The differences arising from the two sample re-constitution methods can be attributed to the differences in particle structure, clearly highlighting the importance of fabric effects in the assessment of the mechanical response of sands. Densification due to increasing confining stress (stress densification) significantly increased the cyclic resistance of loose air-pluviated sand with strong implications in relation to the interpretation of observations from centrifuge testing. This effect, however, was not prominent in the case of water-pluviated or dense samples. The initial static shear stresses reduce the cyclic shear resistance of loose air-pluviated sand in simple shear loading, in contrast to the increase in resistance reported based on data from triaxial testing. Dense sands indicated a increase in cyclic resistance in the presence of initial static shear stress.

Previous cyclic loadings generating high excess pore water pressures (or significant shear strains) reduced the liquefaction resistance of sand against future cyclic loading, while

cyclic loading generating small excess pore water pressures (or small shear strains) increased the liquefaction resistance of sand. However, densification due to post-cyclic consolidation, sometimes, contributed to increasing the liquefaction resistance by compensating for the weakening in the liquefaction resistance due to the large pre-shearing.

The volumetric strains accumulated during drained cyclic loading were independent of the time rate of shear strain, and they increased with increasing shear strain amplitude and the number of cycles. The proportionality of shear-induced volumetric strain to the cyclic shear-strain amplitude, based on drained cyclic shear tests with small shear strain amplitudes, was not observable when the material is subjected to relatively large amplitudes of cyclic strain. A three-parameter shear-volume coupling model was developed for cyclic loadings associated with large strains.

TABLE OF CONTENTS

LIST OF TABLES

LIST OF FIGURES

ACKNOWLEDGEMENTS

The author wishes to express his most sincere gratitude to his supervisor Dr. D. Wijewickreme and co-supervisor Dr. P. M. Byrne for their support, guidance and encouragement throughout this research. The author is grateful to Dr. Y. P. Vaid for his input in relation to advance laboratory testing of sands as well as numerous valuable discussions.

The author also wishes to extend his sincere thanks to Drs. R. J. Fannin, J.A. Howie, L.Yan, and R.G. Campanella for the lessons they taught.

The author would like to express his thanks to his colleagues; Ganan, Ricardo, Megan, Errnest, Sun-Sik, Mahmood, Keith, Chris, Abdul, Ali, Alex, and Mavi for the interesting, critical, and helpful discussions and conversations.

Technical assistance of Messrs. Harald Schremp, Bill Leung, Scott Jackson, and John Wong of the Department of Civil Engineering Workshop is also deeply appreciated.

Financial support provided by the National Research Council of Canada (NSERC), the University of British Columbia, and the Vancouver Geotechnical Society is acknowledge with deep appreciation.

Finally, the author would like to extend his deepest gratitude to his wife, Thamy, for her understanding, support, and encouragement.

DEDICATED

TO MY PARENTS

CHAPTER 1

INTRODUCTION

Earthquake-induced ground displacements are one of the primary hazards to structures located in seismically active areas with liquefiable soils such as those in the Fraser River Delta of British Columbia, Canada. The prediction of ground displacements using numerical models forms a critical part in seismic evaluation, design, and retrofit of structures founded on these soils. Ideally, the acceptability of numerical models requires proper validation using recorded data from field case histories. The needed field data (i.e. soil and groundwater conditions, input ground motions, displacements etc.), however, are often not available with sufficient accuracy and detail, and this, in turn, has hindered the confirmation of numerical models.

It is well known that the behaviour of soils is stress level dependent. Therefore, the use of small-scale models under natural gravity (1g) conditions, which causes stress levels that are significantly smaller than those encountered in the field, is not considered suitable to generate data for verification of numerical models. Centrifuge systems can be used to invoke a high gravitational field on small-scale soil models, thus overcoming the above stress level deficiency in 1g models, and providing an opportunity for more realistic imposition of field stress conditions. Extensive research over the past twenty five years has demonstrated the potential of centrifuge testing in examination of the response of well-defined geotechnical boundary value problems (Arulanandan and Scott, 1993; Boulanger et al., 1999; Phillips et al., 2002), and the approach has been increasingly considered as a meaningful basis for generating data for validation of numerical models.

Efforts to validate numerical models predicting earthquake response of geotechnical problems have been undertaken by many researchers (Finn et al., 1986; Beaty and Byrne, 1998). For example, the current research program at the University of British Columbia (UBC), Vancouver, Canada, is aimed at validating a fully-coupled effective stress approach called UBCSAND (Byrne et al., 2004) using data generated from centrifuge tests conducted at C-CORE (Centre for Cold Oceans Resources Engineering) research facility at the Memorial University of Newfoundland, St. John's, Canada. The centrifuge models used in the program are constructed using dredged Fraser River sand, and the generated data from centrifuge testing provide the basis for verification of the above numerical approaches as well as the modelling of some typical problems faced by the profession in relation to geotechnical earthquake engineering works in liquefiable loose deltaic sand deposits.

In the modelling of a given problem, the numerical procedure should accurately capture the mechanical response of the soils. Fundamental understanding of this mechanical response can only be derived from controlled laboratory element testing of representative samples. In this regard, for laboratory element testing to be meaningful, the samples should essentially replicate the soil conditions existent in the subject centrifuge model. Since the mechanical response of soils is well known to be dependent on its particle fabric/structure (Oda, 1972; Ladd, 1974; Mulilis et al., 1977; Vaid et al., 1999; Leroueil and Hight, 2003), in addition to other influencing factors such as soil type, void ratio, and confining stress, it is critical that the anticipated particle fabric in the centrifuge specimen is also closely replicated in the samples used for laboratory element testing.

In centrifuge testing of sand models, the physical model is commonly prepared by placing dry sand using the method of air-pluviation. For example, in the Geotechnical Centrifuge Center at Rensselaer Polytechnic Institute (RPI), centrifuge samples are prepared by pouring the sand from a predetermined height using a funnel with essentially the same width as the centrifuge box (Taboada and Dobry, 1993), and the centrifuge facility at the University of California, Davis (Boulanger et al., 1999) also uses the method of air-pluviation. The specimens of Fraser River sand test specimens at the C-CORE centrifuge facility, supporting the current research on the verification of numerical models by UBC, will also be prepared using air-pluviated sand (Phillips, 2003). Any required dense zones in the physical model are achieved by tamping after the process of air-pluviation.

While databases are available for element tests conducted on water-pluviated and moist-tamped sands with regard to liquefaction (Vaid and Chern, 1983, 1985; Ishihara, 1993; Vaid and Sivathayalan, 2000; Kammerer et al., 2002; Robertson et al., 2000; Polito and Martin, 2001), laboratory testing that has been undertaken to understand the mechanical response of air-pluviated sands is scarce. Finn and Vaid (1977) and Vaid and Finn (1979) reports a series of cyclic simple shear tests conducted on dry medium Ottawa sand ASTM designation C-109 using a modified Cambridge-type simple shear device. Most of their detailed work, particularly in the investigation of the effect of initial static shear, focused on relative densities above 50%. DeGregorio (1990) and Vaid and Sivathayalan (2000) also report tests conducted on loose air-pluviated sands, and they have compared the results with those from counterpart sand specimens prepared using water-pluviation. Although the investigations have been mainly limited to undrained monotonic loading conditions, they reveal that air-pluviated sands behave in a significantly more contractive manner in comparison to their water-pluviated counterparts, again, highlighting the potential sensitivity of the soil response to particle structure. In spite of this work, the current published information on laboratory tests on air-pluviated sands does not provide an adequate reliable database for validating the numerical modelling of centrifuge test specimens prepared using air-pluviation.

As per above considerations, there is a need to obtain data from controlled element tests on samples that closely mimic the soil fabric and stress conditions of the centrifuge specimens for the validation of numerical approaches using centrifuge tests. In recognition of this, a detailed laboratory element testing research program was undertaken focusing on the cyclic shear response of air-pluviated Fraser River sand. In particular, the following aspects of the mechanical response of sand were addressed:

- Cyclic undrained response of sand without initial static shear stress bias (loose and dense conditions);
- The effect of stress densification on the cyclic shear resistance of sand (loose and dense conditions);
- The effect of initial static shear stress on the cyclic undrained response of sand (loose and dense conditions);
- Effect of cyclic pre-shearing on the cyclic undrained response of loose sand;
- The cyclic drained response of sand (loose and dense conditions); and
- The effect of imparted vibrations during sample preparation in the undrained response of sand (limited tests).

The NGI-type (Bjerrum and Landva, 1966) cyclic direct simple shear test (DSS) device at UBC, which is considered to be more effective in simulating seismic loading than the triaxial device, was used to carry out the testing. Unlike laboratory studies conducted on samples prepared using now well-established methods of water-pluviation, it was recognized that the re-constitution of soil specimens to mimic the particle fabric in the centrifuge physical soil models is non-routine. Since this is an important prerequisite as well as an integral component of this study, great importance was given to the development of pluviation techniques for sample re-constitution and associated verification of sample quality.

CHAPTER 2

LITERATURE REVIEW

2.1 GENERAL

Cyclic loading response of sand is a subject that has been extensively studied by many researchers over the past thirty years. Primarily due to the difficulties in obtaining "undisturbed" samples, most of the work has been carried out on reconstituted sand samples that are prepared using techniques of pluviation and moist tamping. In particular, the method of water pluviation is commonly selected to prepare sand samples since the soil fabric in such samples is considered to mimic the deposition conditions in natural alluvial deposits. Because of this increase focus, there is a relatively large database available from laboratory element tests on water-pluviated samples, for example, in comparison to data from samples prepared using air-pluviation technique.

As indicated in Chapter 1, centrifuge testing plays a critical role in the verification of numerical procedures. Most centrifuge models are prepared using air-pluviated sand, and the soil behaviour is known to be affected by the particle fabric. As such, there is a strong need to obtain data from element tests on specimens that have been prepared using air-pluviation for calibration of constitutive models used in numerical procedures.

This chapter presents a review of literature primarily with regard to the undrained cyclic shear response of sand. An overview of the role of centrifuge and laboratory element testing to validate numerical models is presented as background material. The method of sample preparation in centrifuge testing is also reviewed in order to assess the requirements for laboratory element testing.

2.2 ROLE OF CENTRIFUGE AND LABORATORY ELEMENT TESTING IN THE VALIDATION OF NUMERICAL PROCEDURES

2.2.1 Centrifuge Testing

Ideally, the acceptability of numerical models requires proper validation using recorded data from field case histories. For example, Zienkiewicz et al. (1991), Beaty and Byrne (1999), and Beaty (2001) have validated their numerical procedures against field case histories. The needed field data, however, are often not available with sufficient accuracy and detail; this, in turn, has hindered the confirmation of numerical models.

It is well known that the behaviour of soils is stress level dependent. Therefore, the use of small-scale models under natural gravity (1g) conditions, which causes stress levels that are significantly smaller than those encountered in the field, is not considered suitable to generate data for verification of numerical models. Centrifuge systems can be used to invoke a high gravitational field (Ng) on small-scale soil models, thus overcoming the above stress level deficiency in 1g models, and providing an opportunity for more realistic imposition of field stress conditions (see Figure 2.1). In addition to the gravitational field, several other physical parameters are subject to scaling effects in centrifuge physical modeling as given in Table 2.1. Extensive research over the past twenty five years has demonstrated the potential of centrifuge testing in the examination of the response of well-defined geotechnical boundary value problems (Arulananthan and Scott, 1993; Boulanger et al., 1999; Phillips et al., 2002), and the approach has

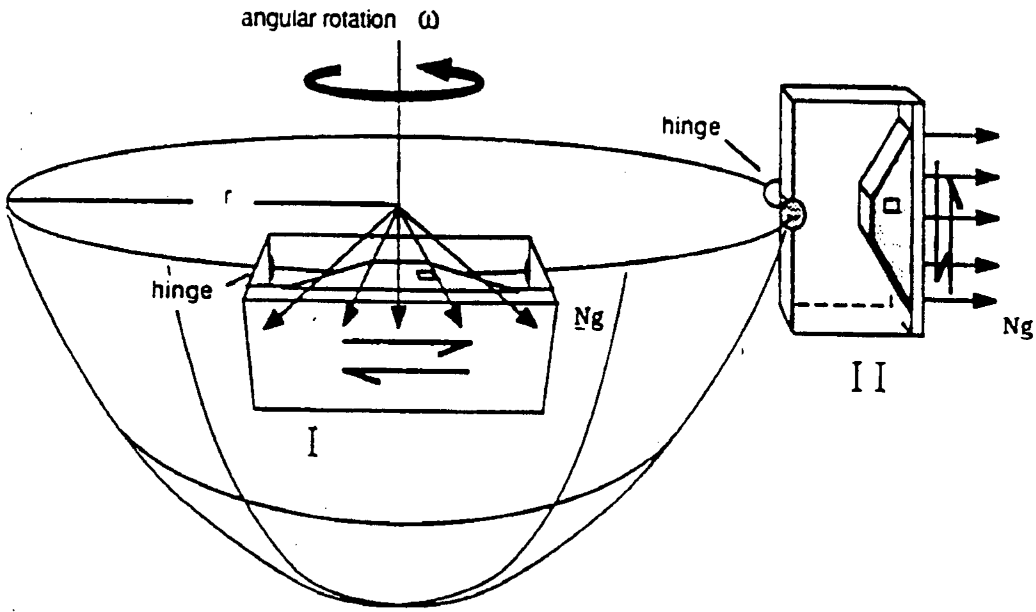

Figure 2.1 Schematic of Centrifuge Set-up (after Schofield and Steedman, 1988).

Table 2.1 Scaling Relations for Centrifuge Tests.

Parameter	Full Scale	Model at Ng's
Linear Dimension	1	1/N
Area	1	$1/N^2$
Volume	1	$1/N^3$
Stress	1	1
Strain	1	1
Force	1	$1/N^2$
Acceleration	1	N
Velocity	1	1
Time-In Dynamic Terms	1	1/N
Time-In Diffusion Cases	1	$1/N^2$
Frequency in Dynamic Problems	1	N

been increasingly considered as a meaningful basis for generating data for validation of numerical models. Several research programs that have been undertaken for the validation of numerical procedures using centrifuge model tests are tabulated in Table 2.2.

2.2.1.1 Specimen Preparation for Centrifuge Testing

In centrifuge testing of sand models, the physical model is commonly prepared by placing dry sand using the method of air-pluviation. In this method, soil is rained through air and the required density is achieved by controlling the pouring rate and/or fall height. For example, in the Geotechnical Centrifuge Centre at Rensselaer Polytechnic Institute (RPI), centrifuge samples are prepared by pouring the sand from a predetermined height using a funnel with essentially the same width as the centrifuge box (Taboada and Dobry, 1993), and the centrifuge facility at the University of California, Davis (Boulanger et al., 1999) also uses the method of air-pluviation. The specimens of Fraser River sand test at the C-CORE centrifuge facility, supporting the current UBC research on the verification of numerical models, will also be prepared using air-pluviated sand (Phillips, 2003). In some cases, when dense zones within test specimens are required, they are prepared by tamping after air-pluviation. It is understood that such tamping will be used for preparing dense specimens of Fraser River sand test at the C-CORE centrifuge facility.

2.2.2 Laboratory Element Testing Considerations

Accurate capturing of element soil behaviour in the constitutive model plays an important role in the numerical verification process, and laboratory element testing is the key to understanding this element behaviour. The relative roles of laboratory element and centrifuge testing in the verification of numerical models can be schematically illustrated as in Figure 2.2.

Table 2.2 Historical events of validation of numerical procedures using centrifuge model tests (Modified after Arulanandan, 1993).

Investigators	Description
Arulanandan, Anandarajah, and Abghari. 1982	Verification of numerical procedure (GADFLEA, 1976) using centrifuge model studies conducted at UCD using a piezoelectric shaker and a stacked ring apparatus.
Steedman, Finn, and Leadbetter. 1984	Verification of numerical procedure -TARA - using centrifuge model studies of a nuclear reactor container vessel conducted at Cambridge University using the Bumpy Road shaker.
Zienkiewicz, Shiomi, and Venter. 1987	Verification of numerical procedure - DIANA - using centrifuge model studies conducted at Cambridge University on the Bumpy Road shaker.
Habbibian and Finn. 1987	Verification of numerical procedure -TARA - using centrifuge model studies of Bolivar coastal dyke conducted at Cambridge University using the bumpy Road shaker.
Arulanandan and Muraleetharan. 1988	Verification of numerical procedure - ELMAI - using centrifuge model studies conducted at Cambridge University by Whitman and Lambe using the Bumpy Road shaker.
Hushmand, Crouse, Martin, and Scott. 1988	Verification of numerical procedure – DESRA - using centrifuge model studies conducted at Caltech using hydraulic actuator developed at Caltech.
VELACS Project. 1993	Verification of numerical procedures using centrifuge model studies conducted at Rensselaer Polytechnic Institute (RPI), University of California, Davis, University of Colorado, California Institute of Technology and Cambridge University.
Byrne, Park, and Beaty. 2003	Verification of numerical procedure - UBCSAND – using centrifuge model studies conducted at Rensselaer Polytechnic Institute (RPI).

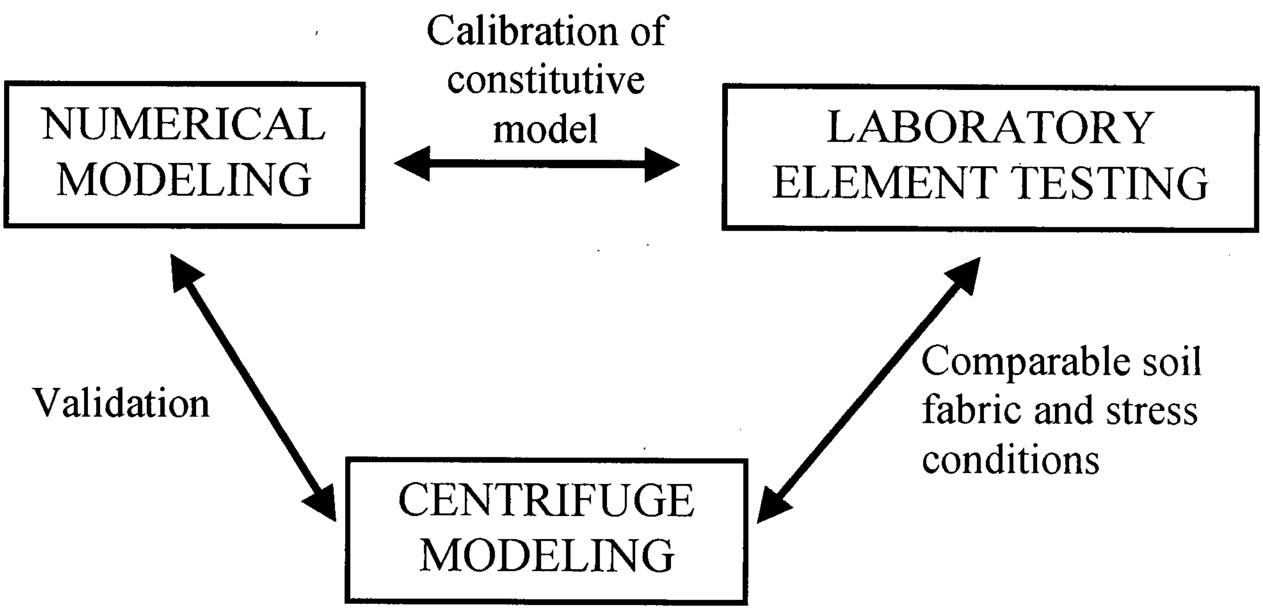

Figure 2.2 Schematic diagram showing the main components in the validation of numerical procedures using centrifuge physical model test data.

In addition to parameters such as density and confining pressures, the fabric of soil specimen and the paths simulated during testing are critical considerations in element testing of soils. The following subsections present a brief summary of the current knowledge on these aspects.

2.2.2.1 Effect of Soil Fabric

The term fabric is used to explain the difference in the particle arrangement/orientation in a soil skeleton. As indicated earlier, sand samples can be reconstituted using many different methods (e.g. water-pluviation, air-pluviation, moist tamping, dry tamping, and vibration). It has been shown that differences in the method of sample preparation would lead to different soil particle structures and, therefore, different stress strain responses (e.g. Oda, 1972; Ladd, 1974, 1977; Mulilis et al., 1977; Oda et al., 1978; DeGregoria, 1990; Vaid et al., 1999). In particular, Ladd (1974, 1977) and Mulilis et al. (1977) have observed that the method of sample preparation will significantly increase or decrease the liquefaction resistance of sand. Tests conducted by Mulilis et al. (1977) have also indicated that the resistance of sand to liquefaction increases with the level of imparted vibrations. Oda et al. (1978) and Vaid et al. (1999) have shown that water pluviated samples very closely mimic the anticipated fabric of water deposited soils.

2.2.2.2 Simulation of Field/Centrifuge Stress Paths

The need for data from laboratory element tests simulating field stress paths (in this case stress paths in centrifuge specimen) has been well accepted since the introduction of Stress Path Method by Lambe (1967). Cyclic triaxial and direct simple shear (DSS) apparatus are widely used to study the cyclic response of sands. Figure 2.3 illustrates typical filed stress conditions under earthquake loading. Figure 2.4 and Table 2.3 present some basic differences in testing

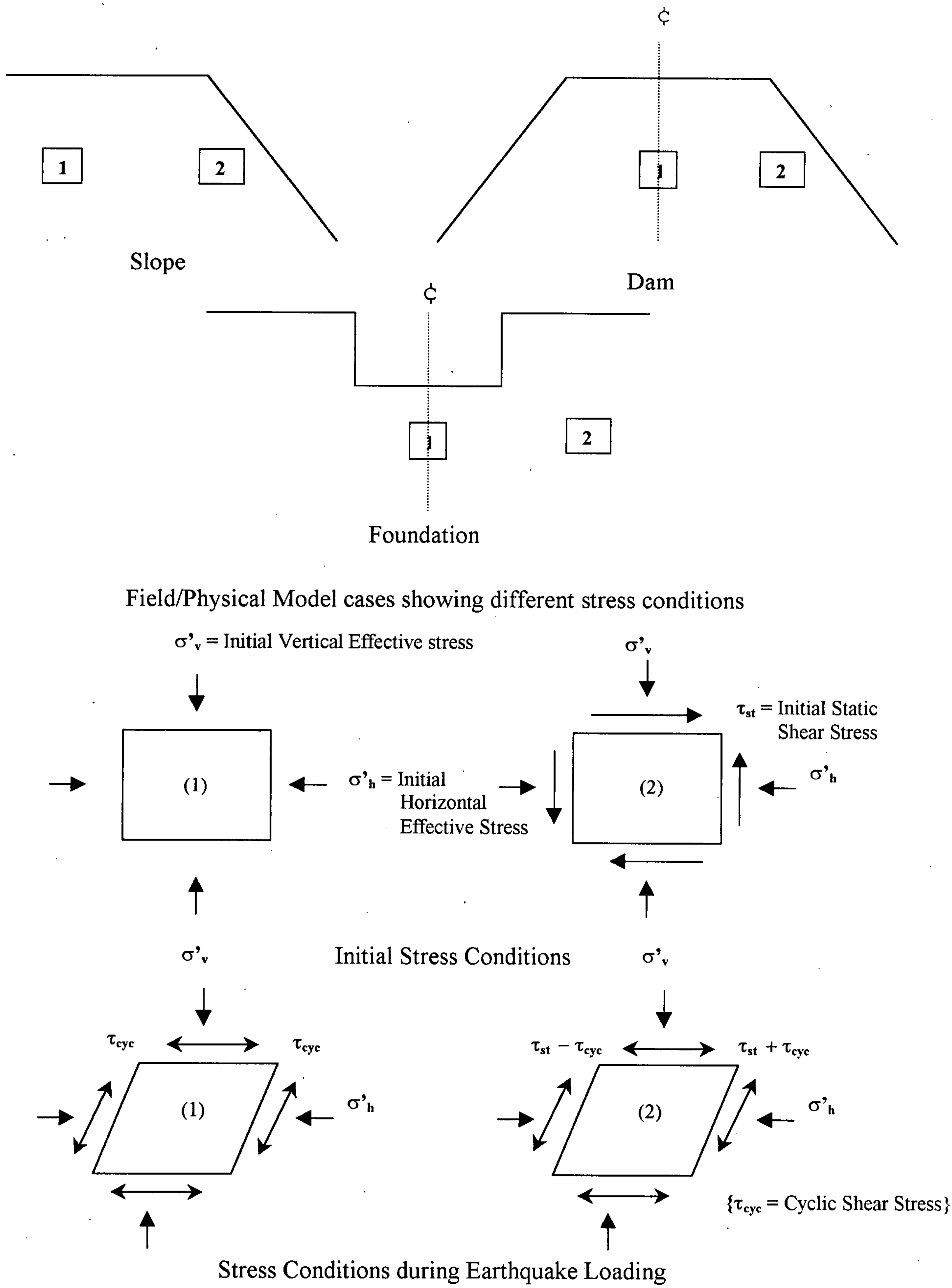

Figure 2.3 Field/Physical Model cases and stress conditions (1) without initial static shear stress (level-ground) and (2) with initial static shear stress (sloping ground).

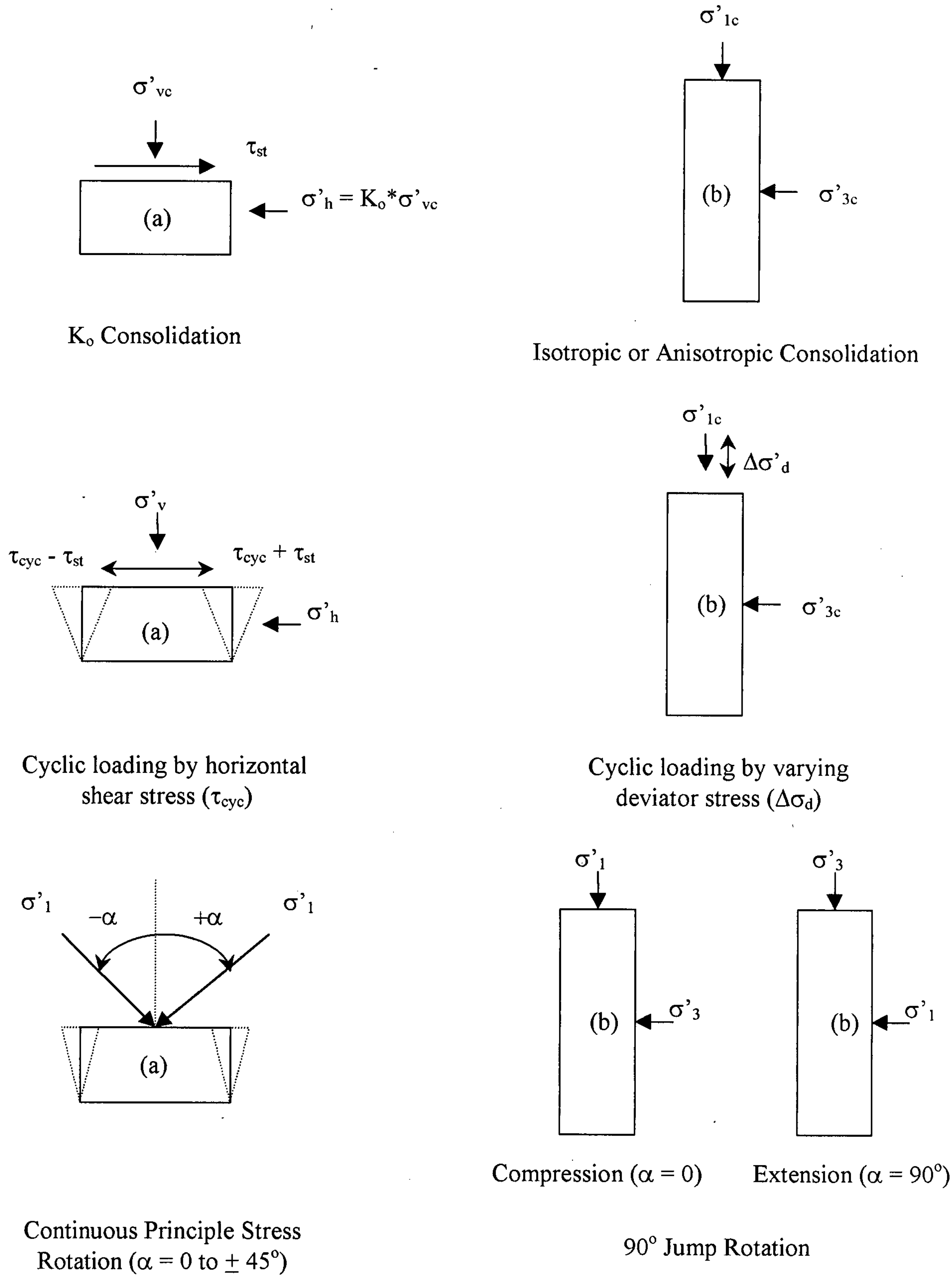

Figure 2.4 Comparison of Stress Conditions in (a) Simple Shear and (b) Triaxial Apparatus.

conditions between simple shear and triaxial apparatus. As may be noted from the figures, the DSS apparatus is considered more capable of replicating the field earthquake loading conditions than the triaxial device (Wijewickreme, 2004). Likely as a result of these differences, the test samples show a larger resistance to liquefaction in triaxial loading condition than in DSS condition (Peacock and Seed, 1968; Finn et al., 1971; Seed and Peacock, 1971; Castro, 1975; Vaid and Sivathayalan, 1996).

Table 2.3: Differences in Simple Shear and Triaxial tests that contributing to the different cyclic resistance to liquefaction.

PARAMETER	SIMPLE SHEAR TEST	TRIAXIAL TEST
Definition of Cyclic Stress Ratio	τ_{cyc}/σ'_{vc}	$\Delta\sigma_d/2\sigma'_{3c}$
Consolidation	K_o	Isotropy or anisotropy
Plane of Loading	Horizontal Plane	Planes of 45° to horizontal
Principle Stress Rotation	Continuous Rotation (0 to $\pm$ 45°)	90° jump Rotation
Intermediate principle stress	Intermediate principle stress always equal to the minor principle stress	Intermediate principle stress jump from minor principle stress to major principle stress during each halt cycles (Compression to extension mode).
Other Factors	Seating errors , Lack of complimentary shear	Necking or bulging of samples, compliance of the system

2.3 SHEAR BEHAVIOUR OF SAND

Understanding of the mechanical behaviour of soil is critically important in the development of constitutive models. Most of the basic understanding of soil behaviour has come from shear tests conducted mainly using the triaxial device, and to a lesser extent using shear devices such as DSS, HCT etc. In recognition of the volume change tendencies associated with shear loading, laboratory testing of soils is often conducted either simulating drained (where provision is made for volume change without generating excess pore water pressures) or undrained conditions (where no volume change is permitted). Because of the volumetric constraint, the samples generally experience pore water pressure changes during undrained shear loading.

In addition to the volumetric constraints, the other important consideration is the type or mode of loading. Monotonic loading tests are often conducted to understand the response of soils to static loading. On the other hand, cyclic loading is used to investigate the soil behaviour under dynamic conditions such as seismic shaking.

The present study is mainly related to investigating the response of air-pluviated sand under cyclic loading conditions. However, in consideration of the relevance to this study, the current understanding of the response of sands under both monotonic (static) and cyclic loadings are reviewed in the following sections. For each loading case, the behaviour of sand under drained and undrained loadings are discussed as separate subsections for clarity.

2.3.1 Drained Monotonic Loading Response

Drained static behaviour of sand has been investigated by many researchers (e.g. Casagrande, 1936; Roscoe et al., 1963; Cole, 1967; Castro, 1969). Casagrande (1936) observed that sand would exhibit significant volumetric deformations during shearing. Typical response of sand observed during drained static loading is given in Figure 2.5. Two types of volumetric responses have been observed (i.e. contractive and dilative responses, respectively). At large strain, the mobilized angle of friction at which soil starts to deform at constant void ratio is called

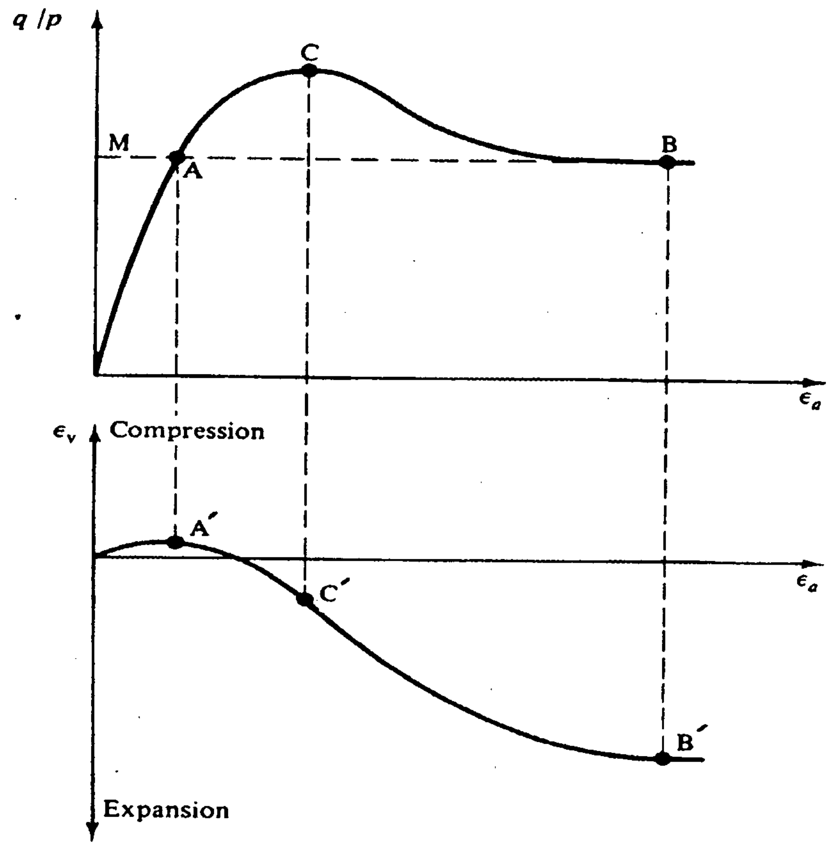

Figure 2.5 Characteristic response of sand during drain static/monotonic loading Condition (after Atkinson and Bransby, 1978).

the constant volume friction angle (ϕ_{cv}). Researchers have found that for a given soil, ϕ_{cv} is essentially same as the mobilized friction angle corresponding phase transformation (ϕ_{PT}) under undrained loading (Chern, 1985; Neguessy et. al., 1988).

Rowe (1962) and Lee and Seed (1967) have identified that, at a given density, there are three main components of shear resistance that comprise the peak mobilized friction angle: intrinsic sliding friction, resistance to dilation, and resistance to particle rearrangement (see Figure 2.6). Furthermore, Vesic and Clough (1968) found that the dilation effects gradually decrease with increasing confinement. This is also in accord with the finding that the contractiveness increases with increasing confining stress in undrained tests.

2.3.2 Undrained Monotonic Loading Response

Numerous investigations on the undrained monotonic behaviour of sand under triaxial and simple shear loading conditions have been reported (e.g. Castro, 1969; Ishihara et al., 1975; Chern, 1985; Ishihara, 1993; Sivathayalan, 1994; Vaid and Thomas, 1995). Typical undrained response of sand in monotonic undrained loading is shown in Figure 2.7. As may be noted, the behaviour has been interpreted in terms of three types of responses. In Type (1) response, the material reaches a peak shear strength and then shows continuous strain-softening. This is termed as liquefaction by Castro (1969), Casagrande (1975), and Seed (1979) and as true liquefaction by Chern (1985). The maximum stress ratio at which the soil starts to strain-soften is called critical stress ratio (CSR) by Vaid and Chern (1983), collapse surface by Sladen et al. (1985), and instability line by Lade et al. (1993). This type of response is considered to result in flow failures under field conditions.

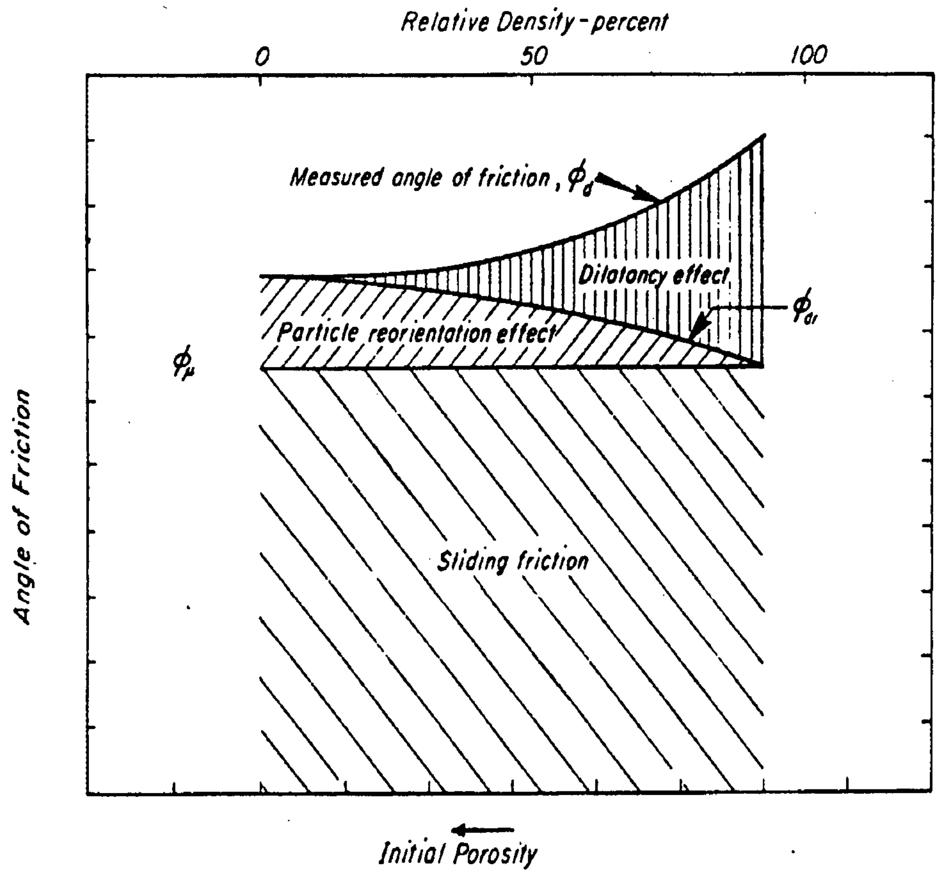

Figure 2.6 Components of shear resistance of sand (after Rowe, 1962; Lee and Seed, 1967).

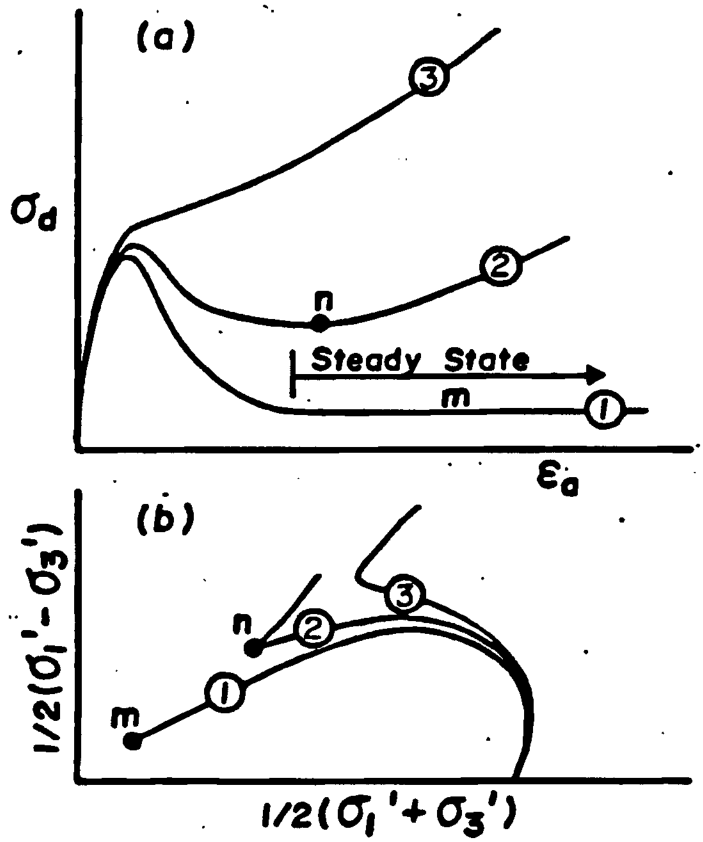

Figure 2.7 Characteristic response of saturated sand under static/monotonic loading conditions (after Vaid and Chern, 1985).

Type (2) response shows initial strain-softening followed by strain-hardening (dilation) and termed as limited liquefaction by Castro (1969). In this type, soil starts to strain soften after reaching CSR and then deform at constant stress ratio and, subsequently, followed by dilative response. The constant stress ratio at which sand undergoes "steady-state-like" deformation has been called the quasi-steady state (QSS) by Ishihara et al. (1975). The term phase transformation (PT) corresponds to the effective stress ratio at which the soil behaviour change from contractive to dilative (or the stress ratio at which the shear induced excess pore water pressure reaches its maximum value). Several research works have confirmed that ϕ_{PT} is unique for a given sand (Bishop, 1971; Ishihara et al., 1975; Vaid and Chern, 1983, 1985; Kuerbis et al., 1988). Furthermore, it has been noted that for a given sand both PT and QSS essentially occur at the same mobilized effective stress ratio, regardless of its initial state (Vaid and Chern, 1985; Ishihara 1993; Vaid and Thomas, 1995).

Type (3) response has no strain-softening region. Sand shows continuous increase in shearing resistance during deformation. Shear-induced excess pore water pressure initially experience an increase indicating a contractive response. This is followed by a decrease in pore water pressure that suggests a dilative tendency.

The soil behaviour can change from Type (1) to Type (3) depending on the initial stress conditions, density states (or void ratio), loading path, and fabric. For example, at same initial stress conditions, the behaviour of sand can change from Type (1) to Type (3) with increasing density (Sivathayalan, 1994). On the other hand, response of soil with same initial density can change from Type (3) to Type (1) with increasing confining stress (Sivathayalan, 1994). Vaid et al. (2001) have shown, from triaxial experiments on water-pluviated samples, that contractive or dilative tendency also depends on initial static shear stress. Loose sand exhibits an increase in strain softening with increasing initial static shear stress.

In consideration of stress paths, for a given initial stress and density condition, sand is more contractive in extension than in compression (Bishop, 1971; Miura and Toki, 1982; Chung, 1985; Vaid et al., 1990, 1995, 2001; Thomas, 1992; Riemer and Seed, 1997). Uthayakumar and Vaid (1998) and Sivathayalan and Vaid (2002) have observed that a sand response can also change from Type (3) to Type (1) with increasing α (angle of major principle stress with respect to vertical direction varying from 0 to 90°). In addition to the above, the particle fabric would also influence the contractive or dilative tendency of sand at identical initial conditions. For example, water-pluviated sand samples exhibit more dilative tendency than the air-pluviated and moist-tamped counterparts (Vaid et al., 1999).

2.3.3 Drained Cyclic Loading Response

Cyclic shear loading can induce significant compressive volumetric strains in unsaturated sands, which can result in undesirable ground settlements and possible damage to structures. In the case of saturated sand, this tendency in volume compression due to cyclic shear loading will lead to progressive generation of pore water pressure and subsequently to liquefaction. With the argument that the soil behaviour is governed by the response of the particle skeleton, data from drained cyclic tests have been used to capture pore pressure generation in undrained cyclic loading (e.g. Byrne, 1991; Lee, 1991). In these cases, the associated volume changes are predicted based on drained test data, and then the generated excess pore pressures are estimated by imposing a volumetric constraint as appropriate.

Laboratory strain-controlled drained cyclic DSS experimental works on sand by Silver and Seed (1971), Seed and Silver (1972); Youd (1972), Martin et al. (1975), and Finn et al. (1982) have shown that there is a progressive decrease in volume with applied number of load cycles. The rate of decrease in volume was noted to gradually decrease with increasing number of load cycles. Finn et al. (1982) found that the soil would become stronger with increasing number of load cycles, and eventually it reaches a steady stress-strain loop. Silver and Seed (1971) and Youd (1972) have observed that the volumetric strains also increase rapidly with increasing cyclic strain amplitude. Furthermore, their results show that the level of confining stress does not have a significant effect on volumetric compression. Youd (1972) has also observed that the frequency of shear strain application has no effect on the shear-induced volume compression. Martin et al. (1975) concluded that the shear-induced volumetric strain is proportional to the applied cyclic shear strain amplitude. Using this observed proportionality, Byrne (1991) has formulated a two-parameter shear-volume coupling model to predict the shear-induced volumetric strains during cyclic loading.

Lee (1991) used a particulate approach to formulate a relationship between shear stress, effective vertical stress, incremental volumetric strain, and incremental shear strain in a drained cyclic simple shear test. He formulated the following bilinear relationship for loading and unloading cases and confirmed the validity of this relationship using data from DSS tests on two different sands:

Loading $$\tau/\sigma_v' = A + B\,\{d\,(\varepsilon_v)/d\,(\gamma)\} \qquad [2.1a]$$

Unloading $$\tau/\sigma_v' = -A - B\,\{d\,(\varepsilon_v)/d\,(\gamma)\} \qquad [2.1b]$$

where A, B are positive constants that depend on the basic friction angle and the number of slip/non-slip contacts. The results indicated larger scatter at the initial levels of stress reversal but showed reasonable agreement elsewhere. The predicted pore pressure using this particulate approach showed larger scatter with increasing number of cycles, and this is likely be due to the fabric changes associated with shearing.

2.3.4 Undrained Cyclic Loading Response

Undrained cyclic loading tests provide an opportunity to understand the soil behaviour during earthquake shaking. As per the case of monotonic loading, three types of responses have been observed: liquefaction, cyclic mobility with limited liquefaction, and cyclic mobility with out limited liquefaction (Castro, 1969; Vaid and Chern, 1985). The typical strain development corresponding to these three cases of responses are shown in Figures 2.8 through 2.10. In the liquefaction type of response, sand suffers continuous contractive deformation (Figure 2.8). On the other hand, in limited liquefaction type of response, once the stress ratio has reached phase transformation (PT) the soil starts to behave in a dilative manner. During the next unloading part of the cycle, larger excess pore pressures would develop and bring the effective confining stress to a zero transition stress stage. Further cyclic loading would cause the soil to exhibit dilative tendency, and, in turn, leading to strain hardening response starting from very low shear modulus (Figure 2.9). In cyclic mobility type response, there is no strain softening, and the shear strains increase gradually with increasing number of load cycles (Figure 2.10).

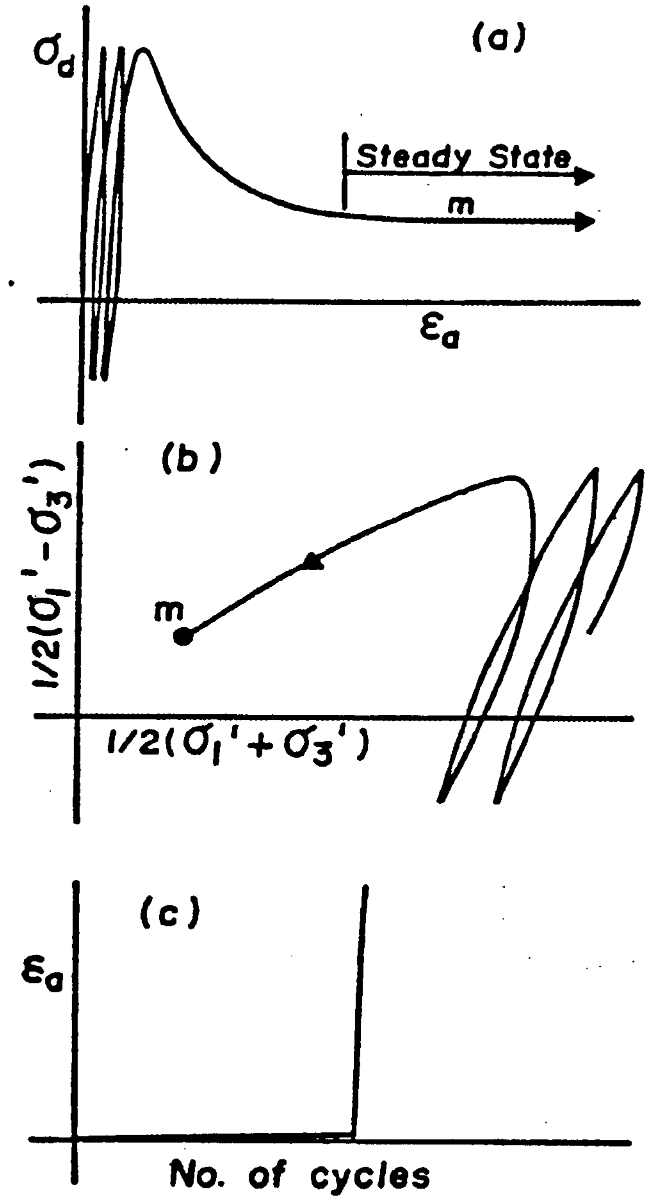

Figure 2.8 True Liquefaction type of deformation during cyclic loading (after Vaid and Chern, 1985).

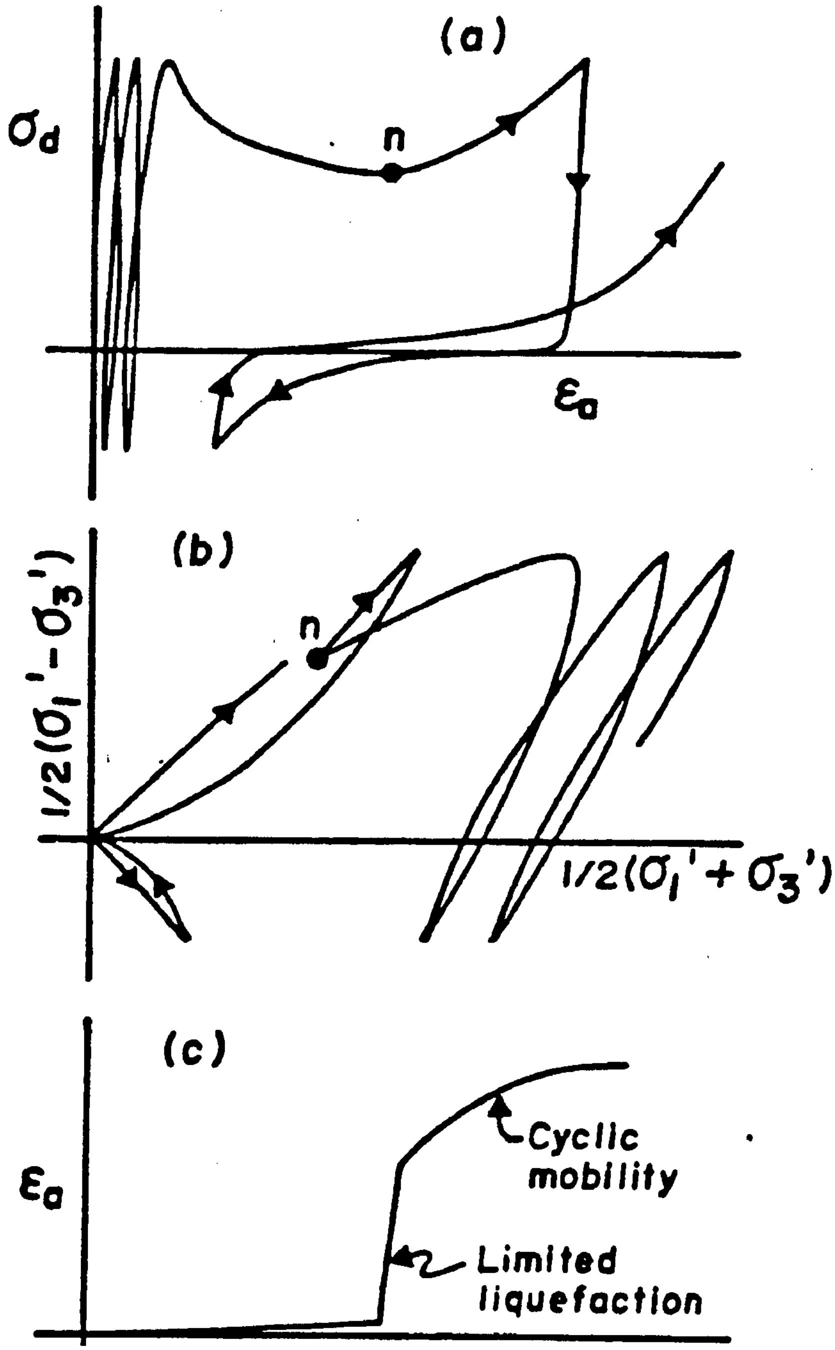

Figure 2.9 Limited liquefaction type of deformation during cyclic loading (after Vaid and Chern, 1985).

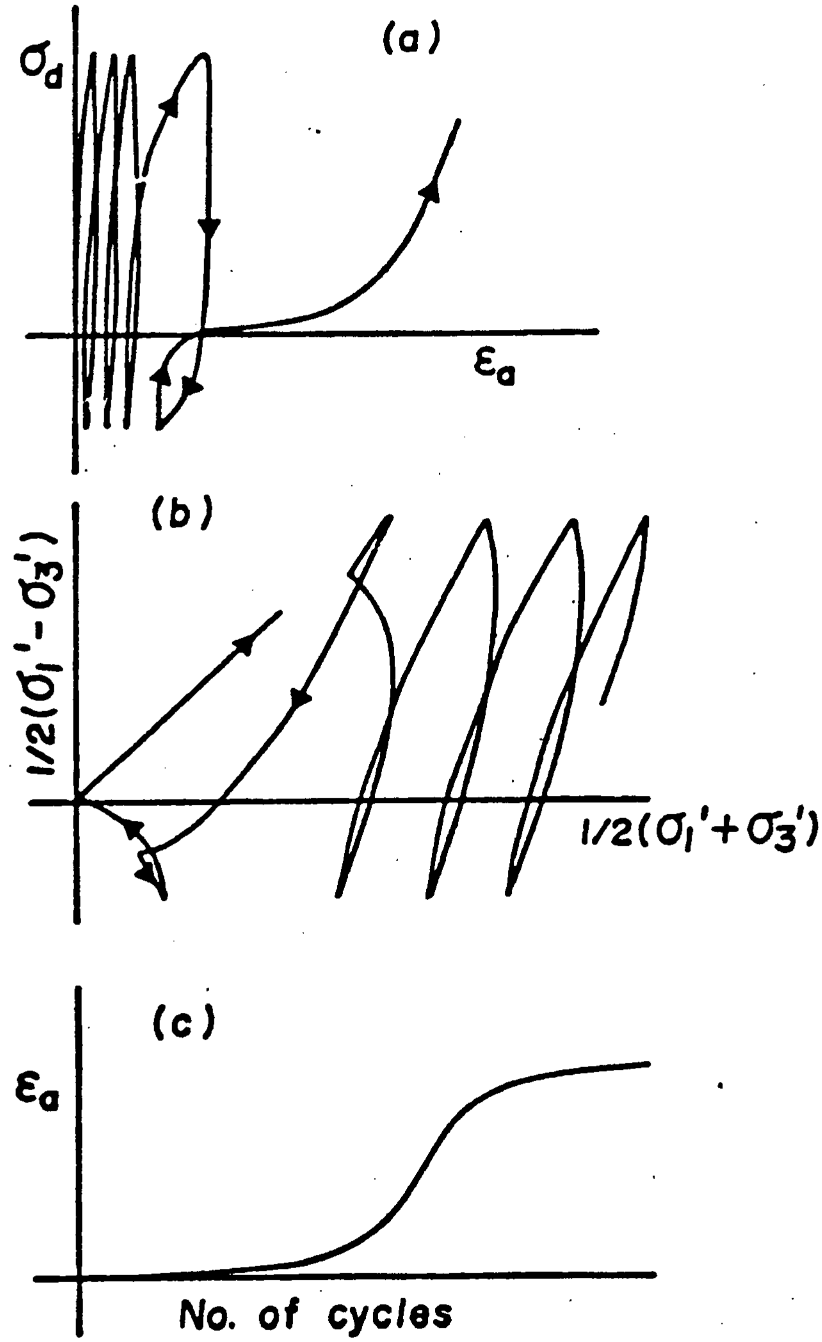

Figure 2.10 Cyclic Mobility type of deformation during cyclic loading (after Vaid and Chern, 1985).

Similar to the case of monotonic loading, the cyclic response of a sand can change from liquefaction to cyclic mobility or vice versa, depending on density, initial static stress, confining stress, magnitude of cyclic load, fabric, past stress/strain history, etc. This dependency of cyclic loading response on some of the above factors is further reviewed in Section 2.4.

2.4 CYCLIC RESISTANCE TO LIQUEFACTION

Generally, cyclic resistance to liquefaction is defined as the cyclic stress ratio (CSR = τ_{cyc}/σ'_{vc} where τ_{cyc} = Amplitude of cyclic shear stress and σ'_{vc} = Initial effective vertical stress) at which a soil sample will reach liquefaction after application of 15 cycles. Liquefaction was originally defined as the point at which the excess pore pressure ratio ($r_u = \Delta u/\sigma'_{vc}$ where Δu = excess pore water pressure and σ'_{vc} = initial effective vertical stress) reaches 100%. Since some soils experience relatively large strains during cyclic loading without reaching r_u = 100% condition, liquefaction has also been defined on the basis of a soil reaching a certain specified strain level {e.g. samples subjected to cyclic loading with initial static bias and with out stress reversal ($\tau_{st} > \tau_{cyc}$) does not reach r_u = 100%}. While a selected strain level is not necessarily an appropriate measure of liquefaction, as an "index" of comparison and for certain discussion purposes, liquefaction is considered to have triggered when the single-amplitude horizontal shear strain (γ) reached a value of 3.75% in a DSS sample. This strain level is equivalent to reaching a 2.5% single-amplitude axial strain in a triaxial sample, which also is a definition for liquefaction previously suggested by the National Research Council of United States (NRC, 1985).

For a given sand, the cyclic resistance to liquefaction will depend on a number of factors such as initial density, confining stress, and static shear stress. The following sub sections will review the influence of some of these factors that are directly connected with the present investigation.

2.4.1 Effect of Confining Stress and Density

The effect of confining stress on the cyclic resistance of soil has been observed by many researchers (e.g. Vaid et al., 1985, 2001; Seed and Harder, 1990; Sivathayalan, 1994; Idriss and Boulanger, 2004). Generally, the cyclic resistance of sand has been observed to decrease with increasing confining stress. Seed and Harder (1990) suggested the following empirical correction factor K_σ to account for this effect of initial confining stress on the cyclic resistance.

$$CRR_{\sigma',\,Drc} = K_\sigma * CRR_{100,\,Drc} \qquad [2.2]$$

where $(CRR)_{\sigma',Drc}$ is the cyclic resistance ratio of a soil sample of a given relative density D_{rc} consolidated to an initial confining stress of σ', and $(CRR)_{100,Drc}$ is the cyclic resistance ratio of a sample of the same soil at the same density consolidated to an initial confining stress of 100 kPa. However, it was later recognized that the experimental results exhibited a significant scatter with respect to the above since the dependency of K_σ on density had not been taken into account. This dependency of K_σ on the relative density of sand was noted by Thomas (1992) and Vaid and Thomas (1995) based on data from cyclic triaxial tests. Furthermore, simple shear tests results by Vaid et al. (1985) and Sivathayalan (1994) has also shown similar dependency of K_σ on the relative density. The effect of confining stress on K_σ was noted to be larger at higher densities, but it has virtually no effect at lower density levels. Hynes and Olsen (1999) have recently compiled and analyzed a large database and derived the following equation for calculating K_σ:

$$K_\sigma = (\sigma'_{vo}/Pa)^{(f-1)} \qquad [2.3]$$

where f is a constant that depends on the relative density. The NCEER/NSF workshop participants have recommended the following values for f: for relative densities between 40% and 60%, f=0.7-0.8; for relative densities between 60% and 80%, f=0.6-0.7 (Youd et al., 2001).

It is well known that the liquefaction resistance increases with increasing density. In general, the density is expected to increase with increasing confining stress (i.e. stress densification). As such, there is a possibility of same compensation between the effect of confining stress and density on the liquefaction resistance. Pillai and Byrne (1994) have demonstrated the importance to consider the effect of stress densification in determining the CRR of insitu sands, from the field and laboratory test results on Duncan Dan sand. Furthermore, Park and Byrne (2004) have demonstrated the method to evaluate the effect of stress densification in numerical models that capture the centrifuge model response.

2.4.2 Effect of Static Shear Stress

The field earthquake Geotechnical problem generally involves configurations having level-ground as well as slopes. In the description of initial stress state, for level-ground conditions, the term "no static shear bias" is commonly used to reflect that there are no initial static shear stresses on the horizontal plane prior to earthquake loading (Seed and Peacock 1971; Vaid and Finn, 1979). In the laboratory, when the objective is to replicate this level-ground condition, cyclic shear tests are conducted on samples consolidated without an initial applied static shear stress (or "no static bias"). On the other hand, samples initially consolidated with an applied static shear stress prior to cyclic shear loading are used to simulate the configuration of sloping ground, and these tests are typically referred to as cyclic shear tests with an "initial static shear stress bias".

It has been found that the presence of initial static shear stress has a profound influence on the cyclic resistance of sand (e.g. Lee and Seed, 1967; Lee et al., 1975; Yoshimi and Oh-oka, 1975; Vaid and Finn, 1979; Vaid and Chern, 1983; Stedman, 1997; Harder and Boulanger, 1997; Vaid et al., 2001). Studies by Lee and Seed (1967), Lee et al. (1975), and Seed et al. (1975) have led to the conclusions that the presence of static shear increases the cyclic resistance to liquefaction. Castro (1969, 1975), Casagrande (1975), Castro and Poulos (1977) and Castro et al. (1982), on the other hand, observed that the increase in static shear stress may decrease the cyclic resistance to liquefaction. Investigation by Vaid and Finn (1979), Vaid and Chern (1983, 1985), Seed and Harder (1990), and Vaid et al. (2001) has indicated that the effect of static shear stress on the cyclic resistance is also influenced by the initial density. For example, it has been found that loose (contractive) sands experience a reduction in cyclic resistance in the presence of initial static shear bias. On the other hand, the cyclic shear resistance of dense (dilative) sands have been noted to increase with increasing level of static bias. Vaid and Chern (1985) have concluded that the cyclic resistance to liquefaction would increase with increasing initial static shear if the deformation mechanism is of "cyclic mobility" type, and vice versa.

Seed and Harder (1990) suggested the following empirical correction factor K_α in order to incorporate the initial static shear effect on cyclic resistance of sand.

$$CRR_{\sigma',Drc,\alpha} = K_\alpha * CRR_{\sigma', Drc,0} \qquad [2.4]$$

where $(CRR)_{\sigma',Drc,\alpha}$ is the cyclic resistance ratio of a soil sample of a given relative density D_{rc} consolidated to an initial confining stress of σ' with an initial static shear bias ratio of α (= τ_{st}/σ'), and $(CRR)_{\sigma',0}$ is the cyclic resistance ratio of a sample of the same soil at the same density/initial confining stress, but with no initial static shear bias (α = 0).

Harder and Boulanger (1997) suggested values for K_α by incorporating the dependency of K_α on density and magnitude of initial static bias mainly based on data from cyclic DSS and torsional shear tests. Vaid and Sivathayalan (2000) and Vaid et al. (2001) have shown that the predicted CRR values using the K_α and K_σ factors as proposed above would underestimate the cyclic resistance ratio regardless of the initial density and stress levels. It has been noted that effect of both static shear stress and confining stress are dependent on the density. As such, it has been suggested both K_α and K_σ are not independent, and, perhaps, the use of a scaling factor $K_{\alpha\sigma}$ that would account for both static shear stress and confining stress is more meaningful.

2.4.3 Effect of Cyclic Pre-shearing (Re-liquefaction Response)

The cyclic resistance to liquefaction has also been noted to be significantly influenced by past liquefaction, or pre-shearing, effects (Finn et al., 1970; Seed et al. 1977; Ishihara and Okada, 1978, 1982; Suzuki and Toki, 1984; Vaid et al., 1989). Finn et al. (1970) noted this effect based on the results obtained from cyclic DSS and triaxial tests. They found that previously liquefied samples exhibit significantly less cyclic shear resistance than virgin samples despite a significant increase in density due to the consolidation followed by liquefaction. Emery et al. (1973) found that the liquefied samples may have top layers that are loose, and this may result in the non-uniform samples that could exhibit a reduction in liquefaction resistance in subsequent loadings. The samples that did not reach liquefaction (i.e. samples subjected to small cyclic strains) showed significant increase in their resistance to liquefaction in comparison to those observed for virgin sample (Finn et al., 1970; Seed et al., 1977). Ishihara and Okada (1978, 1982) have distinguished between the small and large pre-shearing by the location of the effective stress state with respect to the "line of phase transformation". Vaid et al. (1989) have suggested the line of critical stress ratio (CSR) as the demarcation between the small and large pre-shearing because larger deformations start to occur after CSR in true and limited liquefaction types of responses. Results from triaxial tests by Ishihara and Okada (1978) and Vaid et al. (1989) have shown that the small pre-shearing would significantly reduce the excess pore water pressure generation during subsequent cyclic loadings. On the other hand, large pre-shearing would significantly increase or decrease the pore pressure generation in next loading depending on the loading direction. If a sample is loaded in the same direction as the direction of pre-shearing (i.e. no strain reversal) then the pore pressure generation was noted to be less than that observed during the previous loading, and vice versa.

2.4.4 Effect of Aging

While significant laboratory investigations have been undertaken to assess the effects of aging on the soil response under monotonic loading (Andersan and Stokoe, 1978; Howie et al., 2001; Gananathan, 2002; Lam, 2003), not much work has been reported with regard to the effect of aging on liquefaction resistance. Seed (1979) indicated that the cyclic resistance would increase with aging based on results from tests on samples that had been subjected to sustained loads for periods ranging from 0.1 to 100 days prior to testing. Samples that had been subjected to longer periods of sustained pressure showed an increased resistance to liquefaction by about 25% in comparison to the unaged samples.

The study on the effect of aging is not within the scope of the current research program. However, this became important consideration in the development of the testing protocols, particular with respect to determining a suitable aging period prior to shearing for the re-constituted samples.

2.5 PROPOSED RESEARCH PROGRAM

The foregoing literature review indicates that major advances have been made in the understanding of the stress strain response of sand mainly based on data from water-pluviated laboratory element specimens. The response of sand depends on many factors such as density, stress conditions, testing apparatus, fabric, and aging. It is clear that there is a need to obtain data from controlled element tests on specimens that closely mimic the soil fabric of the centrifuge specimens for the validation of numerical models using centrifuge tests.

In recognition of the above, and with the knowledge that the centrifuge samples are prepared mainly using the method of air-pluviation, a detailed laboratory element testing research program was undertaken focusing on the cyclic shear resistance of air-pluviated sand. The NGI-type (Bjerrum and Landva, 1966) cyclic direct simple shear (DSS) device at the University of British Columbia (UBC), which is considered to be more effective in simulating seismic loading than the triaxial device, was used as the testing apparatus.

Experimental procedures, material tested, the development of air-pluviation technique, evaluation of sample uniformity, and assessment of test repeatability are described in Chapter 3. Chapter 4 presents the experimental results, and it also provides a detailed discussion on the important and relevant findings. Summary and conclusions derived from this study are presented in Chapter 5.

CHAPTER 3

EXPERIMENTAL ASPECTS

This chapter describes the experimental aspects of the study presented in this thesis. The selection of testing apparatus and the development of sample preparation techniques to characterize the cyclic loading response of Fraser River sand were conducted in a manner that would directly support and complement the numerical modelling and centrifuge testing proposed as a part of the overall liquefaction study undertaken at the University of British Columbia (UBC).

Initially, a description of the UBC direct simple shear (DSS) apparatus, including the stress and strain controlled loading systems, instrumentation, and data acquisition system is presented. Brief descriptions of material tested, the development of sample reconstitution method, associated uniformity evaluation and test procedures are then addressed. Typical experimental results are also presented to demonstrate the test consistency and repeatability. An outline of the experimental program is provided at the end of the chapter.

3.1 TESTING APPARATUS

The direct simple shear and triaxial apparatus have been used by many researchers to study the cyclic shear response of sands. While the cyclic triaxial test has been widely used because of its simplicity and common availability, the DSS loading is considered to effectively mimic the anticipated stress conditions under cyclic loading. Furthermore, simple shear tests can be conducted in constant volume condition, which eliminates the error due the compliance as well as making the testing easier by eliminating the complicated saturation requirements (Finn and Vaid, 1977; Finn et al., 1978). In recognition of the above, the cyclic direct simple shear apparatus was selected for the characterization of Fraser River sand presented in this thesis.

3.1.1 Simple Shear Apparatus

The UBC simple shear apparatus is of the NGI type (Bjerrum and Landva, 1966). A schematic diagram of the apparatus is given in Figure 3.1. A cylindrical soil sample, 70 mm in diameter and ~20 mm in height, is placed in a reinforced rubber membrane. The reinforced rubber membrane is stiff enough to constrain any lateral deformations and therefore, the soil behavior will be in a state of zero lateral strain during consolidation and cyclic loading, which is considered suitable to simulate the anticipated stress conditions in the field as well as in the centrifuge model (see Figures 2.3 and 2.4). Simple shear tests can be conducted in undrained condition or constant volume condition. In the case of undrained test, undrained condition is imposed by suspending all drainage conditions. In constant-volume DSS tests, as an alternative to suspending the drainage of a saturated sample, a constant volume condition can be enforced even in dry soil by constraining the sample boundaries (diameter and height) against changes. The sample diameter is already constrained against lateral strain using reinforced rubber membrane, and the height constraint is attained by clamping the vertical movement of the top and bottom loading caps. It has been shown that the decrease (or increase) of vertical stress in a constant-volume DSS test is

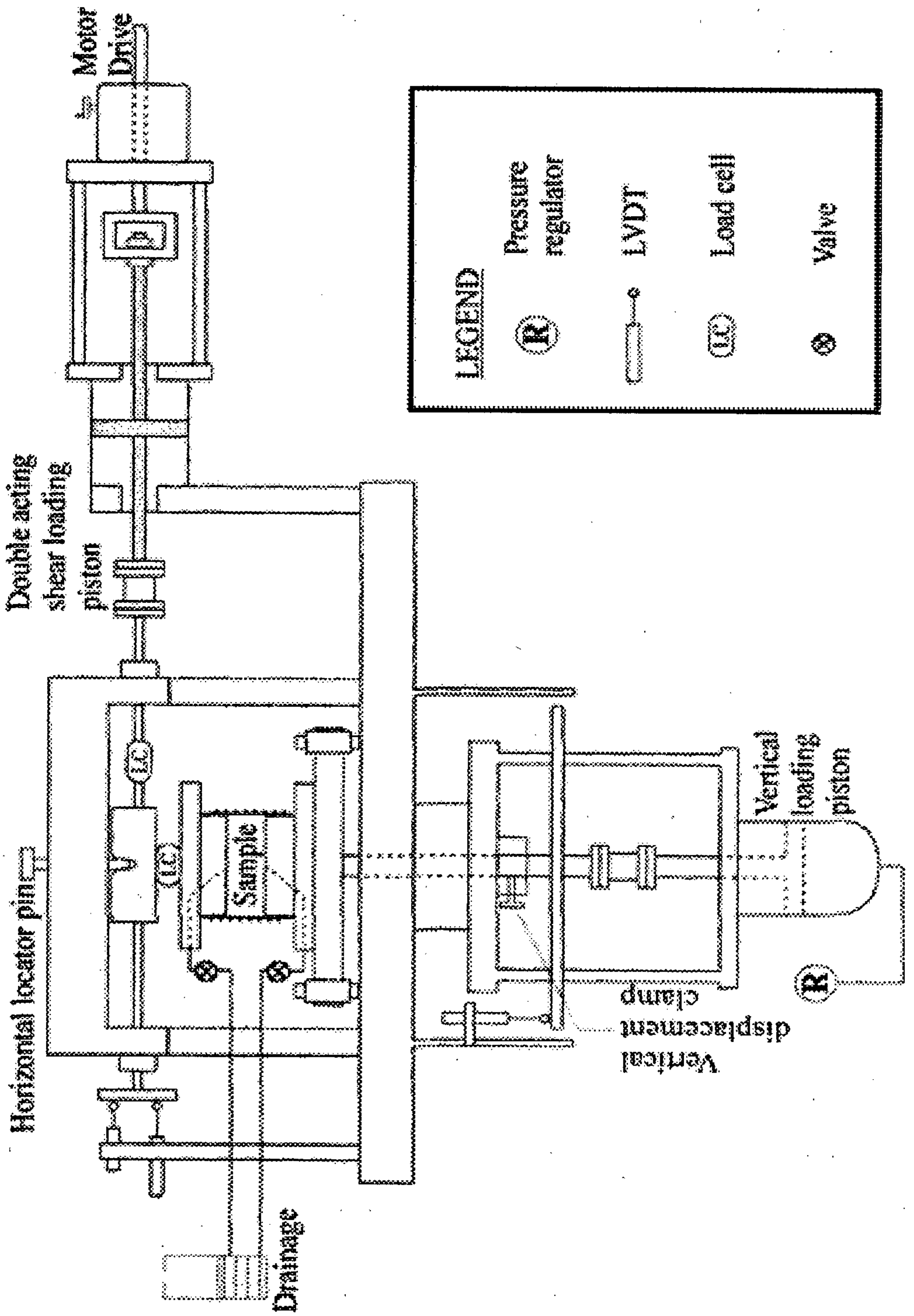

Figure 3.1 Schematic diagram of UBC simple shear apparatus.

essentially equal to the increase (or decrease) of excess pore water pressure in an undrained DSS test where the near constant volume condition is maintained by not allowing the mass of pore water to change (Finn et al., 1978; Dyvik et al., 1987).

3.1.2 Loading System

The UBC DSS apparatus consists of horizontal and vertical loading systems (see Figure 3.1). The vertical loading system consists of a single acting air piston, which can be precisely controlled by an external manually controlled air pressure regulator. A double acting frictionless air piston that is coupled in series with a constant speed motor drive is used to apply the horizontal load. The coupled horizontal loading system enables the system to provide a smooth transition from stress-controlled to strain-controlled loading and vice versa.

Cyclic loading in stress-controlled mode is applied by changing the pressure on one side of the double acting piston by the means of electro-pneumatic regulator, while holding the pressure on the other side constant. The electro-pneumatic regulator is coupled with a data acquisition system and computer, which enables to apply essentially any prescribed form of cyclic loading. Generally, a sinusoidal waveform is used, and the magnitude and duration of the waveform can be changed, at anytime, during the test. Each chamber of the double acting piston is coupled with a volume booster, in order to maintain the amplitude of cyclic loading at present value during large deformations.

Cyclic loading or monotonic loading in strain-controlled mode is applied by the means of constant speed motor. The motor speed and direction can be changed manually, as required.

3.1.3 Data Acquisition and Control System

The UBC DSS device uses a high-speed data acquisition and control system. A 12-bit "PCL718" high-speed data acquisition card is used for signal input and output. This card consists of five A/D input channels and a D/A output channels.

Input channels are dedicated to collect data from the two load cells (monitoring vertical load and horizontal load) and three LVDTs (one for monitoring vertical displacement and two for horizontal displacement). From the two LVTDs that are used to measure horizontal displacements, one is assigned for the measurement of small displacements and the other for large displacements. This approach increased the measuring resolution of small displacements. All transducers are excited using a 5V d.c voltage. Input signals from load cells are amplified by a factor of 1000. The resolution is further improved by averaging 60 readings for each data channel. The high-speed data acquisition system is capable of gathering about 500 sets of data per second.

The D/A channel is used to control the electro-pneumatic transducer that supplies the pressure to one chamber of the double acting air piston. The electro-pneumatic transducer is of "SMC IT2051-N33" type that is capable of 90 kPa full scale pressure output for a 1000 kPa input pressure.

3.1.4 Measurement Resolution

Carefully selected transducers and sophisticated data acquisition system yield a high resolution of measurement and precise control of the test specimen. In the data reduction program, the measured shear load is corrected for shaft friction, strength of reinforced membrane, and spring force from the displacement transducers. The resolution of each measurement, for a 70 mm in diameter and 20 mm in height sample, is given in Table 3.1.

Table 3.1 Measurement resolutions of UBC simple shear apparatus.

MEASUREMENT		RESOLUTION
Vertical/ normal stress		± 0.25 kPa
Horizontal/shear stress		± 0.25 kPa
Shear strain	Small Range (<13%)	± 0.01 %
	Large range (>13%)	± 0.05 %
Vertical strain		± 0.01 %

3.2 MATERIAL TESTED

The Fraser River sand used in this study had an average particle size D_{50} = 0.26 mm, D_{10} = 0.17 mm, and uniformity coefficient c_u = 1.6 (see Figure 3.2). This dredged sand from the Fraser River in the Lower Mainland of British Columbia, Canada, has been extensively used in laboratory research at UBC over the past 10 years. Because of its presence and judged susceptibility to liquefaction in large parts of the highly populated Fraser River Delta, it has been selected as the soil material for the centrifuge model testing conducted to provide data for the verification of numerical models at UBC. The maximum and minimum void ratios (e_{max} and e_{min}) for the sand determined as per American Society for Testing and Materials Standards ASTM-4254 and ASTM-4253 are 0.94 and 0.62, respectively. Fraser River sand is composed of 40% quartz, quartzite, and chert, 11% feldspar, and 45% unstable rock fragments (Garrison et al., 1969). The sand grains are generally angular to sub-rounded in shape. A microscopic view of the sand particles is shown in Figure 3.3.

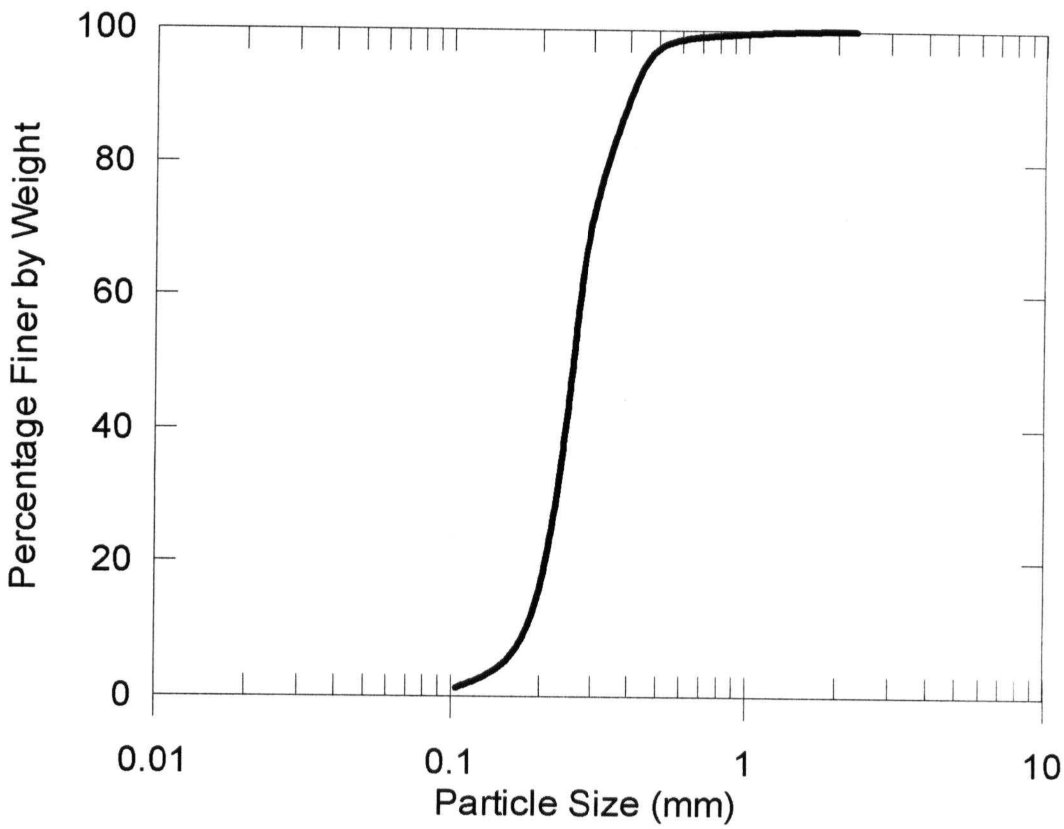

Figure 3.2 Grain size distribution of Fraser River sand (Park, 2003).

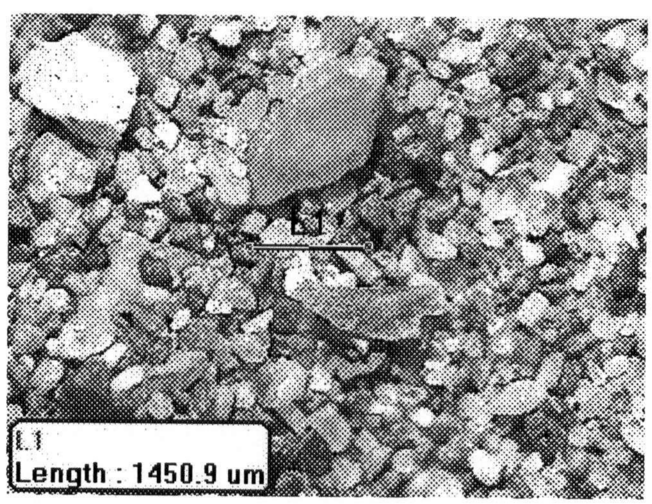

Figure 3.3 Microscopic view of Fraser River sand particles.

3.3 DEVELOPMENT OF AIR-PLUVIATION METHOD

One of the most important considerations was to develop a specimen preparation technique that would essentially replicate the granular structure imparted in centrifuge specimens prepared by raining of sand in air. Previous work by several researchers (Vaid and Negussey, 1986; Rad and Tumay, 1987; Cresswell et al., 1999) has indicated that the as-placed density of air-pluviated sand is dependent on the fall height as well as the mass rate of deposition of sand particles. Hence, there was a need to develop the characteristic relationships between as-pluviated density, flow rate, and fall height for Fraser River sand. This information was considered useful not only in the preparation of sand specimens for element testing, but also as input for the preparation of larger centrifuge specimens.

A simple raining technique that allows relatively independent control of both fall height and mass flow rate of sand is most preferable for the preparation of samples. Methodologies that have been previously developed by others (Rad and Tumay, 1987; Cresswell et al., 1999) were found to be relatively complex. As a result, a simple pluviation technique was developed, and Figure 3.4 shows the mechanical details of the arrangement. The set-up essentially consists of two concentric plexi-glass cylinders where the outer diameter of the inner cylinder is only very slightly smaller than the inner diameter of the outer cylinder. The inner cylinder can be rotated with respect to the outer cylinder as desired, and it has the effect of reducing side friction and arching effects as well as the ability to control the flow rate. A steel wire mesh with a selected opening size (1 mm sq. mesh) is mounted to the bottom of the outer cylinder, thus providing for raining of sand over a circular footprint. This footprint was designed to be essentially equal to that of the circular mold for the soil test specimen (~70 mm diameter) to ensure that the sand surface at any given time during placement would always be generally flat. The objective was to ensure that the sand,

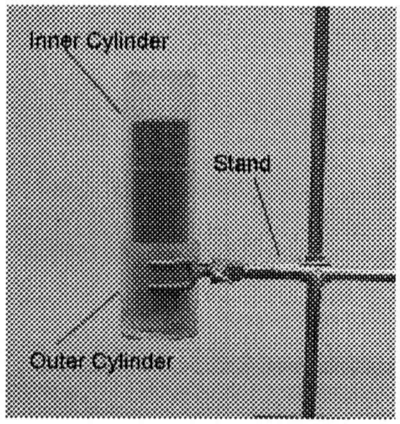

(a)

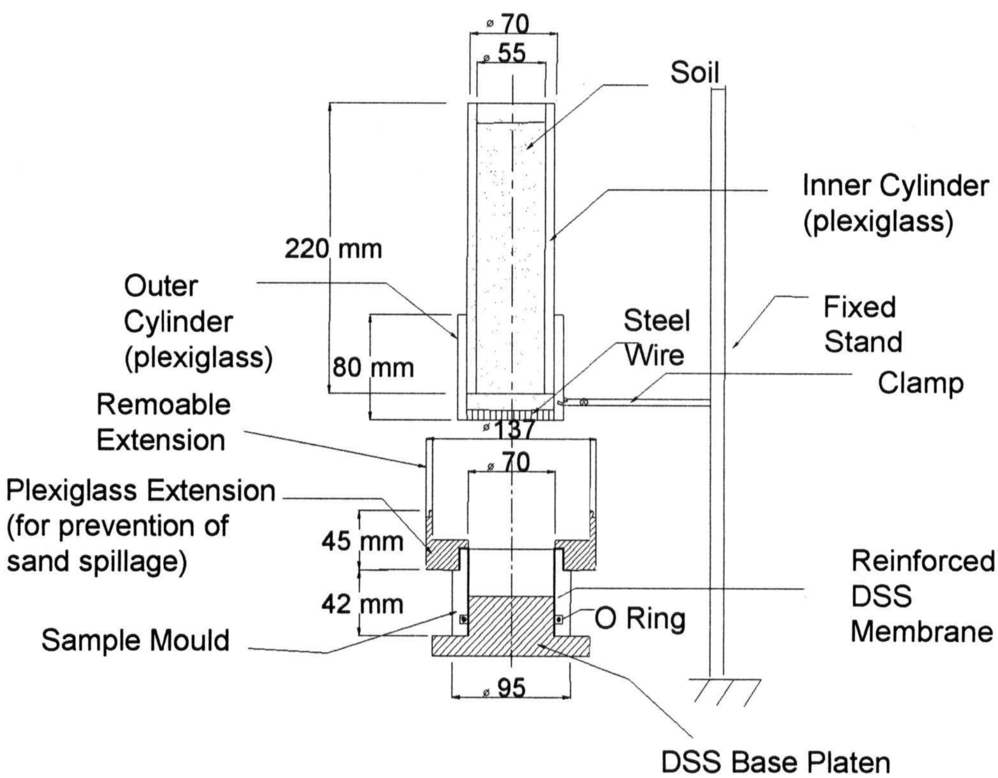

(b)

Figure 3.4 Mechanical details of air-pluviation arrangement.
(a) photograph (b) schematic diagram.

once deposited in the mold, would not be subjected to significant local lateral movements (or internal failures) that could result in changes to the particle structure after initial deposition.

In the air-pluviation process, the inner cylinder is initially filled with Fraser River sand. While holding the raining arrangement stationary, the sand is then allowed to fall freely through the bottom mesh until the sand flow would eventually stop (unassisted) due to the arching of soil across the inner cylinder above the mesh. At this point, the specimen mold is carefully positioned below the pouring arrangement so that their two footprints are aligned. The inner cylinder is then rotated with respect to the outer cylinder causing a breakage of the arching effect, and resumption of the flow of soil. The flow rate could be adjusted by manually controlling the rate of rotation of the inner cylinder. Over 100 air-pluviated specimens of Fraser River sand were made using different combinations of fall heights and flow rates. The characteristic variations of relative density with flow rate and average fall height determined from this work is shown in Figure 3.5.

The results clearly indicate that the as-placed density increases with increasing fall height and decreasing mass flow rate. Similar trends have been observed by Vaid and Negussey (1986) for medium Ottawa sand. The noted increase in placement density with increasing drop height can be explained relatively easily as a result of higher kinetic energy associated with particles dropping over a larger distance. The reason for the noted decrease in as-placed density with increase in mass flow rate is not so readily explained. It may be that with increasing mass flow rate, the opportunity for the expulsion of entrapped air between particles upon landing is more constrained in the case of higher mass flow rates than that possible under lower flow rates. It is possible that this constrained expulsion of entrapped air, and the resulting increased level of energy dissipation, could potentially lead to the observed lower as-placed densities at higher mass flow rates.

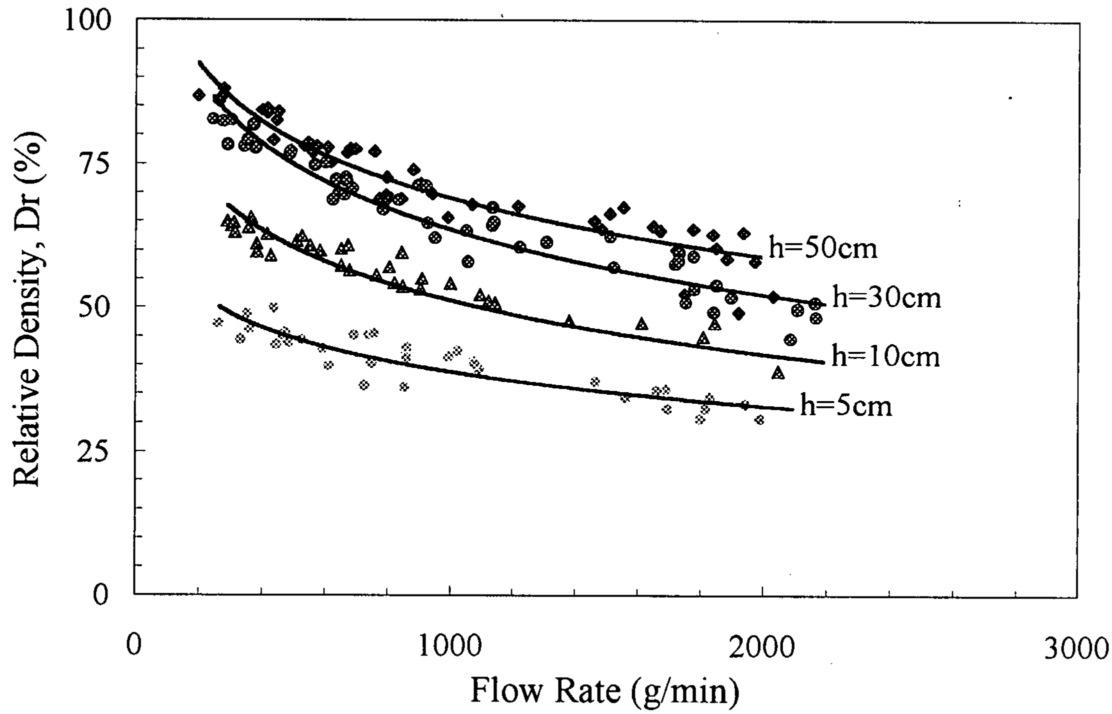

Figure 3.5 Characteristic variation of relative density of air-pluviated Fraser River sand as a function of flow rate and average fall height (h).

The tests described above were carried out with a 1 mm sieve opening. It was identified that the raining of sand for the preparation of centrifuge specimens might also be undertaken using a 2.5 mm sieve that would lead to larger mass flow placement rates than that obtained from the 1 mm sieve size. To allow for this option, the laboratory sand deposition arrangement was modified to have a 2.5 mm screen. Due to the larger sieve size, the arching effect did not manifest across the walls of the plexi-glass cylinders, and as a result, the sand mass flow rate was essentially constant, and an inner cylinder to vary the rate of flow was not required. Since the flow rate is kept constant, the required as-placed density was achieved by selecting the fall height.

3.4 UNIFORMITY OF SOIL SPECIMENS

While considerations related to the particle structure in sample preparation can be addressed partly by the mode of placement, the uniformity of the sample in terms of its density is another important consideration in laboratory testing. In this regard, investigations were undertaken to assess the density variation of the air-pluviated samples prepared using the methods described above.

The uniformity of sand specimens is often assessed using the density of dissected sections obtained from gel-impregnated samples (Emery et al., 1973; Vaid and Negussey, 1986; Vaid et al., 1999). Since the air-pluviated samples are obviously in a dry condition, a simple, but accurate, siphoning technique was developed to "dissect" specimens instead of using more intricate gel-impregnation techniques. The process essentially involved extracting, at a given time, about a 6 mm thickness of the 20 mm-high simple shear sample using a siphoning arrangement (see Figure 3.6). As noted in the figure, a suction of 20 kPa was applied to the siphon tube. The inlet of the siphon tube was then carefully traversed over

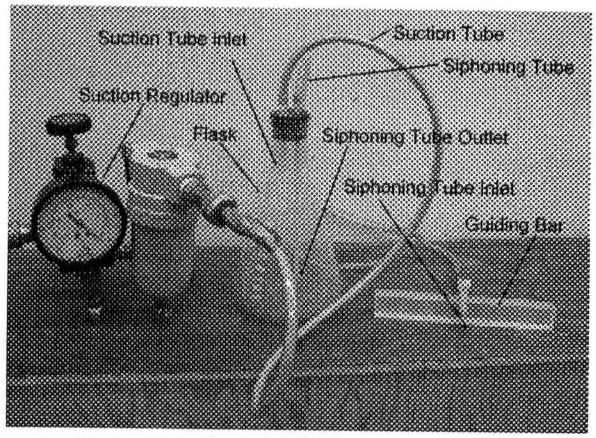

(a)

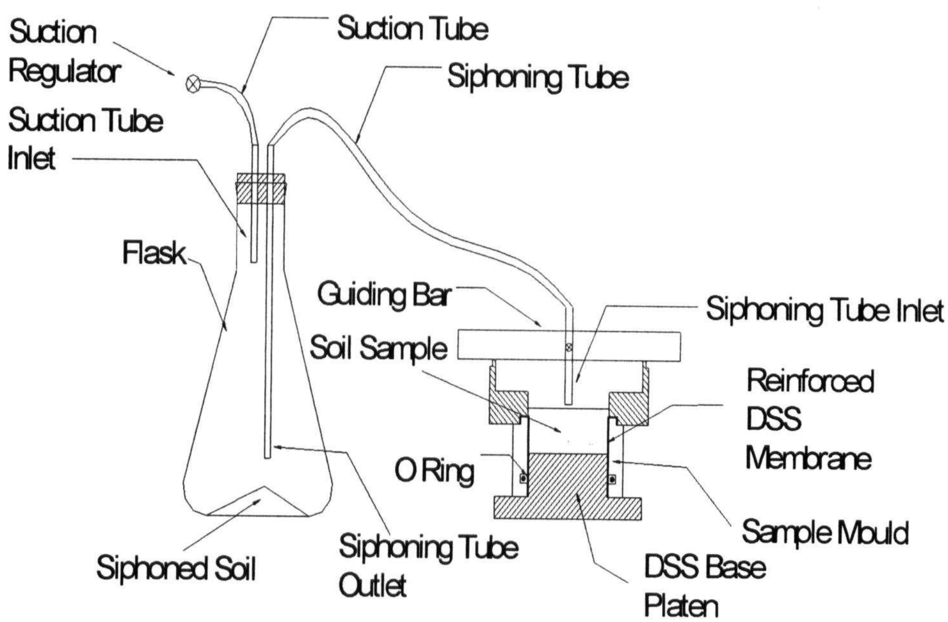

(b)

Figure 3.6 Mechanical details of siphoning arrangement for determination of the uniformity of density in air-pluviated samples. (a) photograph (b) schematic diagram.

the sample, using a guide, so that only the upper soil is removed and a flat surface left on the remaining soil. The height and the weight of each removed portion were recorded, thus enabling calculation of the corresponding in-place relative density. The relative density variation with depth was determined using this approach on a number of samples, and typical results are shown in Figure 3.7.

The results presented in Figure 3.7 indicate that the air-pluviation technique allows the preparation of samples that are relatively uniform, with densities of a given zone deviating not more than ±5% from the corresponding average relative density. Uniformity checks, using gel-impregnation techniques, conducted by Vaid and Negussey (1986) have shown that samples can be prepared using water-pluviation to achieve relative densities within ±3% from the average relative density. On the other hand, samples prepared using moist-tamping seem to have given rise to wide non-uniformities with up to ±10% deviations from the average (Vaid et al., 1999). It is worthwhile noting that, unlike the small 6-mm thick portions considered in the determination of density for the present study, the results reported by Vaid et al. (1999) have been derived using the densities assessed using dissected portions having much larger volumes (i.e. using ~20 mm-thick portions). Due to limitations on the measurement accuracy (of height and mass), the estimated relative density from smaller soil volumes would be more susceptible to scatter than those computed from larger volumes. As such, part of the wider variation of ±5% noted above might be a result of the relatively thin (6 mm) dissections used for the evaluation of air-pluviated samples. The uniformity of density in specimens prepared using the new air-pluviated technique, therefore, was judged to be comparable to those obtained from water-pluviation, and considered acceptable from the point of view of laboratory element testing. Having assessed the

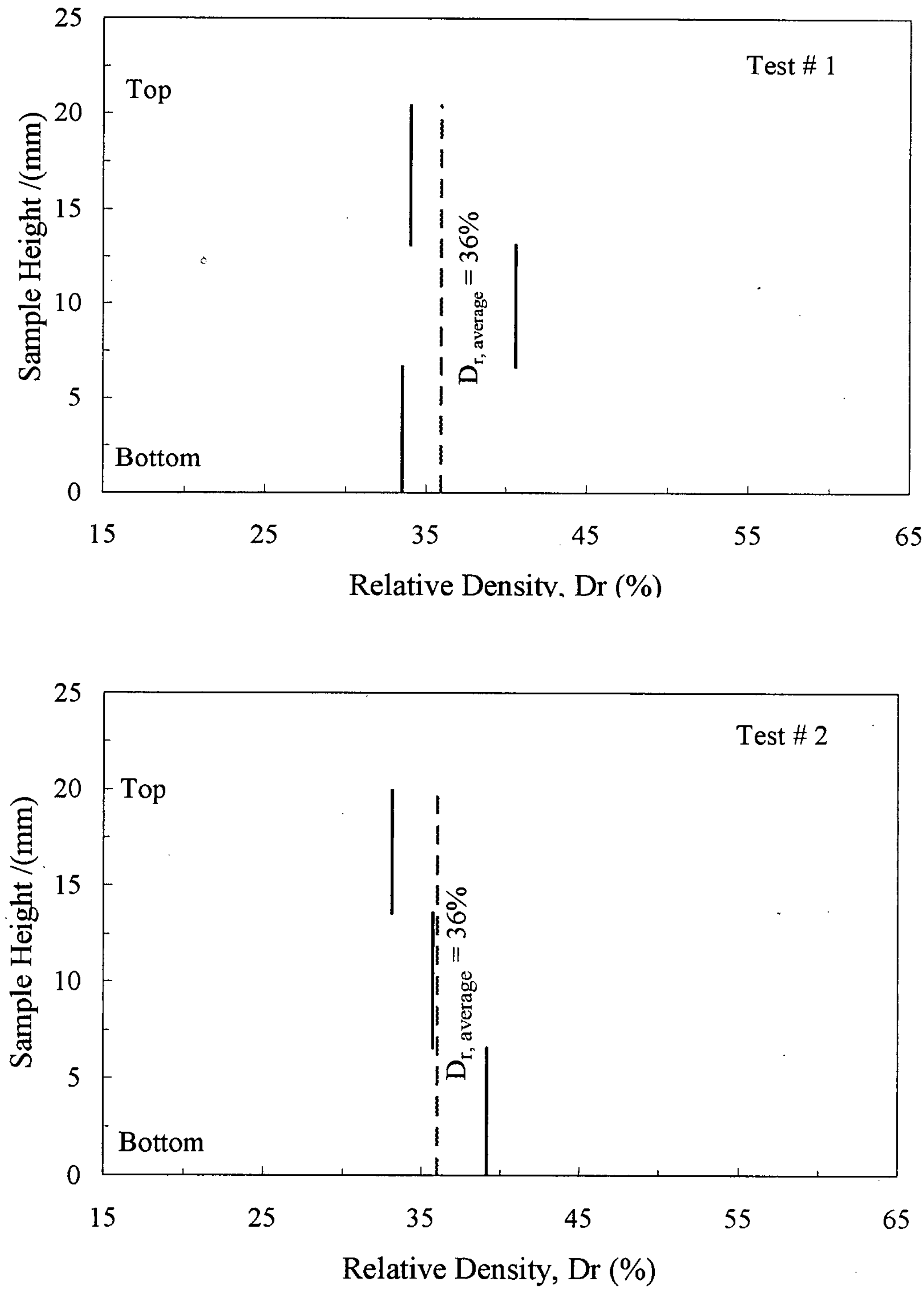

Figure 3.7 Typical variation of relative density demonstrating the uniformity of air-pluviated samples.

acceptability, all samples for the characterization of sands for this research program were prepared using the above air-pluviation methodology and considering the deposition characteristics developed thereof.

3.5 TEST PROCEDURE

3.5.1 Sample Setup

In preparation for air-pluviation, the reinforced rubber membrane was placed in position and the bottom of the rubber membrane was sealed with the bottom pedestal using an o-ring (see Figure 3.1). Then the split mould was kept in position and vacuum was applied to stretch the membrane and create the sample cavity. Soil was deposited from a predetermined height as to obtain sample types as discussed below in this section. Excess soil was siphoned off using the same methodology that have been used to evaluate the uniformity of test specimens (see Figure 3.6).

Three different types of sand samples as defined below were prepared for the testing program presented herein:

3.5.1.1 Type (1) Samples

Type (1) samples were prepared by air-pluviating the sand, using the method described in Section 3.3 (see Figure 3.4). The drop height was selected in such a way to achieve an as-placed relative density of 34% with the intent of achieving a target relative density at the end of consolidation (D_{rc}) of 40% at a vertical confining stress of 100 kPa. After placement of sand, the vertical stress was brought to 20 kPa using the vertical loading system, and the rubber membrane was sealed with the top cap using an o-ring.

It is noted that due to the difference in the applied vertical stress, the samples that were consolidated to σ'_{vc} values of 50 kPa and 200 kPa resulted in samples having D_{rc} = 38% and 44%, respectively. These σ'_{vc} - D_{rc} combinations were specifically chosen since it represented the target loose density of the centrifuge models planned for the validation of numerical models at UBC. The above approach essentially meant that two controlling parameters, σ'_{vc} and D_{rc}, would be allowed to vary simultaneously in "parallel samples" in a given test series; this is somewhat different from the conventional approach in laboratory research where the effects arising from only one influencing factor are generally isolated by varying only that factor during a given test series. However, this atypical approach was considered essential herein since integral capturing of the stress densification effects on the response of sand was a necessity to generate data for the simulation of centrifuge tests.

3.5.1.2 Type (2) Samples

Type (2) samples were prepared by initially, air-pluviating the sand into the mold same as per Type (1) samples and then, manually tamping on the sample surface using a "plunger-type" tamper that has a footprint essentially similar to the sample size, but with a small 2° vertical tapering. The tapering was needed to eliminate the frictional resistance between the tamper and reinforced membrane during the tamping process. Upon completion of tamping to achieve a relative density of 77%, a confining stress of ~10 kPa was applied to the sample using the vertical loading system, and then sample mold was given a small amount of external tapping using a soft hammer to ensure proper seating. This further densified the sample and increased the relative density to 79%. The samples prepared as above reached a target relative density of 80% at a confining stress of 100 kPa. Again, samples that were consolidated to other confining stresses resulted in different densities due to stress densification. For example, samples with 200 kPa had a relative density of 81%.

3.5.1.3 Type (3) Samples

The effect of imparted vibration during sample preparation on the stress strain response of sand were investigated using a limited number of samples prepared using an approach slightly different from the above methods (Type (3) Samples). In this instance, the sand was initially deposited into the sample cavity formed by the membrane lined split mould essentially with no drop height. This was achieved by placing a 2.5 mm square steel wire mesh at the bottom of the split mold and then placing sand using a funnel maintained at almost zero fall height. Upon filling the cavity of the mold, the wire mesh was retracted in a slow and gentle manner. This enabled the sand to pass through the mesh essentially at zero height of drop and, in turn, to reconstitute a uniform air-pluviated sample with an initial relative density of 7%. The sample was then densified to a relative density of 36% by gentle tapping using a soft hammer while being subjected to a 10 kPa effective stress from the vertical loading system. The sample prepared as above eventually reached a relative density of 40% at a confining stress of 100 kPa.

3.5.1.4 Final Setup

All the transducers were properly positioned and initial outputs were set to their zero values, and readings were taken as appropriate during all the sample preparation steps. All vertical load applications were done gently to avoid sudden impacts and possible disturbance. Finally, the horizontal loading system was connected with the top pedestal and the vacuum, split mould and horizontal locator pin, which was used to hold the top pedestal in place were subsequently removed. During this final set up period, the transducer readings were monitored to assess and confirm that no undesirable movements or loads were imparted.

3.5.2 Consolidation Phase

After completion of sample setup, the vertical confining stress was increased to the target value corresponding to a given test. In the case of tests with initial static shear stress, a shear stress was also applied manually using the horizontal loading piston (see Figure 3.1). The volume change during the consolidation phase with respect to time was recorded using the data acquisition system. The primary consolidation process for sand was almost instantaneous. The samples were then kept at their consolidation stress conditions for 30 minutes in order to allow for same aging effects that would be anticipated in the centrifuge model. (Note: An aging time of 30 minutes was considered suitable based on discussions that were made with the centrifuge testing experts)

3.5.3 Shearing Phase

Upon completion of the consolidation phase, the vertical displacement constraint was set to meet the requirements of a given test. For example, in the case of constant volume tests, the ram of the vertical loading piston was clamped so that there would not be any change of sample height during the shearing process. On the other hand, for drained tests, this loading ram was allowed to move freely under the applied vertical consolidation stress. The monitored value of the vertical load cell allowed the estimate of σ_v' at a given time during a constant-volume DSS tests. In drained tests, the volume changes were obtained from vertical displacement measurements.

As indicated earlier, the horizontal shear loading was applied either using double acting piston or constant speed motor depending on whether the test was stress-controlled or strain-controlled, respectively. In stress-controlled constant-volume cyclic tests, the loading was applied in the form of a sinusoidal wave with a frequency of 0.1 Hz. Even though this frequency is less than the frequency content of typical earthquake loadings, it enabled a better control of loading as well as data acquisition. The undrained behaviour of sand is known to be essentially frequency independent; therefore, this approach is commonly adopted as reasonable in laboratory cyclic loading of soils. Strain-controlled cyclic loading drained tests were conducted by applying the cyclic loading at strain rates of 10% or 20% strain per hour, and strain-controlled monotonic tests were conducted at a strain rate of 10% strain per hour. The selection of low strain rates, again, enabled well-controlled tests with reliable measurements.

All the cyclic tests except the tests that were carried out to study the repeated cyclic response of sand were terminated once the sample reached significantly large deformations (~10% horizontal shear strain for constant-volume tests) or the required number of cycles (for drained tests). On the other hand, the cyclic tests that were carried out to study the repeated cyclic response of sand (see next section) were terminated once the sample reached the target r_u value. All the monotonic loading tests were conducted up to a horizontal shear strain level of ~6%.

3.5.4 Re-consolidation and Re-shearing Phases

After completion of the cyclic loading phase of undrained/constant volume cyclic loading tests, samples were re-consolidated to the initial confining stresses to obtain an indication of the potential post liquefaction, or post-cyclic volume changes. Since the samples generally had a residual shear strain at the end of a given cyclic loading, before re-consolidation, the samples were manually reset in a strain-controlled manner to reach approximately zero shear stress and strain level.

In those tests where the repeated cyclic shear response was sought, the samples re-consolidated as above were again sheared in cyclic loading and re-consolidated as needed before. In some tests, this process was repeated until a third round of cyclic loading.

3.6 REPEATABILITY OF THE TEST RESULTS

The ability to obtain repeatable results is an important consideration in affirming confidence in an experimental program. Repeatability of results from a given type of test indicates the suitability of the technique of sample preparation in terms of replicating sample uniformity, density and soil structure/fabric. It also confirms the quality of the loading and measuring systems in terms of their measuring accuracy, and the ability to duplicate loading paths. Typical results from repeated testing of samples in cyclic shear are shown in Figures 3.8 and 3.9. Figure 3.8 shows the repeatability in stress-controlled constant volume cyclic loading tests, and Figure 3.9 shows that for the strain-controlled drained cyclic loading tests. The observed very good repeatability illustrate the care taken during sample preparation, in addition to the quality of the techniques of preparation, loading, and data acquisition.

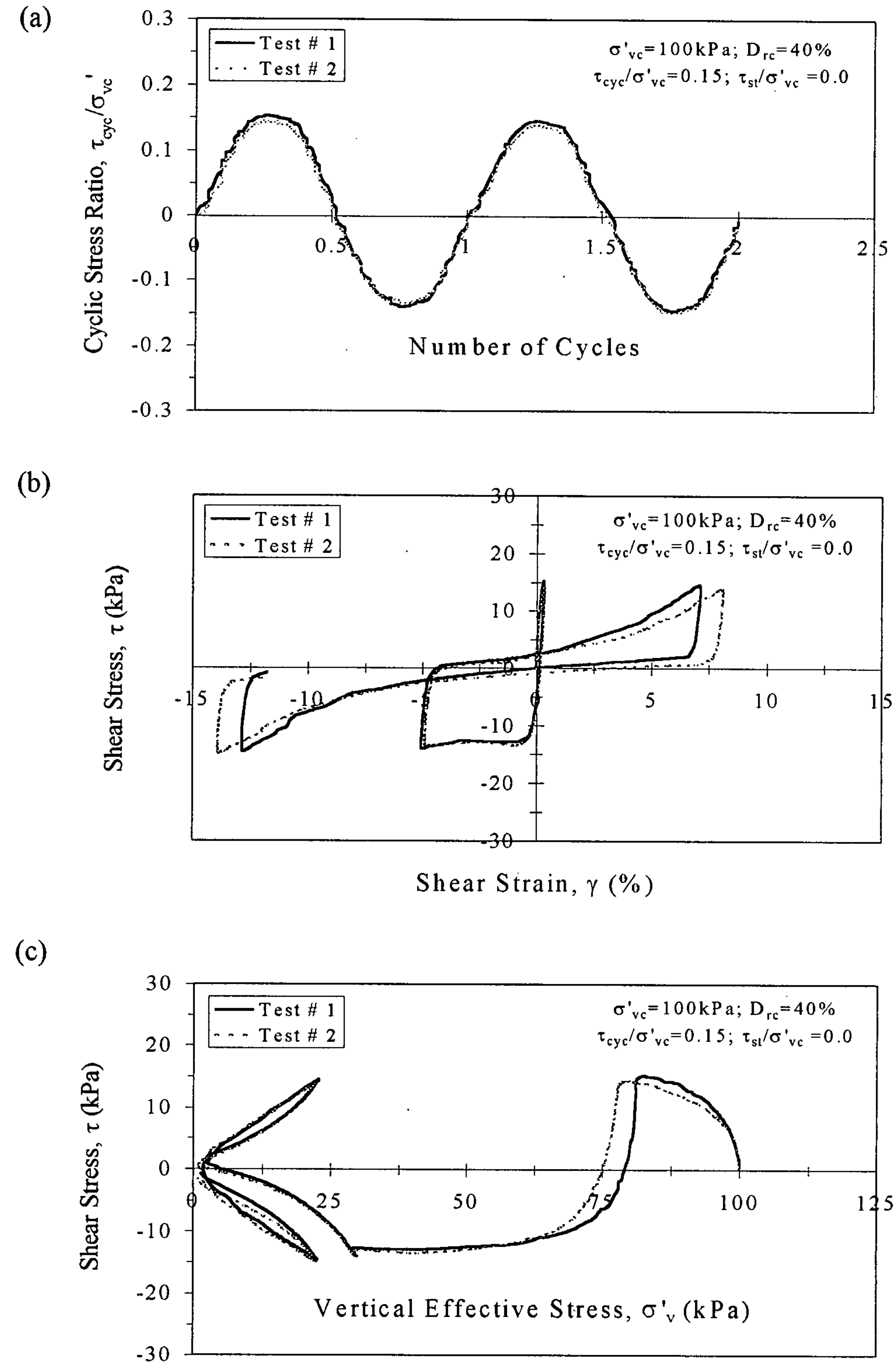

Figure 3.8 Typical results showing repeatability in undrained cyclic response of sand.

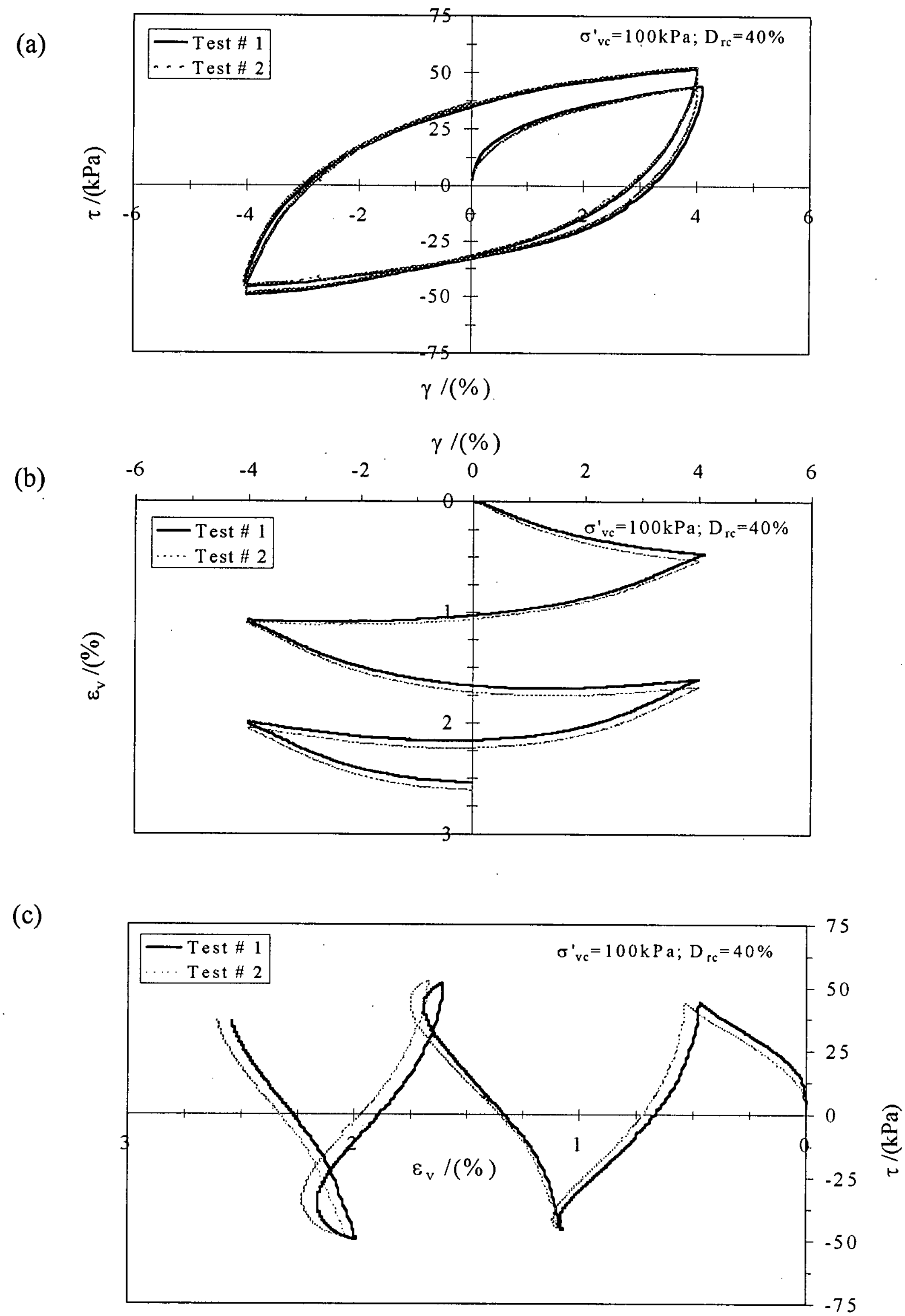

Figure 3.9 Typical results showing repeatability in drained cyclic response of sand.

3.7 TEST PROGRAM

A testing program was developed with the main objective of characterizing the fundamental cyclic loading response of air-pluviated Fraser River sand. The stress and density conditions of the samples, and loading parameters were selected so as to provide input to verification of numerical models conducted at UBC. The research program has six main components as described below.

3.7.1 Characterization of Undrained Cyclic Loading Response of Loose Fraser River Sand (Type (1) Samples)

A series of cyclic loading tests were carried out on loose air-pluviated {Type (1) samples as described in Section 3.5.1.1} Fraser River sand in constant volume simple shear conditions, and the test program is summarized in Table 3.2. Most of the tests were conducted to explore the response at two vertical confining stress (σ'_{vc}) levels, 100, and 200 kPa, with the exception of some additional tests performed at σ'_{vc} = 50 kPa with no static shear stress bias. Consolidation shear/normal stress levels and cyclic stress ratios were selected in such a way to capture a combination of loading scenarios and initial stress conditions (e.g. with shear stress reversal, without shear stress reversal and transient zero shear stress condition). As indicated in Section 3.5.1.1, due to the difference in the applied vertical stress, the samples that were consolidated to σ'_{vc} values of 50 kPa and 200 kPa resulted in samples having D_{rc} = 38% and 44%, respectively.

3.7.2 Characterization of Undrained Cyclic Loading Response of Dense Fraser River Sand (Type (2) Samples)

Table 3.3 summarizes the cyclic loading tests conducted on dense {Type (2) samples as described in Section 3.5.1.2} Fraser River sand under constant-volume simple shear conditions. Tests were performed to explore the response of the sand without initial static bias at two vertical confining stress (σ'_{vc}) levels, 100, and 200 kPa. All the samples were prepared with a target relative density of 80%. The samples that were tested with a confining stress of 200 kPa had their relative density (D_{rc}) increased to 81% due to stress densification. An additional set of tests was conducted to study the response with initial static bias with stress reversal at a vertical confining stress of 100 kPa.

3.7.3 Characterization of Drained Cyclic Loading Response of Loose Fraser River Sand (Type (1) Samples)

DSS tests were also carried out on loose air-pluviated {Type (1) samples} Fraser River sand to make direct observation on the cyclic shear-volume coupling response (see Table 3.4). The tests were conducted on samples with an initial relative density of 40% and vertical confining stress of 100 kPa. Samples were sheared with constant cyclic shear strain amplitudes (γ_{max}) for a range of γ_{max} values from 2% to 8%.

3.7.4 Characterization of Drained Cyclic Loading Response of Dense Fraser River Sand (Type (2) Sample)

A DSS test was carried out on dense {Type (2) Sample} Fraser River sand to make direct observation on the cyclic shear-volume coupling response (see Table 3.4). The test was conducted on samples with an initial relative density of 80% and vertical confining stress of 100 kPa. Sample was sheared with a constant cyclic shear strain amplitude (γ_{max}) of 4%.

3.7.5 Characterization of Repeated Cyclic Loading Response of Loose Fraser River Sand (Type (1) Samples)

A limited numbers of cyclic loading constant-volume simple shear tests were carried out to study the multiple cyclic loading response of loose {Type (1) samples} Fraser River sand (see Table 3.5). Tests were carried out on loose samples with a relative density of ~40% at a confining stress of 100 kPa. Cyclic loading was stopped at predetermined pore water pressure ratio levels, and the samples were then subjected to re-consolidation to the original 100 kPa stress level and subsequent shearing. As may be noted from Table 3.5, some of the samples were re-consolidated upon the completion of second cyclic loading and again subjected to another round of cyclic loading. In order to assist the presentation of results and discussion in Section 4.1.4, the cyclic loading phases have been identified using different test numbers as shown in Table 3.5.

3.7.6 Monotonic Loading Response of Loose Fraser River Sand

A monotonic constant-volume simple shear test was also undertaken on Type (1) sample. Another sample was prepared to achieve the same density as Type (1) sample when subjected to σ_{vc}' = 100 kPa, except it was a Type (3) sample as described as in Section 3.5.1.3. The later test allowed observing the effect of imparted vibrations during sample preparation on stress strain response of sand and, in turn, assessing the inherent fabric differences between Type (1) and Type (3) samples (see Table 3.6).

Table 3.2 Summary of constant-volume stress-controlled cyclic simple shear tests on loose Fraser River sand {Type (1)}.

Test Series No.	Initial Vertical Consolidation Pressure σ'_{vc} (kPa)	Relative Density $D_{rc\,(\%)}$	Static Shear Stress Ratio (τ_{st}/σ'_{vc})	Cyclic Shear Stress Ratio (τ_{cyc}/σ'_{vc})
A1	50	38	0	0.08, 0.10, 0.12
B1	100	40	0	0.08, 0.10, 0.12, 0.15
B2			0.10	0.65, 0.08, 0.10
B3			0.05	0.10
C1	200	44	0	0.08, 0.10, 0.12, 0.15
C2			0.10	0.60, 0.08, 0.10
C3			0.05	0.10

Table 3.3 Summary of constant-volume stress-controlled cyclic simple shear tests on dense Fraser River sand {Type (2)}.

Test Series No.	Initial Vertical Consolidation Pressure σ'_{vc} (kPa)	Relative Density $D_{rc\,(\%)}$	Static Shear Stress Ratio (τ_{st}/σ'_{vc})	Cyclic Stress Ratio (τ_{cyc}/σ'_{vc})
E1	100	80	0	0.25, 0.30, 0.35
E2			0.1	0.35, 0.40, 0.45
F1	200	81	0	0.20, 0.25, 0.30

Table 3.4 Summary of strain-controlled drained cyclic simple shear tests on Fraser River sand.

Test Series No.	Initial Vertical Consolidation Pressure σ'_{vc} (kPa)	Relative Density $D_{rc\,(\%)}$	Sample Type	Strain Rate (%strain/hrs)	Cyclic Shear Strain Amplitude γ_{max} (%)
G1	100	40	(1)	10	2, 4, 5, 8
G2				20	2, 8
H1		80	(2)	20	4

Table 3.5 Summary of cyclic constant-volume simple shear tests to study repeated cyclic loading response of loose Fraser River sand {Type (1)}.

Sample No.	Initial Relative Density D_{rc} (%)}	Cyclic Loading	Cyclic Loading Phase No.	Pore Water Pressure Ratio at which Cyclic Loading was terminated (%)
R1	41	1st	R11	100
		2nd	R12	100
R2	41	1st	R21	46
		2nd	R22	100
R3	41	1st	R31	88
		2nd	R32	100
R4	40	1st	R41	100
		2nd	R42	100
		3rd	R43	100
R5	40	1st	R51	54
		2nd	R52	100
		3rd	R53	100

Table 3.6 Summary of strain-controlled monotonic undrained simple shear tests.

Initial Vertical Consolidation Pressure σ'_{vc} (kPa)	Relative Density D_{rc} (%)	Strain Rate (%strain/hrs)	Sample Type	Sample Preparation Method
100	40	10	(1)	Air-Pluviation
			(3)	Air-Pluviation with external tapping

CHAPTER 4

RESULTS AND DISCUSSION

This chapter presents a detailed examination of the results obtained for the test program outlined in Chapter 3. Initially, the results from the monotonic constant-volume (undrained) direct simple shear tests conducted on loose air-pluviated Fraser River sand is presented. The observed response from cyclic constant-volume direct simple shear tests on loose samples, with different initial stress conditions, are then presented and discussed. The observations on the repeated cyclic loading response of loose air-pluviated Fraser River sand are evaluated. The observed response from cyclic constant-volume direct simple shear tests on dense samples, with different initial stress conditions, are then presented and discussed. This is followed by the results from drained cyclic simple shear tests. Differences in soil fabric due to the imparted vibrations during sample preparation are inferred based on monotonic tests.

4.1 UNDRAINED RESPONSE OF LOOSE FRASER RIVER SAND

4.1.1 Monotonic Loading Response

Figure 4.1 presents the stress path and stress-strain response from a constant-volume, monotonic, strain-controlled DSS test on loose air-pluviated Fraser River sand (Type (1)

(a)

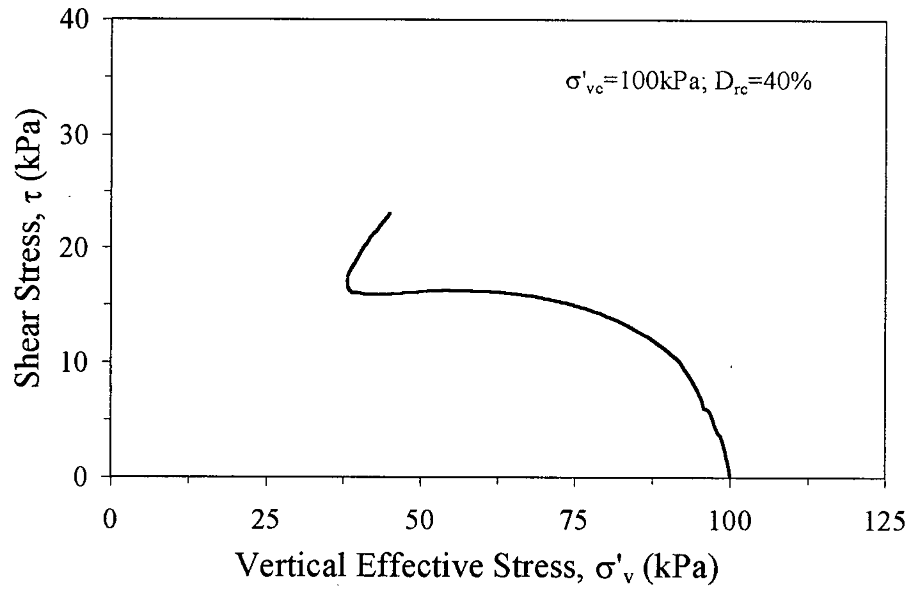

(b)

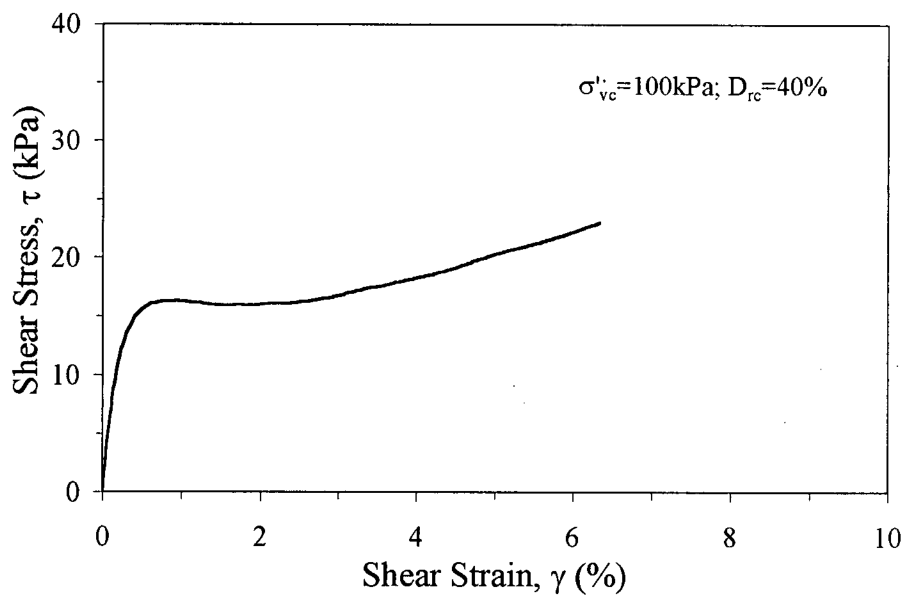

Figure 4.1 Monotonic (a) stress path and (b) stress-strain response of loose air-pluviated Fraser River sand.

sample) consolidated to a vertical stress (σ'_{vc}) of 100 kPa (D_{rc} = 40%). Under this static loading, the sample deformed with a slight strain-softening response, which was then followed by a strain-hardening response. This behaviour is essentially similar to the response described as "limited liquefaction" type by Isihara et al. (1975), Vaid and Chern (1985), Vaid and Thomas (1995), and Vaid et al. (2001) based on observations mainly from cyclic undrained tests conducted on water-pluviated sands.

4.1.2 Cyclic Loading Response – Without Initial Static Shear Stress Bias

Figures 4.2 through 4.5 present the response of Type (1) sand during cyclic DSS loading of samples, consolidated to σ'_{vc} = 100 kPa and D_{rc} = 40%, without application of initial static shear stress (i.e. τ_{st} = 0) as per Series B1 (Table 3.2). As may be noted, the points of liquefaction, defined as the point of γ = 3.75%, is also identified. For example, the test depicted in Figure 4.2 (Sample L1) was loaded with a cyclic stress ratio (τ_{cyc} / σ'_{vc}) of 0.08 (Note: τ_{cyc} = cyclic shear stress amplitude). The sample exhibited significant drop in σ'_{vc} (or rise in pore water pressure) with increasing number of cycles, with liquefaction triggering in about the 18th cycle [Note: As discussed earlier, decrease of vertical stress in a constant-volume DSS test is essentially equal to the increase of pore water pressure in an undrained DSS test]. Figure 4.5 shows the response of Sample L4, which was loaded with a cyclic stress ratio of 0.15. This sample, having subjected to more severe cyclic loading than Sample L1, reached liquefaction in a relatively smaller number of cycles with deformations occurring in a strain-softening manner. Upon liquefaction, both the specimens experienced transient $\sigma'_{vc} \sim 0$ conditions (or excess pore water pressure ratios amounting to ~100%) when

(a)

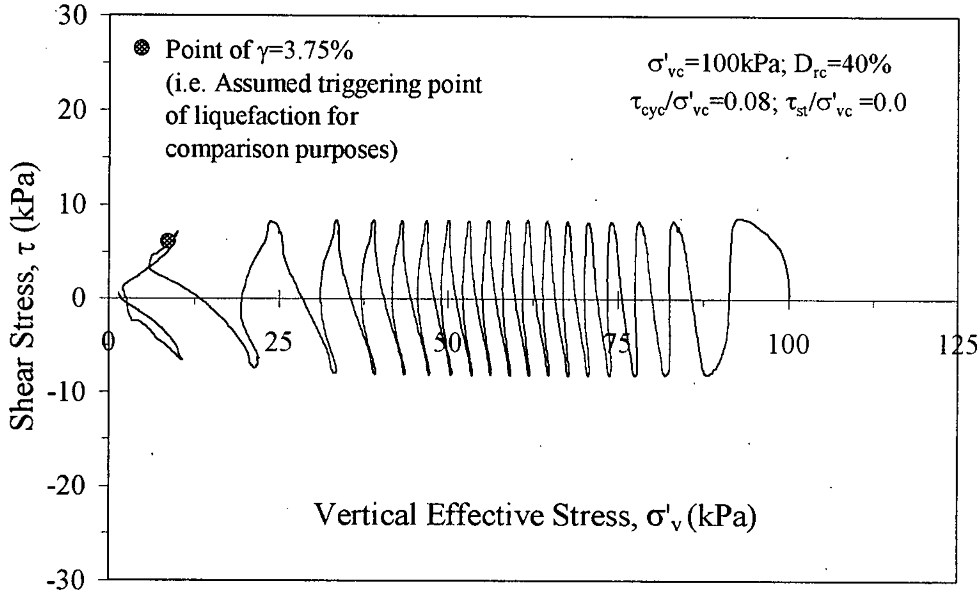

(b)

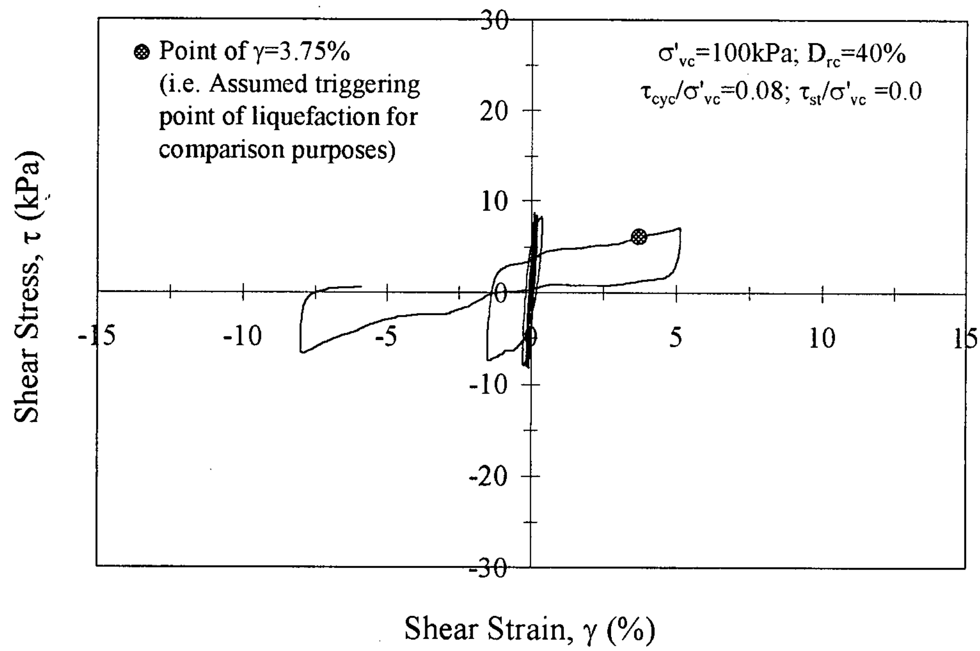

Figure 4.2 Cyclic (a) stress path and (b) stress-strain response of loose sand without initial static shear stress – Sample L1.

(a)

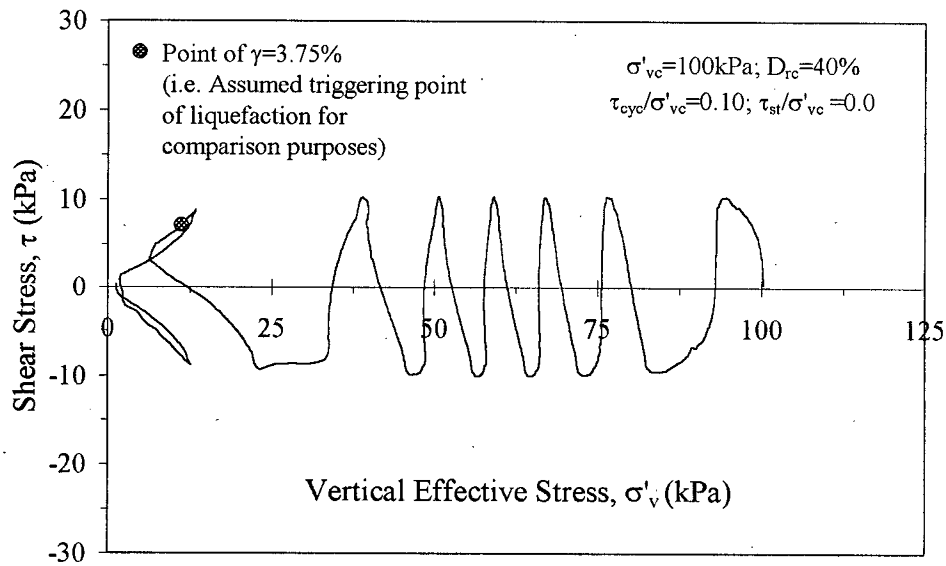

(b)

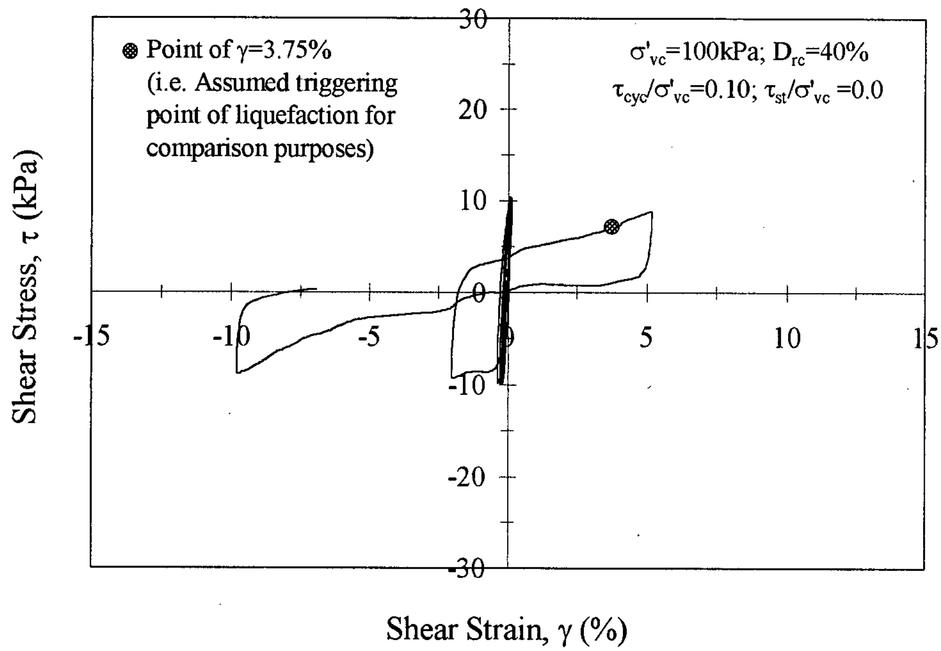

Figure 4.3 Cyclic (a) stress path and (b) stress-strain response of loose sand without initial static shear stress – Sample L2.

(a)

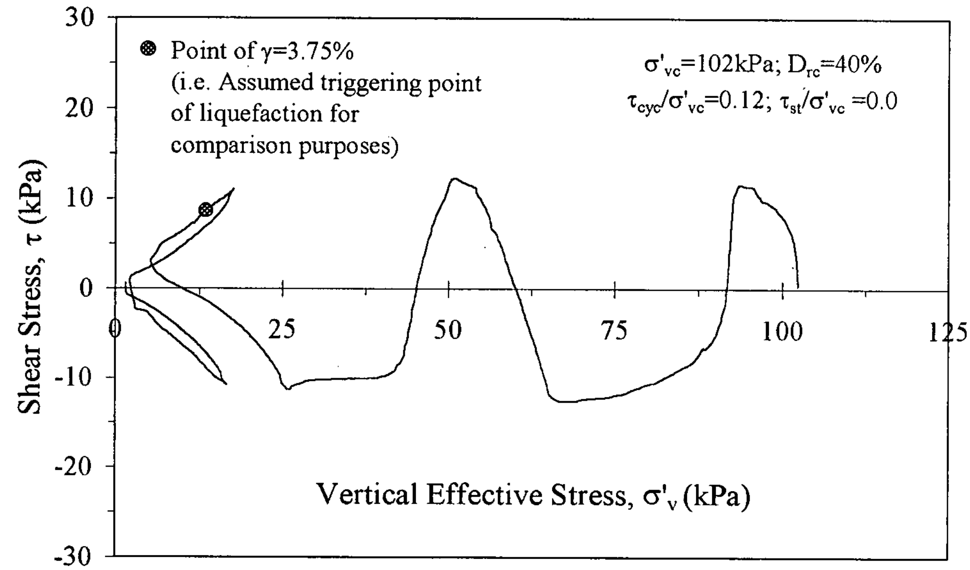

(b)

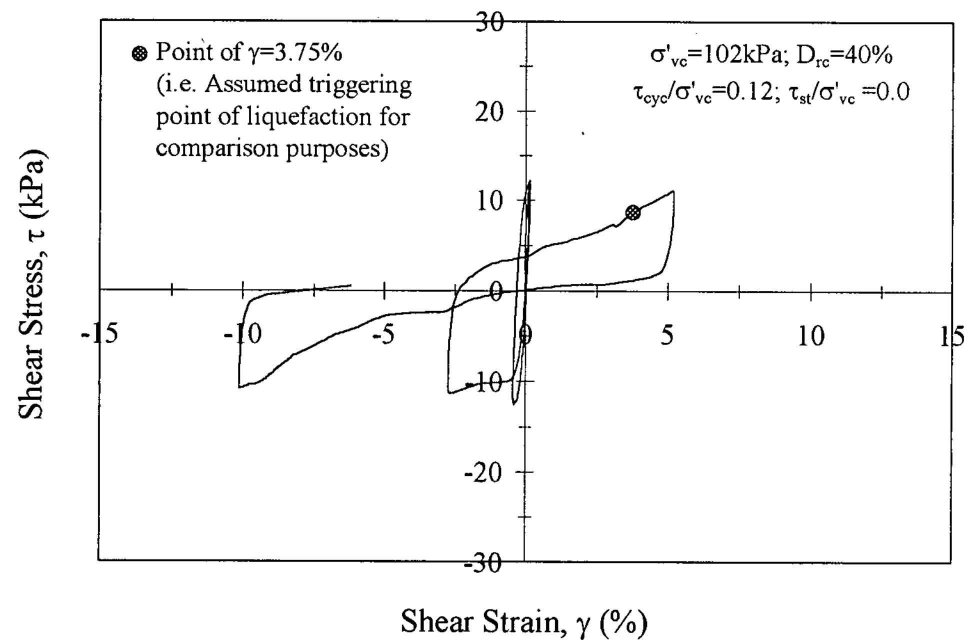

Figure 4.4 Cyclic (a) stress path and (b) stress-strain response of loose sand without initial static shear stress – Sample L3.

(a)

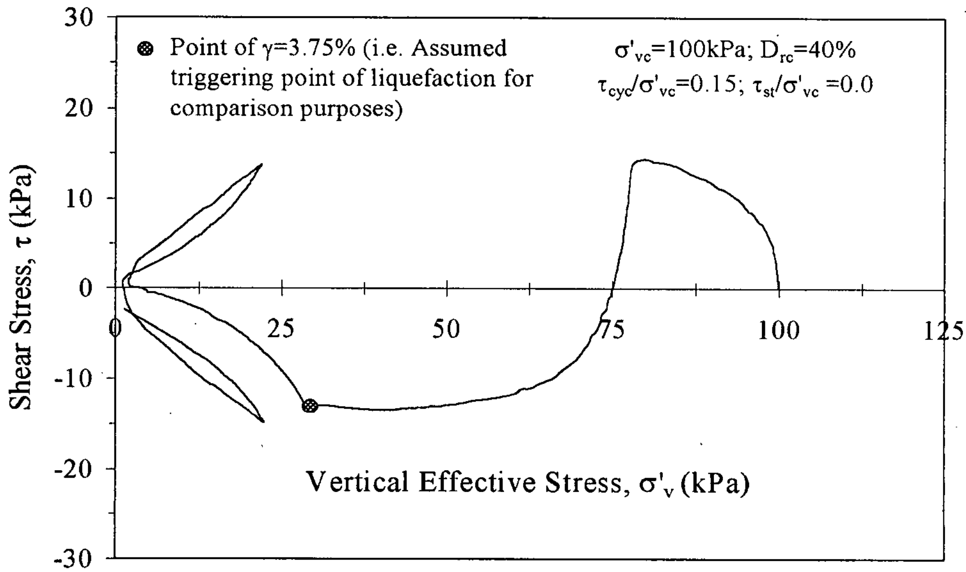

(b)

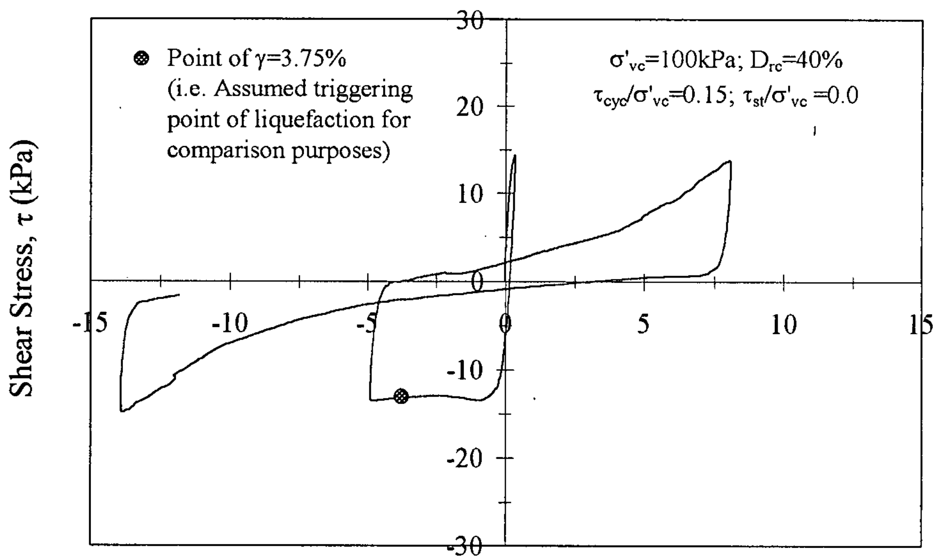

Figure 4.5 Cyclic (a) stress path and (b) stress-strain response of loose sand without initial static shear stress – Sample L4.

the shear stress reached a value of zero during cyclic loading. Similar responses can be noted for test results presented in Figures 4.3 and 4.4. The observed trends of stress-strain and pore water pressure development under cyclic loading discussed above are generally similar to those noted by others (Chern, 1985; Vaid and Chern, 1985; Thomas, 1992; Sivathayalan, 1994) from tests on water-pluviated loose sand.

4.1.2.1 Air-Pluviated Samples Vs Water Pluviated Samples

Curve I in Figure 4.6 shows the variation of applied cyclic stress ratio (τ_{cyc}/σ'_{vc}) versus number of cycles required to trigger liquefaction (N_L) developed from DSS tests on four identical samples (Samples L1 through L4) of air-pluviated Fraser River sand having D_{rc} = 40% (or void ratio e_c = 0.812) under a vertical stress of σ'_{vc} = 100 kPa. The results obtained by Sivathayalan (1994) for water-pluviated Fraser River sand for two void ratio levels (Curves II and III) using the same DSS device are also superimposed on the same plot. The Fraser River sand used in the current study was different from the batch used by Sivathayalan (1994), and the minimum and maximum void ratios (e_{max} and e_{min}) determined using ASTM standards for the two batches were also found to be different. The value of D_{rc} = 40% referred to in Curve II has been calculated with respect to e_{max} and e_{min} used by Sivathayalan (1994), and, as a result, it has a void ratio different from that corresponding to the samples having a D_{rc} = 40% as per e_{max} and e_{min} of the current study. On the other hand, the Curve III corresponds to tests conducted by Sivathayalan for samples having a void ratio at the end of consolidation e_c = 0.81, which is identical to the void ratio of samples having D_{rc} = 40% shown in Curve I from the current study.

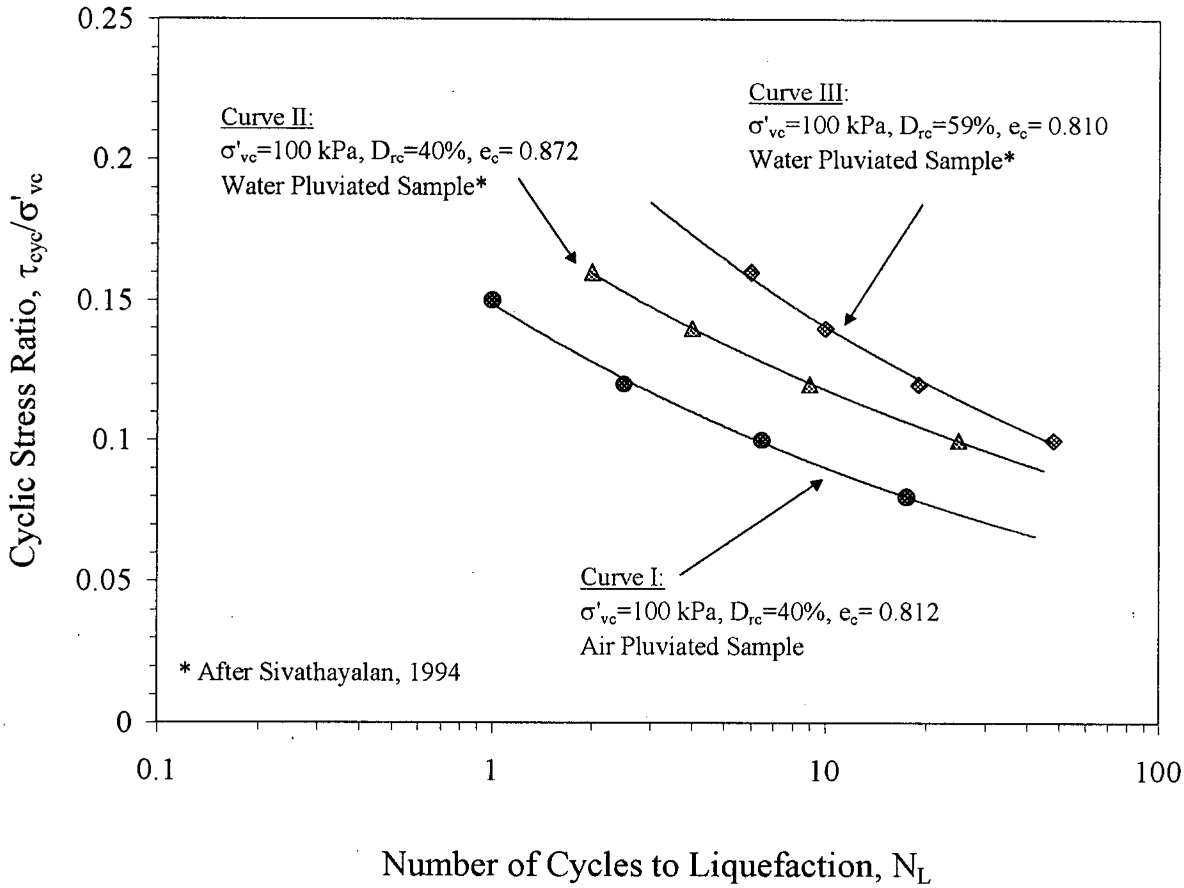

Figure 4.6 Comparison of cyclic resistance curves for loose air-pluviated and water-pluviated sands.

The results in Curves I through III indicate that, regardless of whether the comparison is made with respect to samples having same void ratio e_c or same relative density D_{rc} at the end of consolidation, the air-pluviated samples are significantly weaker in resisting cyclic loads in comparison to their water-pluviated counterparts. These findings from cyclic loading further corroborate the increased liquefaction susceptibility of air-pluviated sands in comparison to water-pluviated sands previously observed by others from undrained monotonic loading tests. The difference in liquefaction susceptibility can be attributed to differences in the particle structure resulting from the two methods of sample re-constitution. In summary, these findings show the importance and relevance of particle structure in governing the liquefaction response of sands in addition to relative density (or void ratio) and level of confining stress that are commonly considered as primary controlling parameters.

4.1.2.2 Influence of Vertical Confining Stress and Effect of Stress Densification on the Cyclic Loading Response of Sand

Figures 4.7 through 4.10 present the response of Type (1) sand during cyclic DSS loading of samples, consolidated to σ'_{vc} = 200 kPa and D_{rc} = 44%, without application of initial static shear stress (i.e. τ_{st} = 0) as per Series C1 (Table 3.2), and that presented in Figures 4.11 through 4.13 are for the samples, consolidated to σ'_{vc} = 50 kPa and D_{rc} = 38%, without application of initial static shear stress (i.e. τ_{st} = 0) as per series A1 (Table 3.2). The tests were aimed at assessing the effect of vertical confining stress and stress densification in an integral manner. All the samples showed similar type of stress-strain response as the results presented for Series B1 at the beginning of this section.

(a)

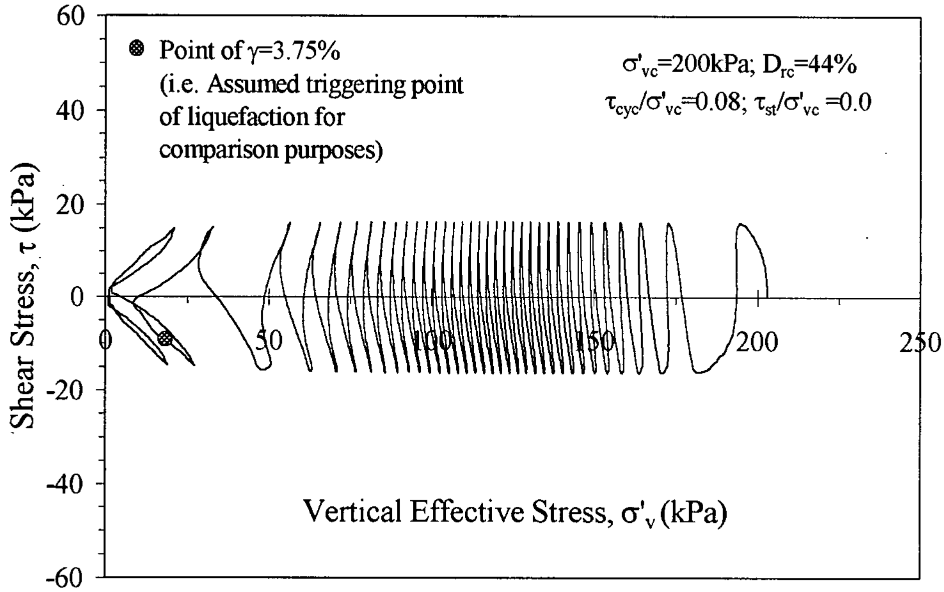

(b)

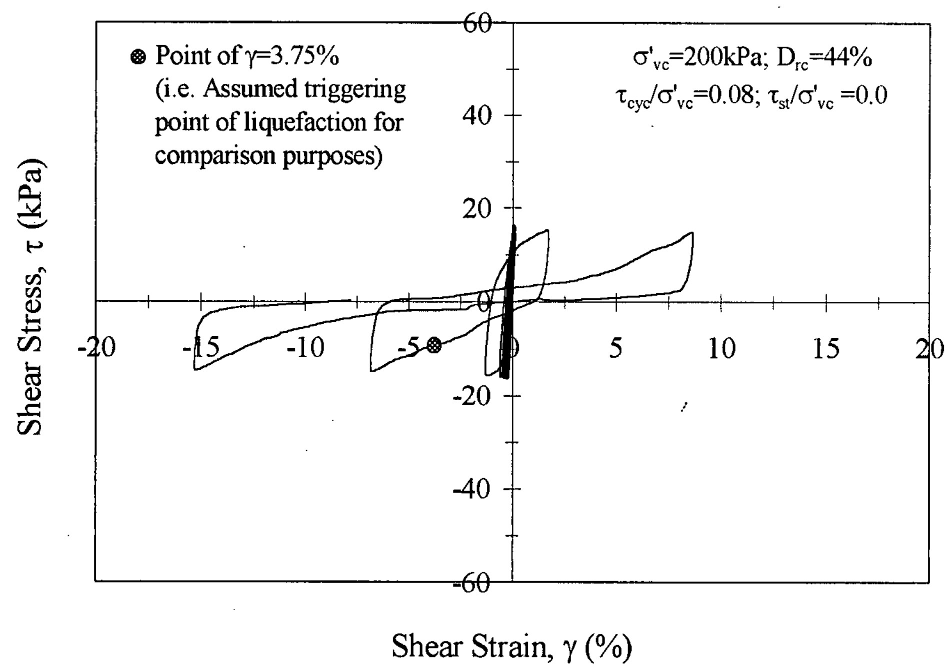

Figure 4.7 Cyclic (a) stress path and (b) stress-strain response of loose sand without initial static shear stress – Sample L5.

(a)

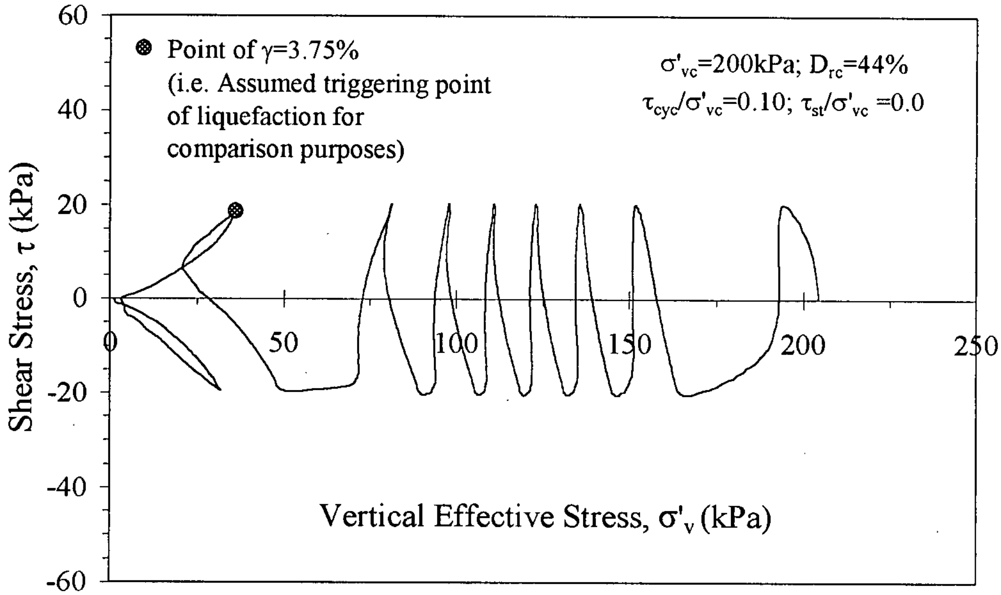

(b)

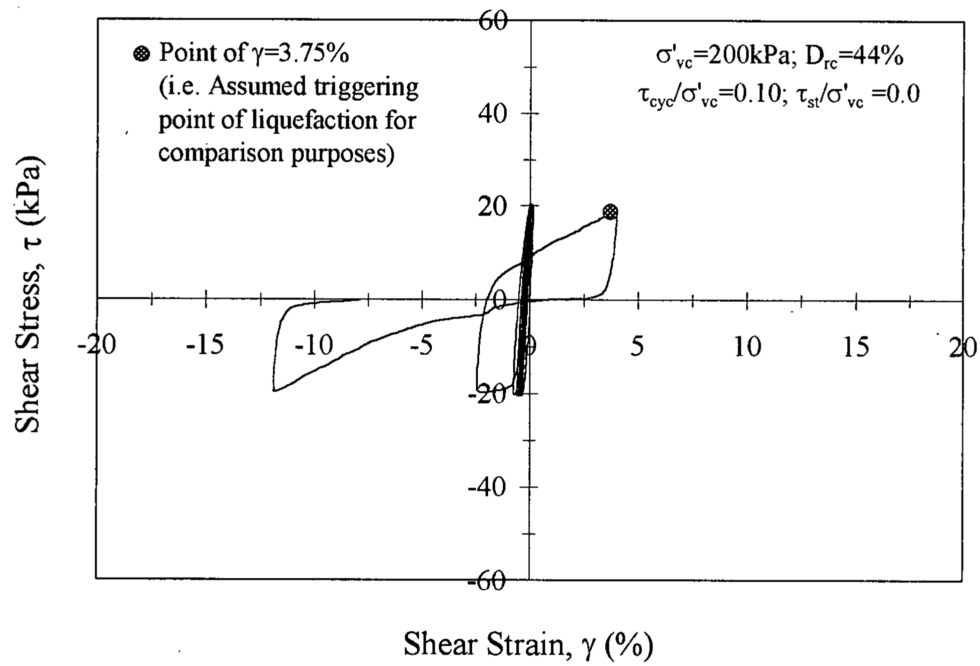

Figure 4.8 Cyclic (a) stress path and (b) stress-strain response of loose sand without initial static shear stress – Sample L6.

(a)

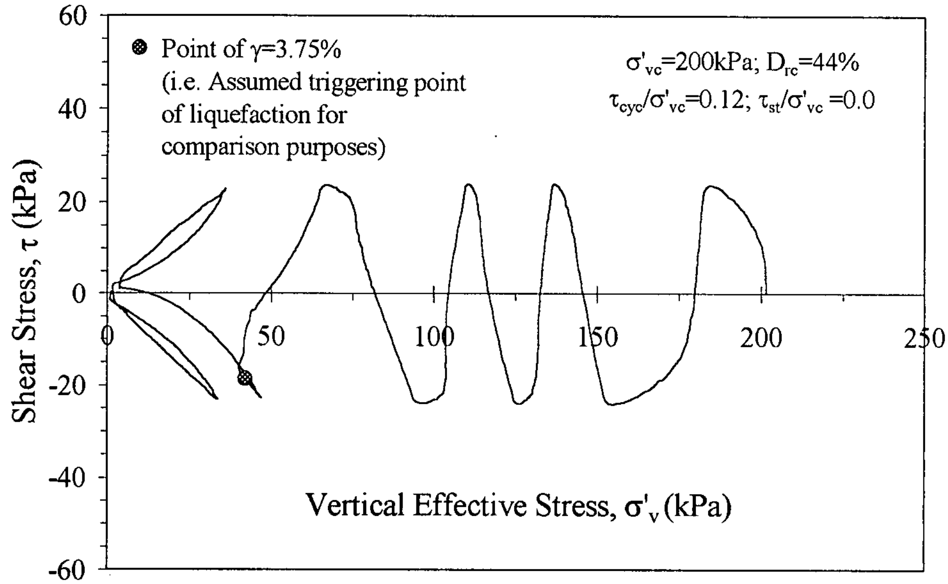

(b)

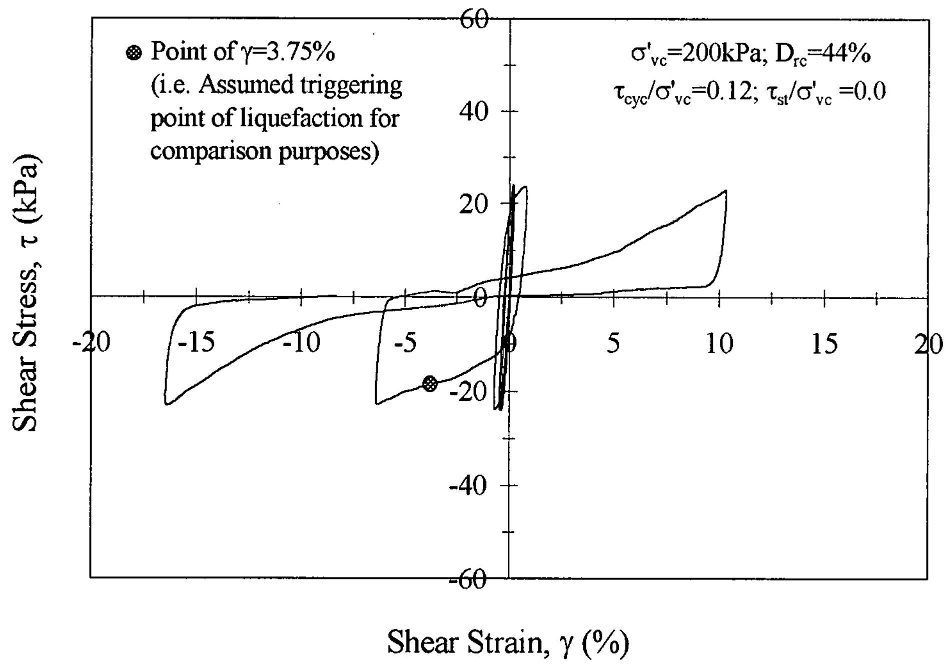

Figure 4.9 Cyclic (a) stress path and (b) stress-strain response of loose sand without initial static shear stress – Sample L7.

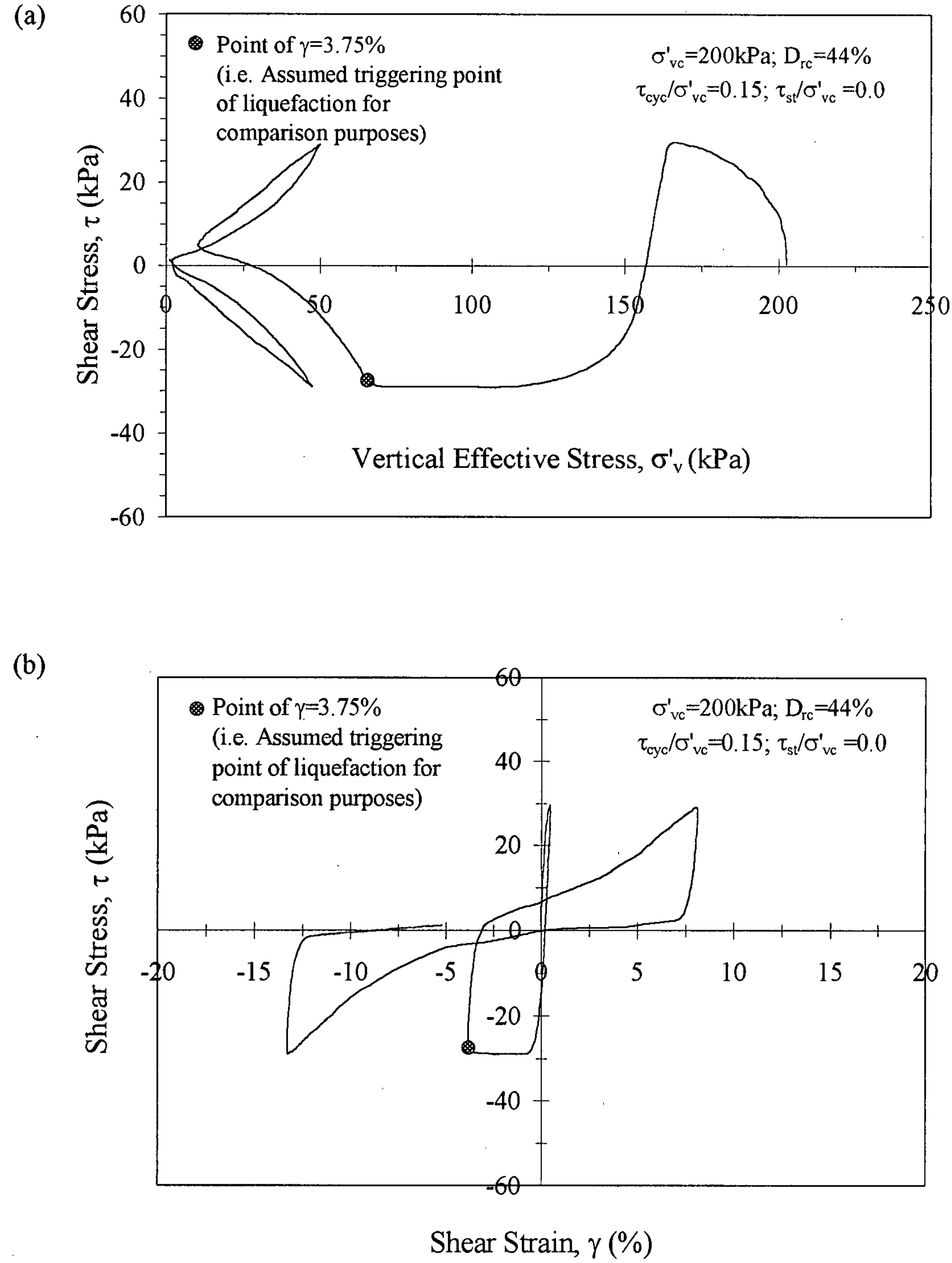

Figure 4.10 Cyclic (a) stress path and (b) stress-strain response of loose sand without initial static shear stress – Sample L8.

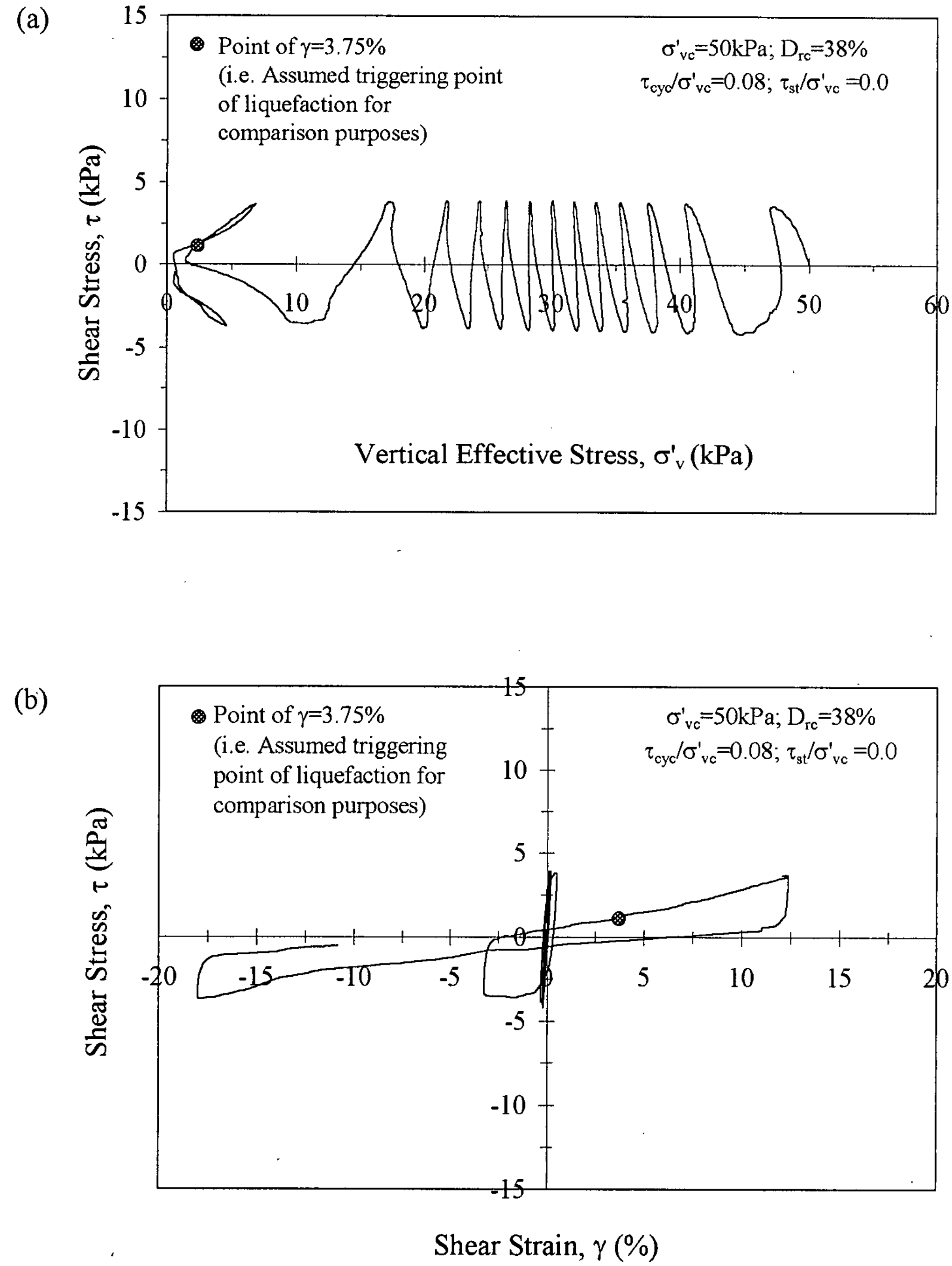

Figure 4.11 Cyclic (a) stress path and (b) stress-strain response of loose sand without initial static shear stress – Sample L9.

(a)

(b)

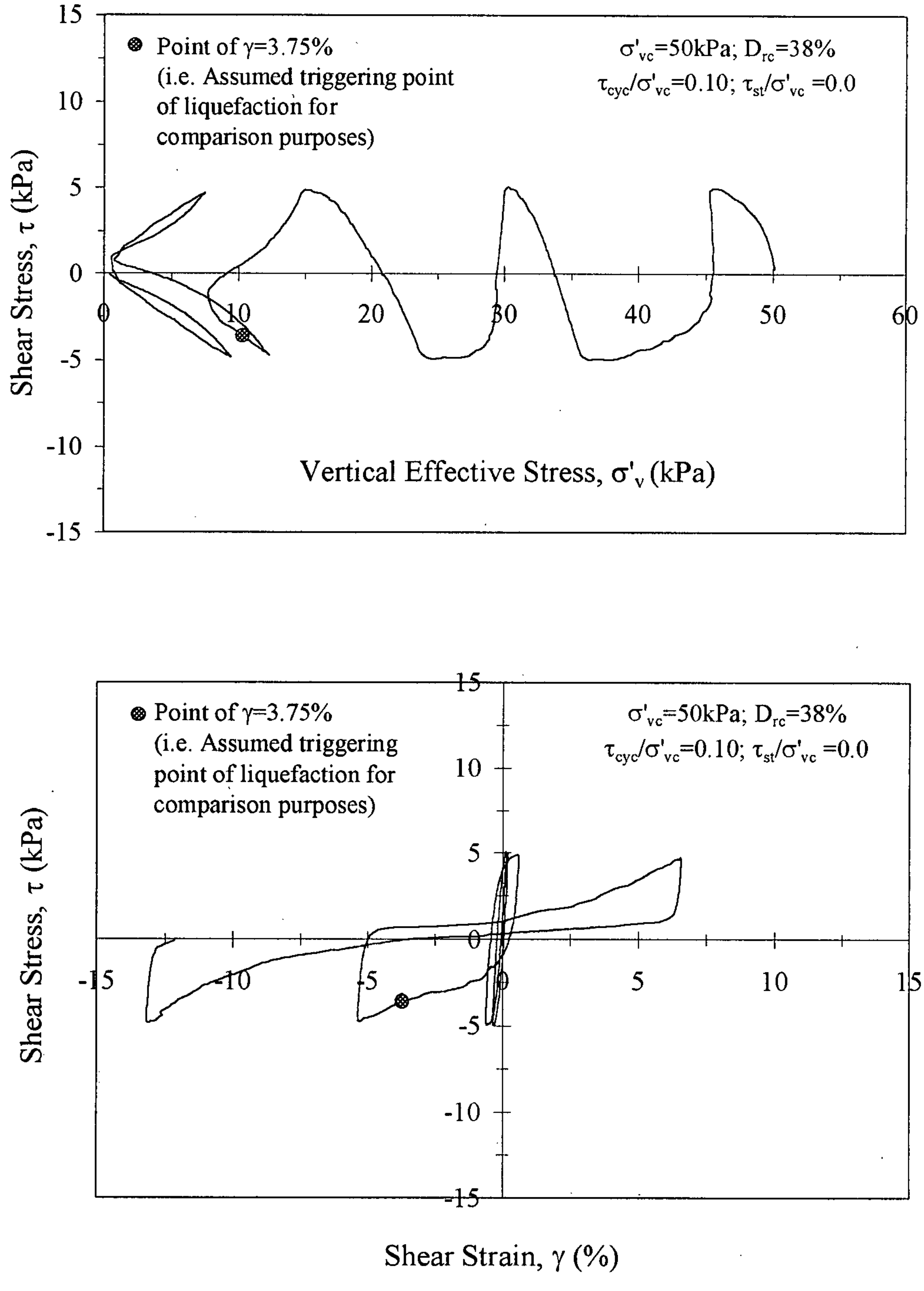

Figure 4.12 Cyclic (a) stress path and (b) stress-strain response of loose sand without initial static shear stress – Sample L10.

(a)

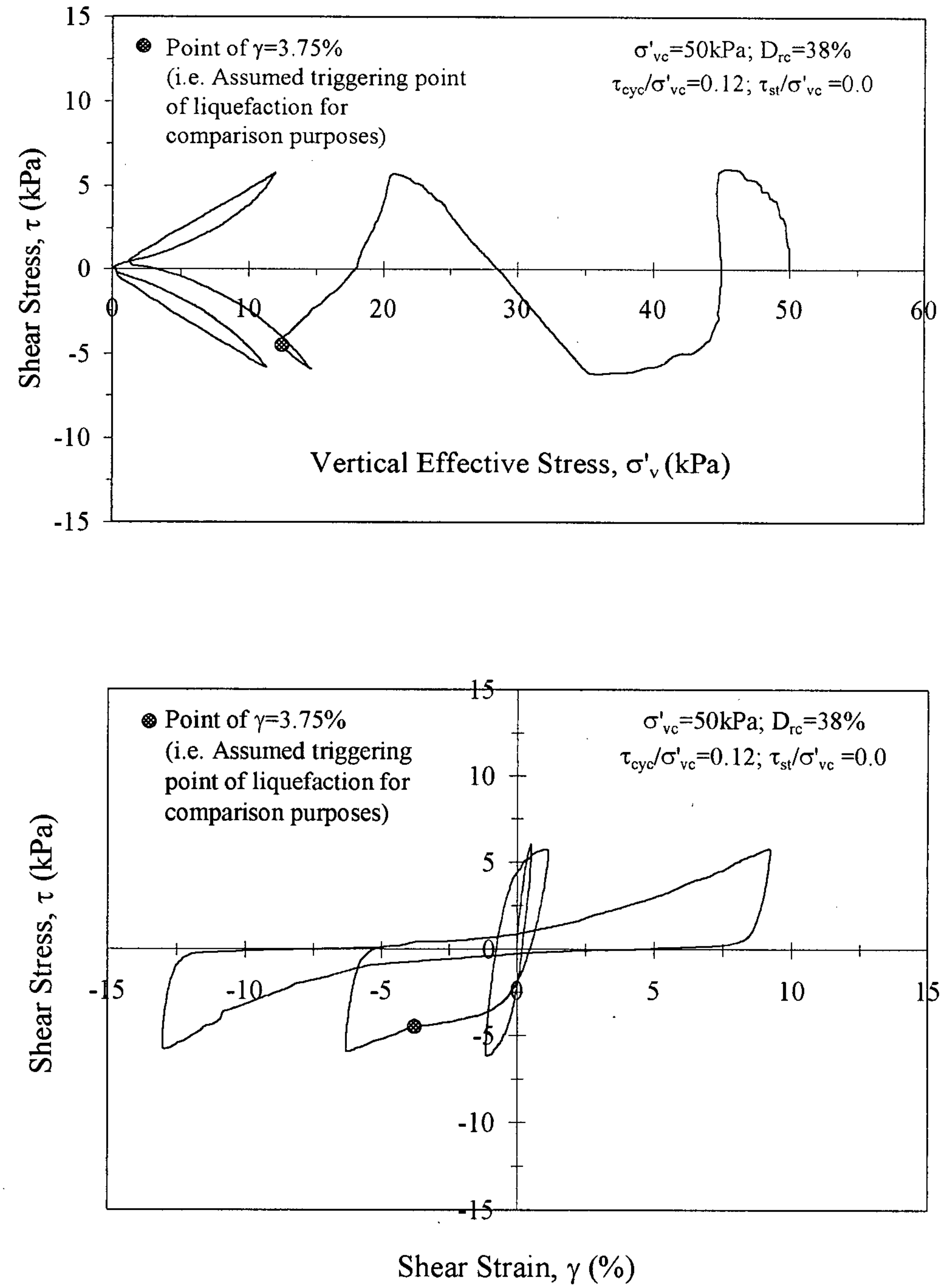

(b)

Figure 4.13 Cyclic (a) stress path and (b) stress-strain response of loose sand without initial static shear stress – Sample L11.

The variation of applied cyclic stress ratio versus number of cycles required to liquefaction (N_L) for cyclic shear tests on air-pluviated loose Fraser River sand conducted on samples consolidated to vertical stresses of: σ'_{vc} = 50 kPa (D_{rc} = 38%), 100 kPa (D_{rc} = 40%), and 200 kPa (D_{rc} = 44%) are shown in Figure 4.14. The results show that, for Type (1) samples formed with the same energy, the number of cycles to liquefaction under a given cyclic stress ratio level increases with the increase in initial vertical confining stress.

Previous work has shown that the cyclic resistance ratio (CRR) of a sand for a given relative density decreases with increasing confining stress (Seed and Harder, 1990). This reduction in CRR has been accounted for using a correction factor (K_σ) defined as:

$$(CRR)_{\sigma', Drc} = K_\sigma * (CRR)_{100, Drc} \qquad [4.1]$$

where $(CRR)_{\sigma', Drc}$ is the cyclic resistance ratio of a soil sample of a given density D_{rc} consolidated to an initial confining stress of σ', and $(CRR)_{100,Drc}$ is the cyclic resistance ratio of a sample of the same soil at the same density consolidated to an initial confining stress of 100 kPa. The value of K_σ has been noted to decrease with increasing confining pressure, for a given relative density. The decrease is larger at higher relative density states (Vaid et al., 2001). As such, considering the cases without initial static shear stress conditions, K_σ can be essentially considered as a function σ' and D_{rc} [i.e. $K_\sigma(\sigma', D_{rc})$].

At first glance, the results presented in Figure 4.14 appear to be not in agreement with the above generally accepted influence of confining stress on the liquefaction resistance using the K_σ correction factor. A closer review indicates that, for air-pluviated sand, the gain in CRR due to stress densification effect has exceeded the potential reduction in CRR arising

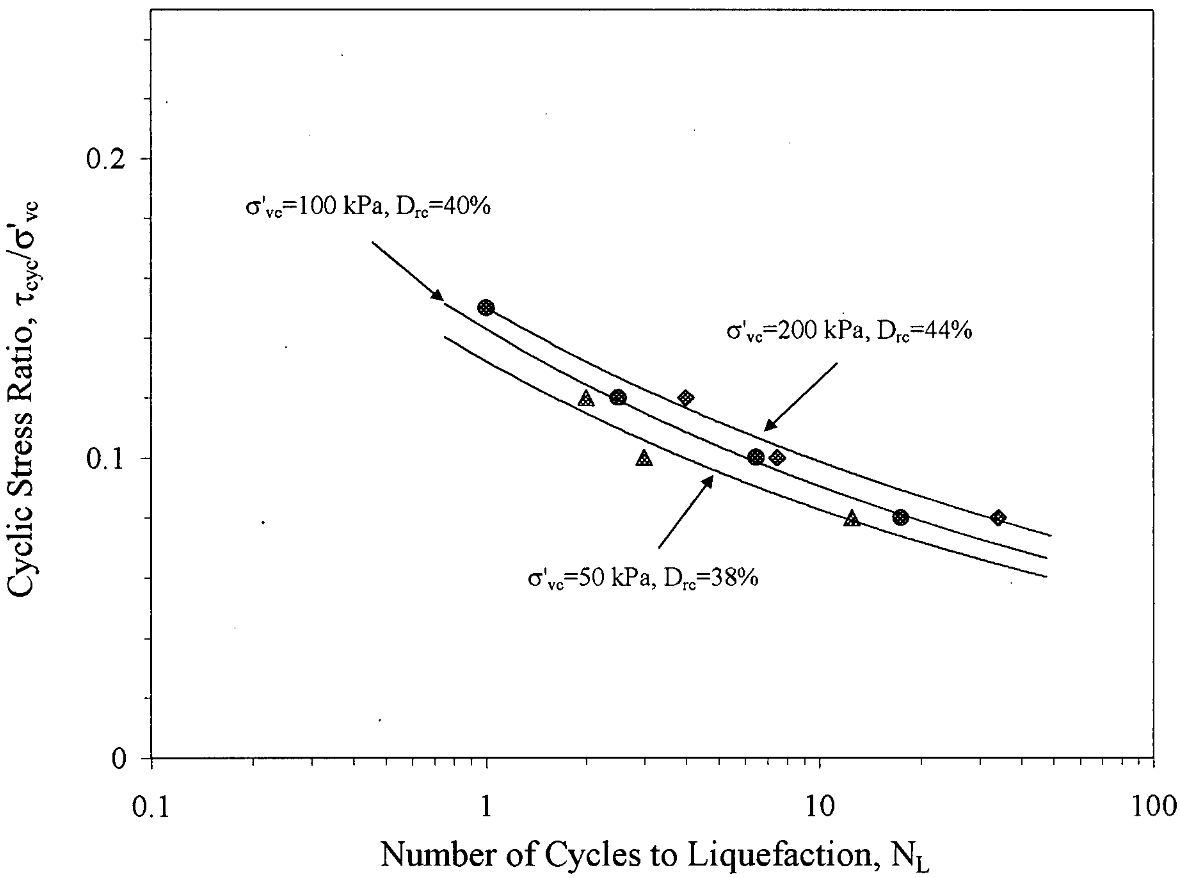

Figure 4.14 Effect of stress densification on cyclic resistance for loose air-pluviated sand.

from increase in σ'_{vc}. This is illustrated in another format in Figure 4.15 where values of CRR corresponding to N_L = 15 cycles from DSS tests on air-pluviated samples are extracted from Figure 4.14 and re-plotted with respect to σ'_v. The different relative densities arising from stress densification corresponding to the three stress levels are also identified in the figure. Published experimental data in Sivathayalan (1994) allowed determination of CRR values for water-pluviated Fraser River sand for (σ'_v and D_{rc}) combinations identical to those for the air-pluviated sands above, and they are also plotted in Figure 4.15 for comparison purposes. For the water-pluviated samples, there appears to be essentially no increase in CRR with increasing confining stress. In this case, the increase in CRR due to increased D_{rc} is balanced by the reduction in CRR due to the stress increase. Clearly, this is different from the noticeable effect of stress densification on the CRR values observed with respect to the air-pluviated samples. Again, this contrast between the two CRR curves can only be attributed to the likely difference in the fabric between air-pluviated and water-pluviated sands. In addition, the above findings also highlight the need to account for stress densification in the numerical analysis of the centrifuge models prepared using air-pluviation. The results also re-confirm the importance of the effect of stress densification in predicting the liquefaction resistance of sand, which has been highlighted by other researchers (Pillai and Byrne, 1994; Park and Byrne, 2004).

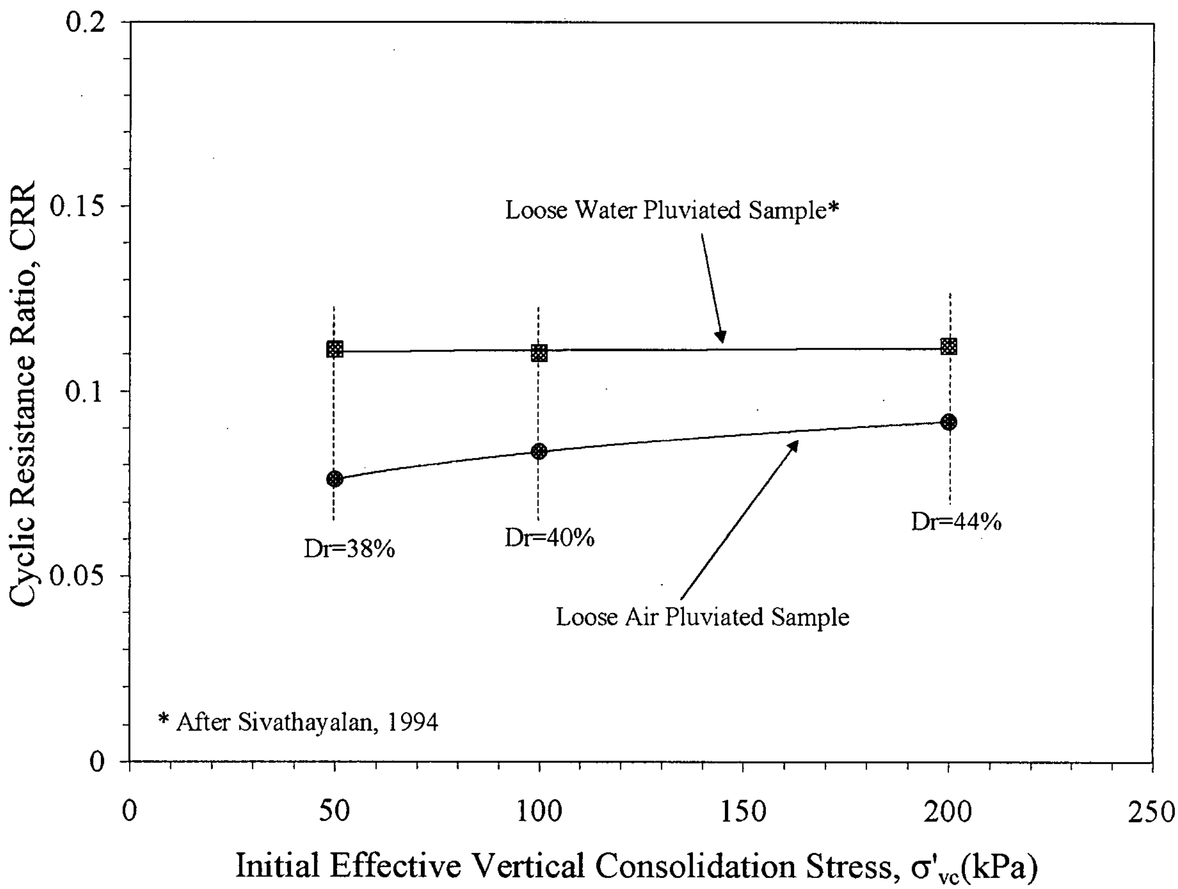

Figure 4.15 Comparison of cyclic resistance curves for loose air-pluviated and water-pluviated sands at same relative density (D_{rc}) and vertical effective stress (σ'_{vc}) conditions.

4.1.3 Cyclic Loading Response – With Initial Static Shear Stress Bias

Figures 4.16 through 4.19 present the response of four Type (1) samples that were initially consolidated to σ'_{vc} = 100 kPa (D_{rc} = 40%) with an initial static shear stress bias (i.e. normalized static shear stress level = $\alpha = \tau_{st}/\sigma'_{vc}$), and then subjected to cyclic loading as per Series B2 and B3 (Table 3.2), and that presented in Figures 4.20 through 4.23 are for another four Type (1) samples that were initially consolidated to σ'_{vc} = 200 kPa (D_{rc} = 44%) with an initial static shear stress bias, and then subjected to cyclic loading as per Series C2 and C3 (Table 3.2). As may be noted from the Figures 4.16 through 2.23, all the samples exhibited reduction in effective stress (or rise in pore water pressure) with increasing number of cycles. If shear stress reversal does not occur during cyclic loading, samples could reach liquefaction without 100% excess pore water pressure generation (e.g. Samples L12, L13, l16, and L17). On the other hand, with cyclic stress reversal (e.g. Samples L15 and L19), or transient shear stress $\sigma'_v = 0$ condition (e.g. Samples L14 and L18), the samples were subjected to liquefaction with transient excess pore water pressure ratio amounting to ~100%. These trends are, again, qualitatively similar to those observed from cyclic tests on water-pluviated sand.

4.1.3.1 Cyclic Resistance (Number of Cycles to Liquefaction)

Figure 4.24 shows the variation of applied cyclic stress ratio (CSR) level versus number of cycles required to liquefaction (N_L) derived from DSS tests conducted on Type (1) samples with an initial static shear stress $\alpha = \tau_{st} / \sigma'_{vc} = 0.1$ (i.e. Test Series B2 and C2 in

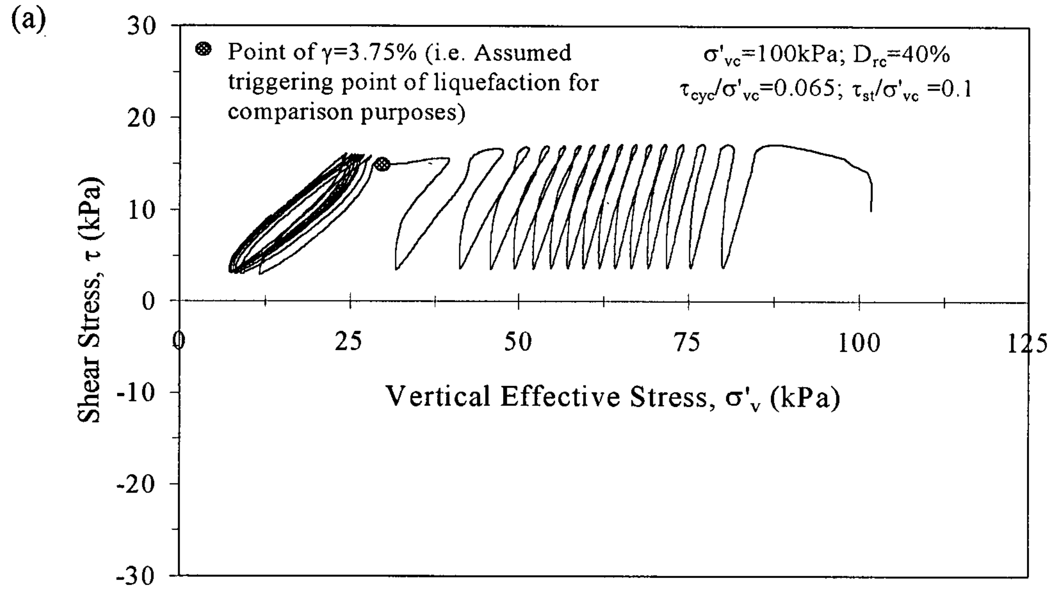

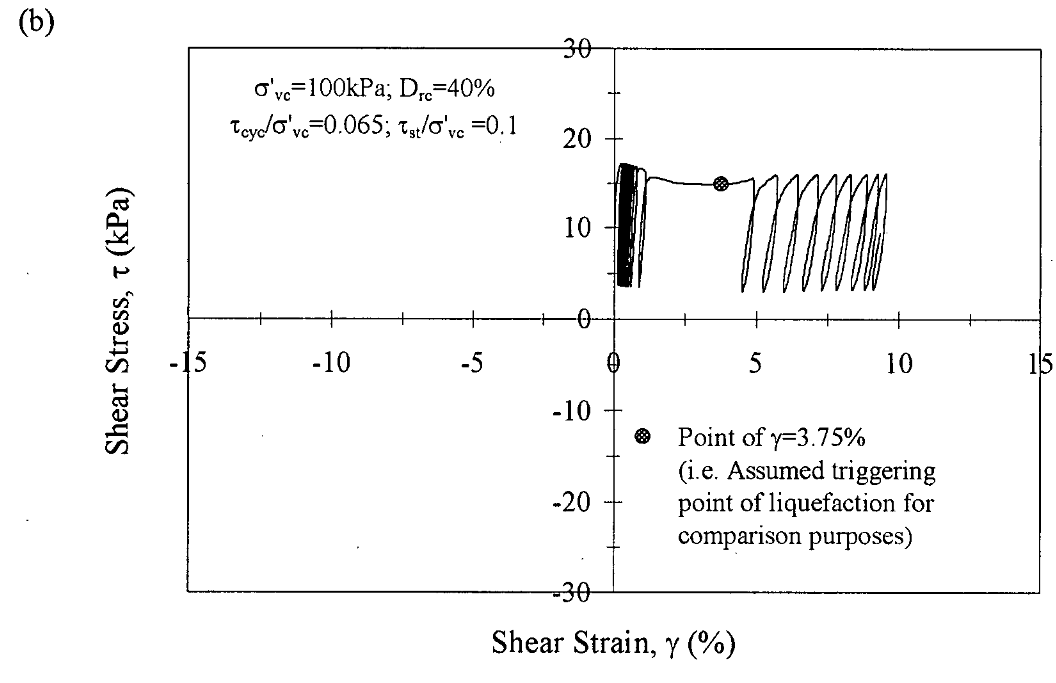

Figure 4.16 Cyclic (a) stress path and (b) stress-strain response of loose sand with initial static shear stress – Sample L12.

(a)

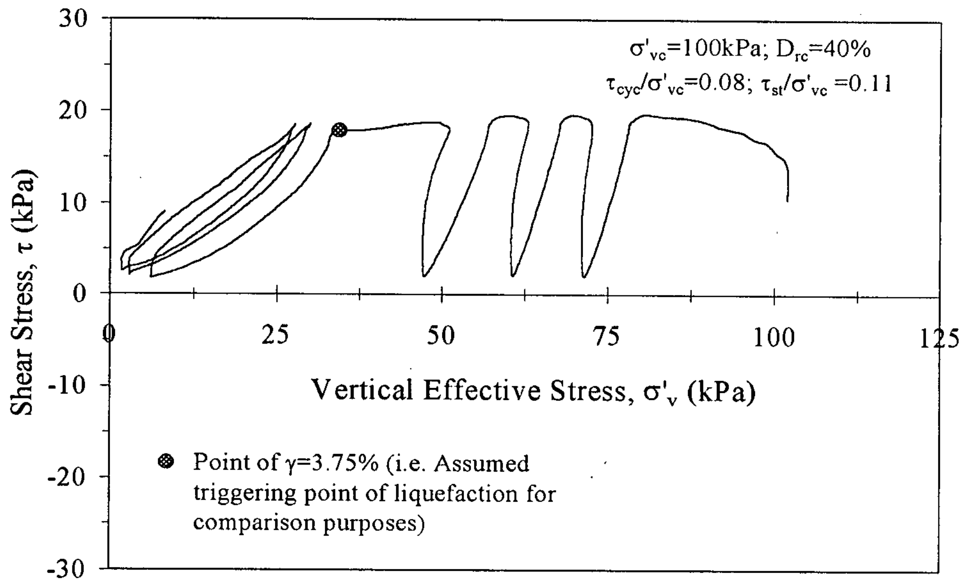

(b)

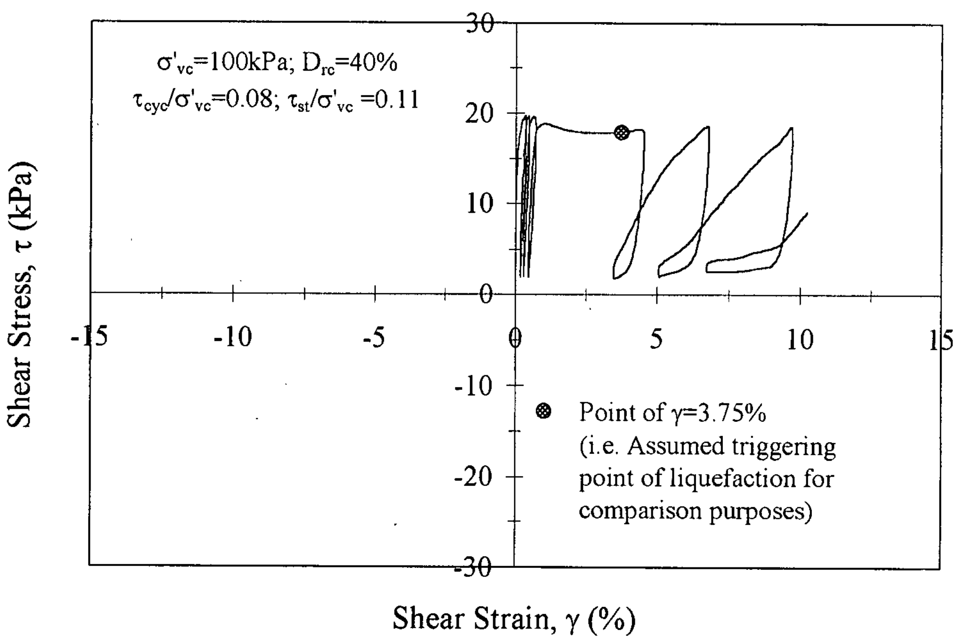

Figure 4.17 Cyclic (a) stress path and (b) stress-strain response of loose sand with initial static shear stress – Sample L13.

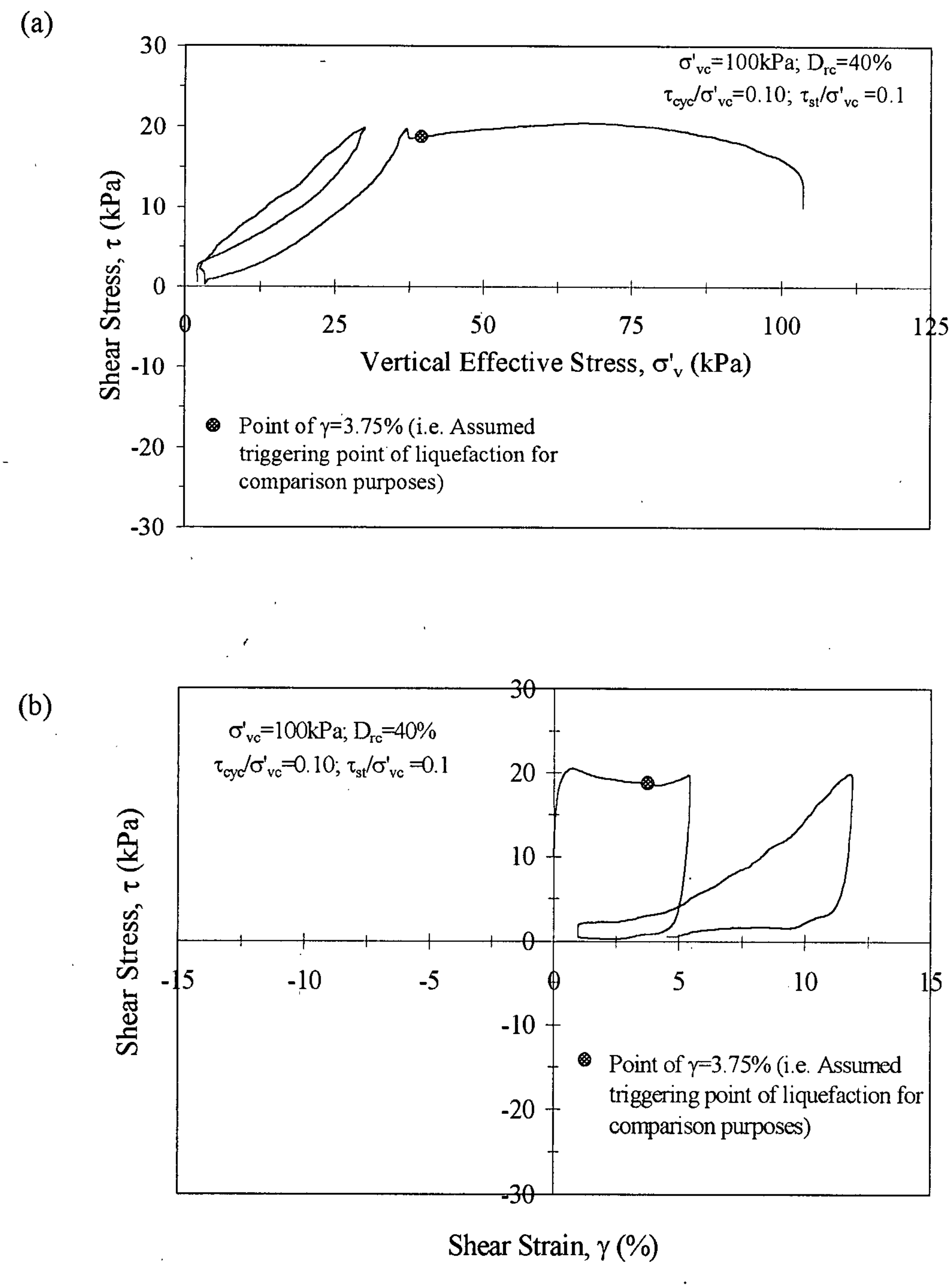

Figure 4.18 Cyclic (a) stress path and (b) stress-strain response of loose sand with initial static shear stress – Sample L14.

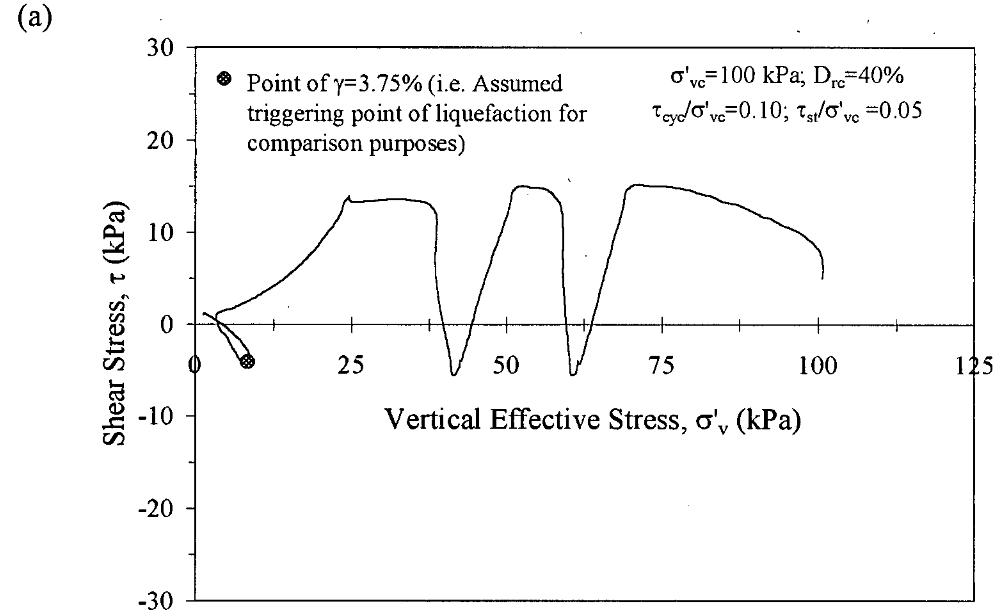

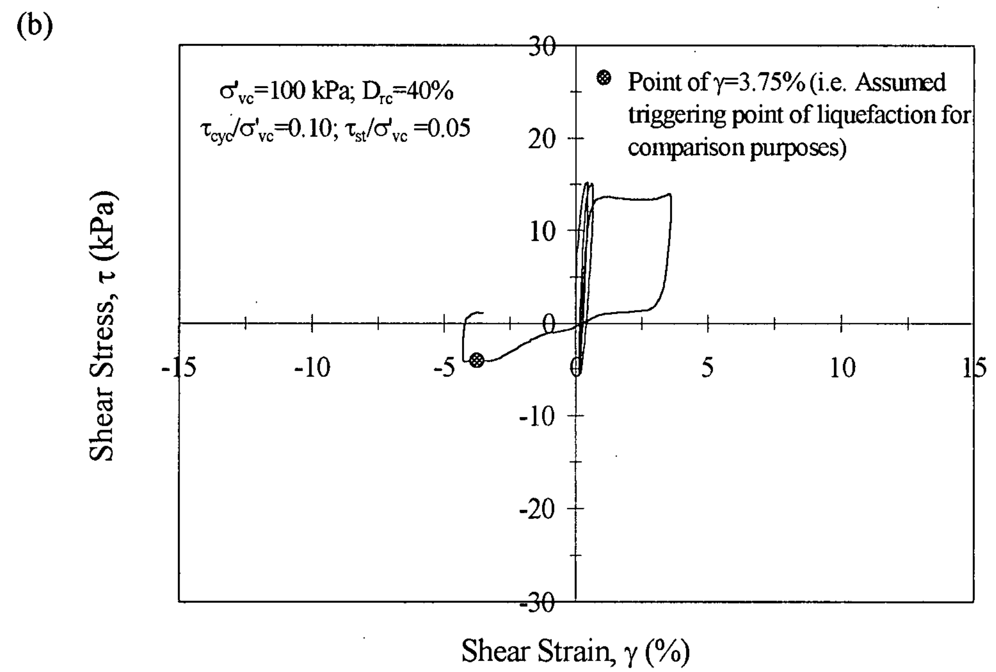

Figure 4.19 Cyclic (a) stress path and (b) stress-strain response of loose sand with initial static shear stress – Sample L15.

(a)

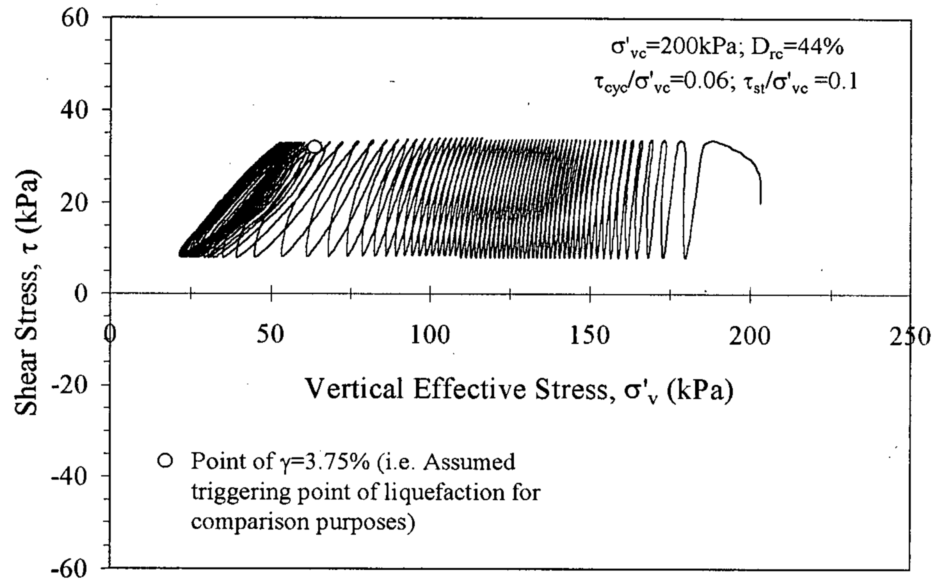

(b)

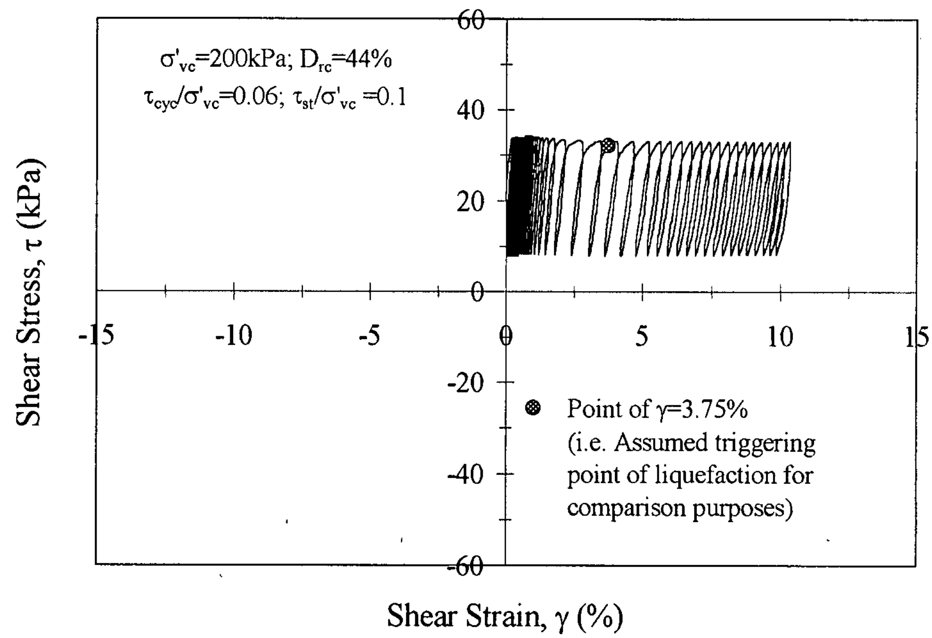

Figure 4.20 Cyclic (a) stress path and (b) stress-strain response of loose sand with initial static shear stress – Sample L16.

(a)

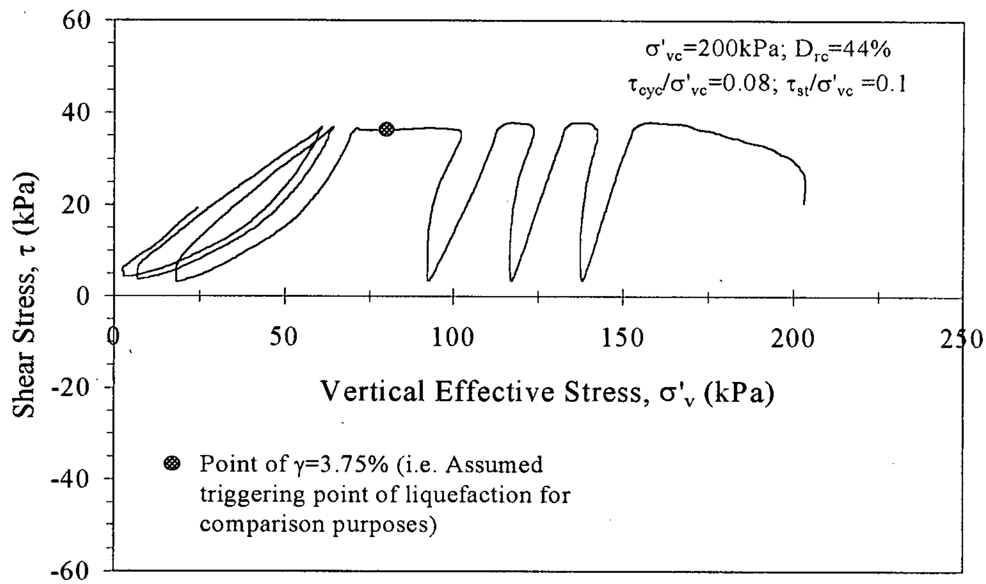

(b)

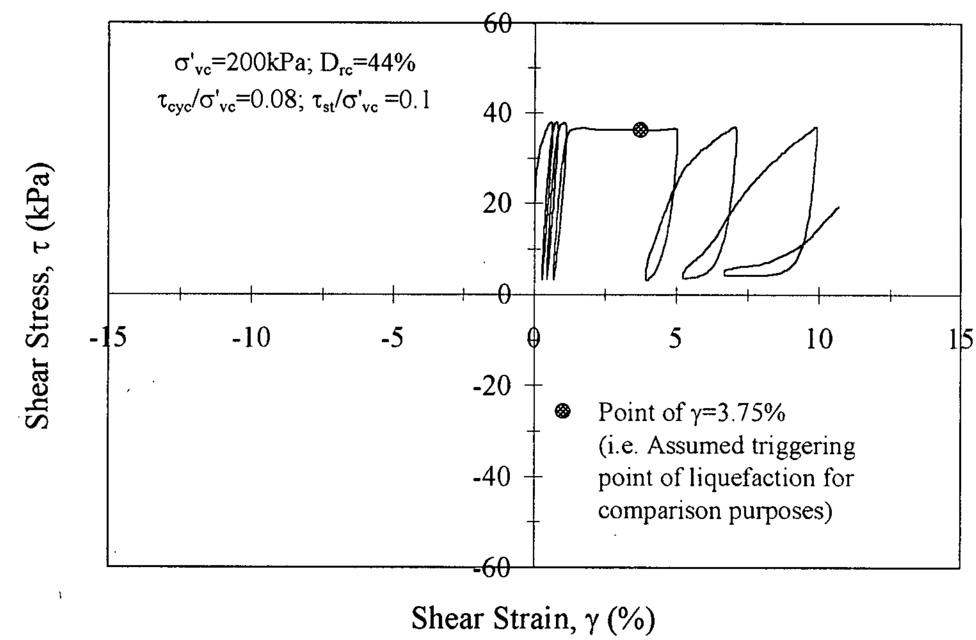

Figure 4.21 Cyclic (a) stress path and (b) stress-strain response of loose sand with initial static shear stress – Sample L17.

(a)

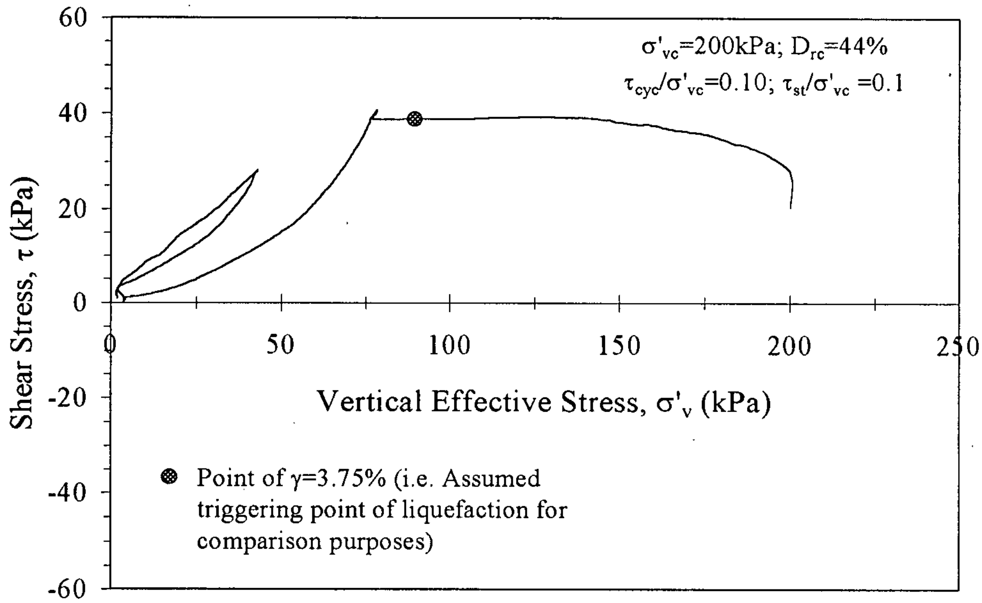

(b)

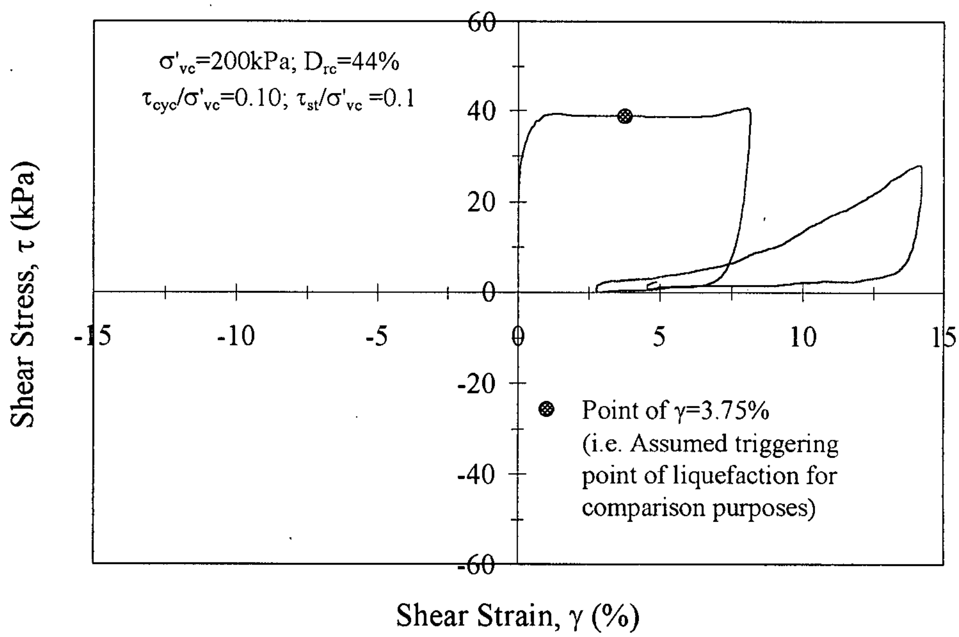

Figure 4.22 Cyclic (a) stress path and (b) stress-strain response of loose sand with initial static shear stress – Sample L18.

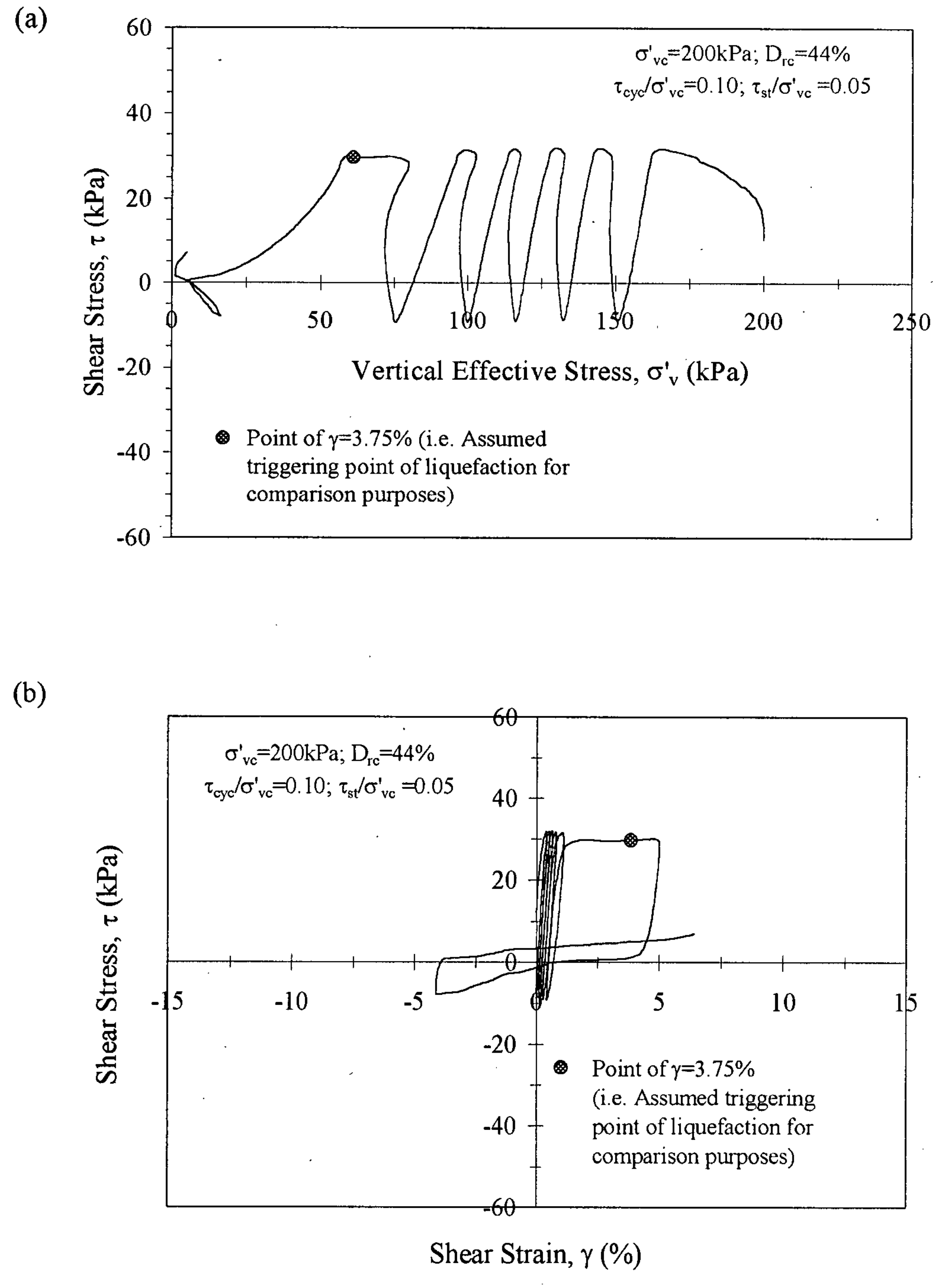

Figure 4.23 Cyclic (a) stress path and (b) stress-strain response of loose sand with initial static shear stress – Sample L19.

Table 3.2). The samples were consolidated to vertical stresses of: σ'_{vc} = 100 kPa (D_{rc} = 40%), and 200 kPa (D_{rc} = 44%), and, the results are compared with those obtained from DSS tests without static bias, but otherwise with identical initial stress level and density conditions.

The effect of increasing cyclic shear resistance due to increasing stress densification is less prominent for the tests involving initial static bias in comparison to those tests with no static bias. The effect of normalized initial static shear stress α on the liquefaction resistance can be examined in the context of commonly used K_α factor defined as:

$$(CRR)_{\sigma',Drc,\alpha} = K_\alpha * (CRR)_{\sigma',Drc,0} \qquad [4.2]$$

where $(CRR)_{\sigma',Drc,\alpha}$ is the cyclic resistance ratio of a given sand at an arbitrary initial confining stress σ' and static bias of α, and $(CRR)_{\sigma',Drc,0}$ is the cyclic resistance ratio of a sample of the same soil at the same density/initial confining stress, but with no static shear bias (α = 0). Considering the values of CRR corresponding to N_L = 15 cycles from Figure 15, a K_α value of ~0.8 is obtained for both the vertical normal effective stresses of 100 kPa (D_{rc}= 40%) and 200 kPa (D_{rc}= 44%). These values are in reasonable agreement with the lower bound of the K_α values for sands suggested by Harder and Boulanger (1997) for α = 0.1 and σ'_{vc} values less than 300 kPa, but for a lower relative density (D_{rc}) condition of 35%. Since Harder and Boulanger (1997) relations are understood to be weighted more heavily towards data obtained from direct simple shear and torsional simple shear tests, they are compatible with the loading mode used in the present study. However, the K_α values for D_{rc}=

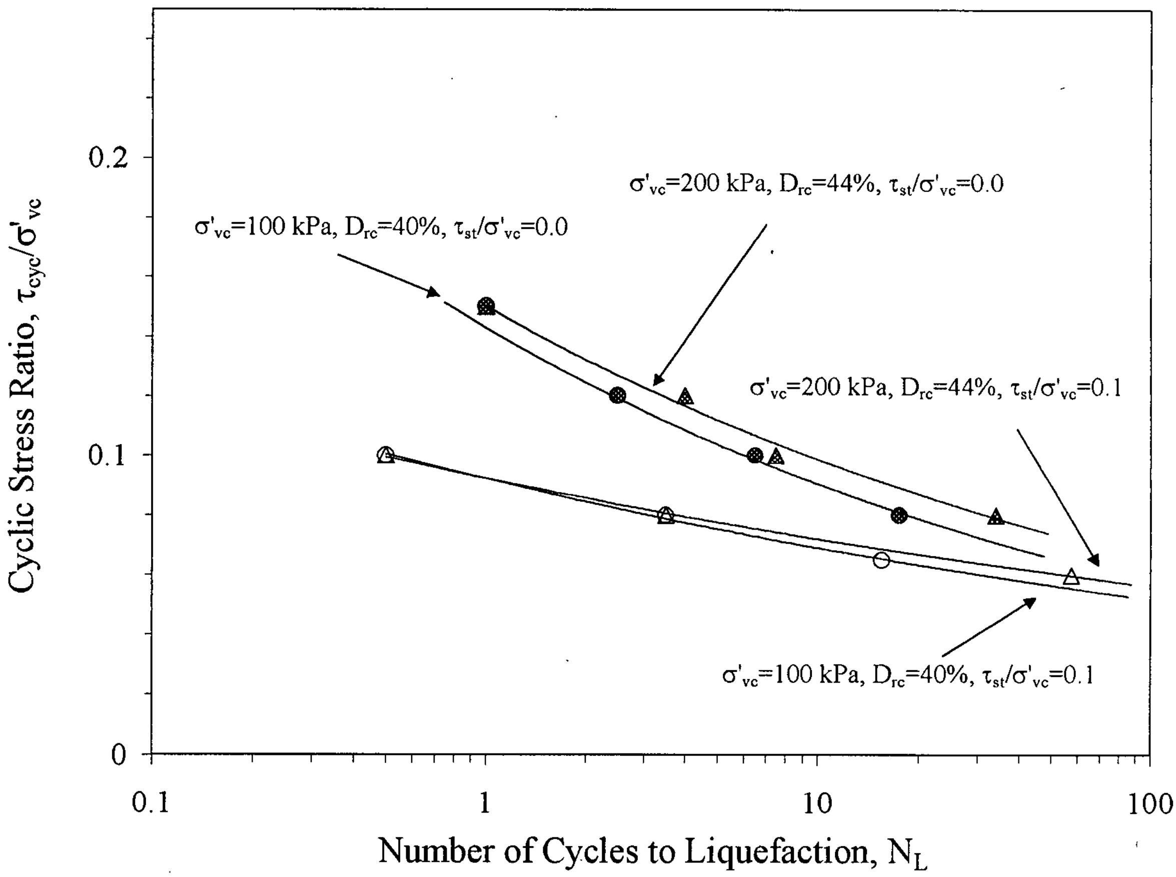

Figure 4.24 Comparison of cyclic resistance curves for loose air-pluviated sand with and without initial static shear stress.

40% observed by Vaid et al. (2001) using triaxial tests for water-pluviated Fraser River sand, tested in a similar consolidation stress level, range between 1.25 and 1.5 indicating increase in cyclic shear resistance due to static bias. The difference in loading mode between the triaxial and simple shear loading, combined with the differences in particle structure associated with air-pluviation, would likely have contributed to the observed inconsistencies.

4.1.4 Repeated Cyclic Loading Response

This section presents the results obtained from repeated cyclic loading tests conducted on initially loose air-pluviated Fraser River sand {Type (1)}. (Note: The testing procedures and test identification numbers are given in Chapter 3 and they are not repeated herein).

Figures 4.25, 4.27 and 4.29 present the stress paths under first and second cyclic loading phases of Samples R1 through R3, respectively, conducted on these loose air-pluviated Fraser River sand specimens. The corresponding stress-strain responses of these three tests are given in Figures 4.26, 4.28 and 4.30. As indicated in Table 3.5, the samples had identical conditions (an initial relative density of 41% at a confining stress level of 100 kPa) and the first cyclic loading of a given sample was stopped upon reaching a certain predetermined excess pore water pressure ratio (r_u) and allowed to consolidate. The samples were then subjected to a repeated cyclic loading.

Sample R1 was subjected to first cyclic loading (Phase R11) until it reached a r_u of 100%. This sample is essentially identical to Sample L2 (see Figure 4.3). Similar to the observed response for Sample L2, the Sample R1 also showed a significant drop in σ'_{vc} with increasing number of cycles. Sample R1 reached liquefaction (i.e. γ = 3.75%) in the 9th cycle; this is slightly more than the seven cycles required for liquefaction of sample L2,

(a)

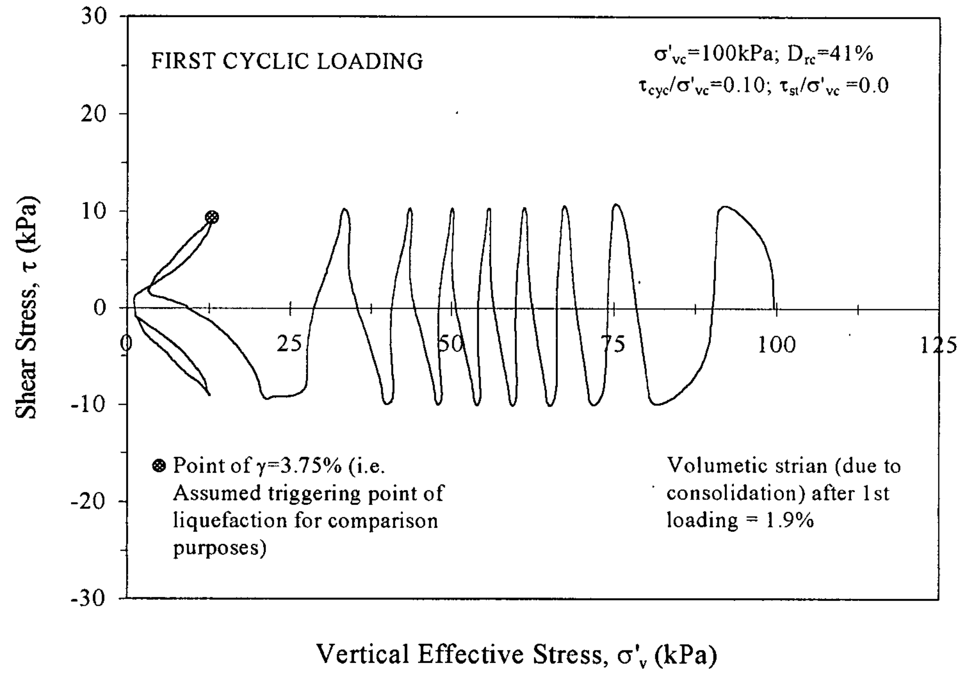

(b)

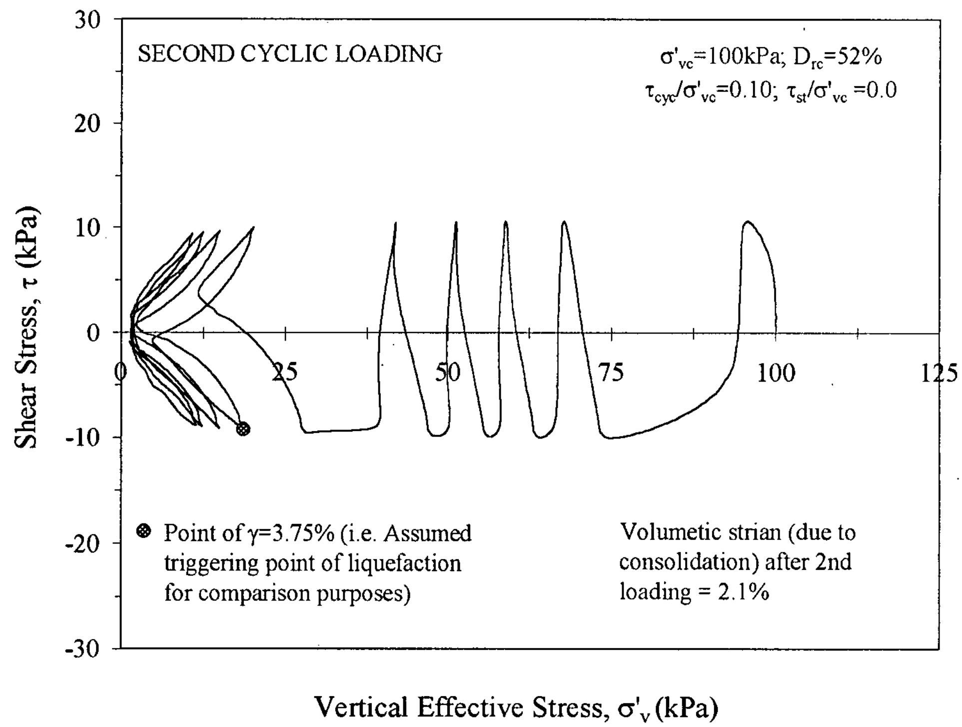

Figure 4.25 Cyclic stress paths of initially loose sand during repeated cyclic loading (a) First Cyclic Loading Phase (R11) (b) Second Cyclic Loading Phase (R12) – Sample R1.

(a)

(b)

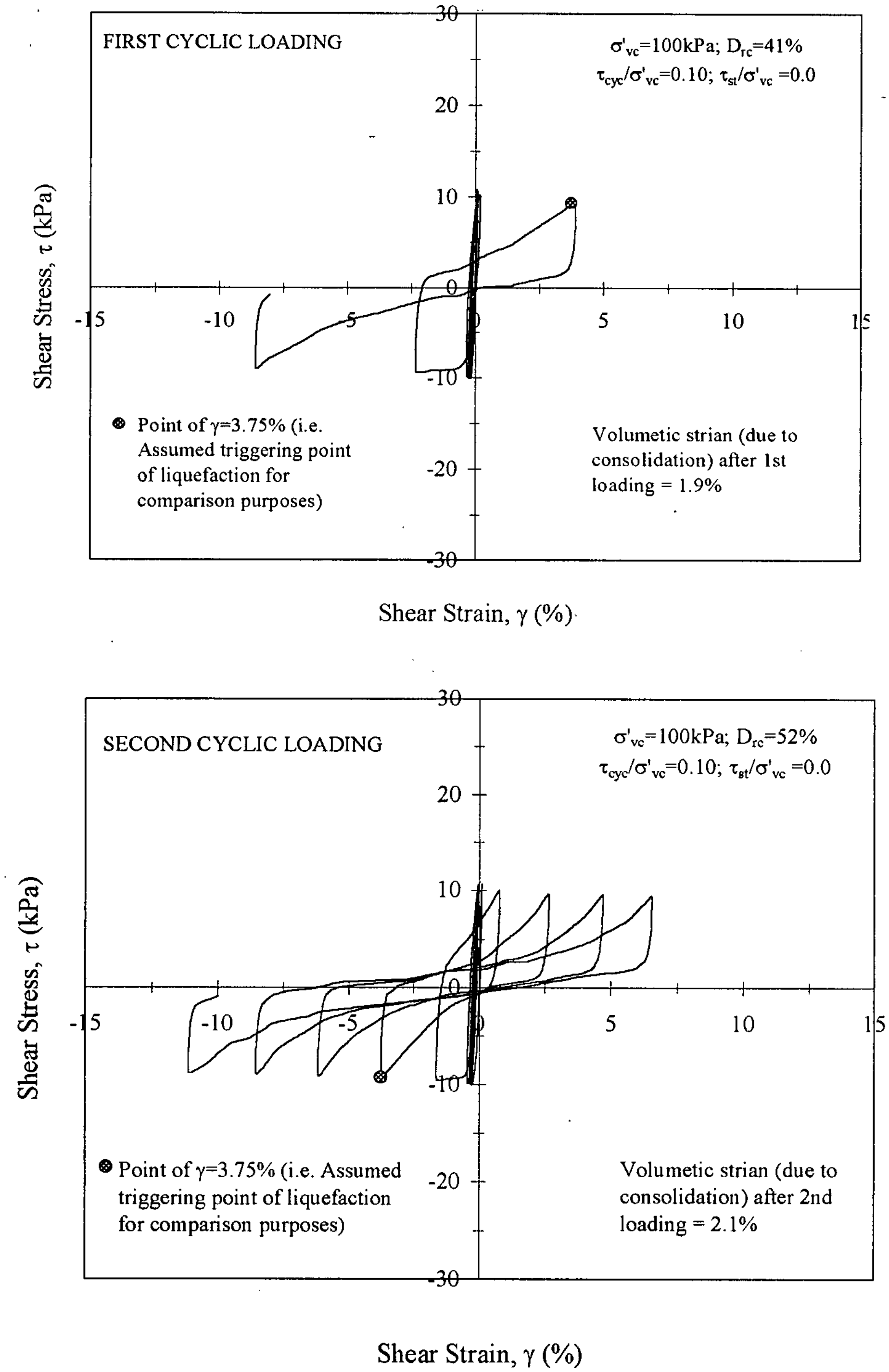

Figure 4.26 Cyclic stress-strain response of initially loose sand during repeated cyclic loading (a) First Cyclic Loading Phase (R11) (b) Second Cyclic Loading Phase (R12) – Sample R1.

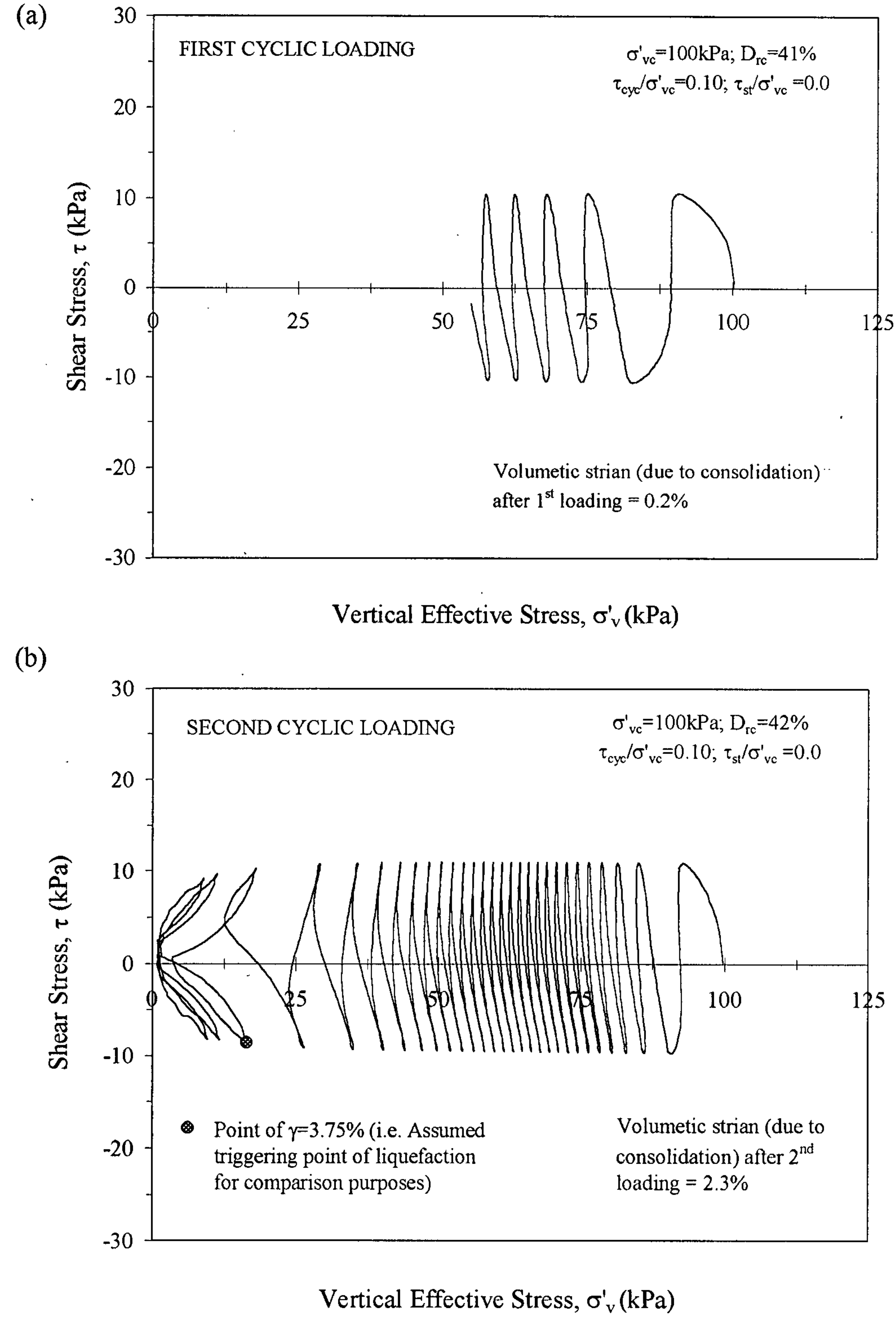

Figure 4.27 Cyclic stress paths of initially loose sand during repeated cyclic loading (a) First Cyclic Loading Phase (R21) (b) Second Cyclic Loading Phase (R22) – Sample R2.

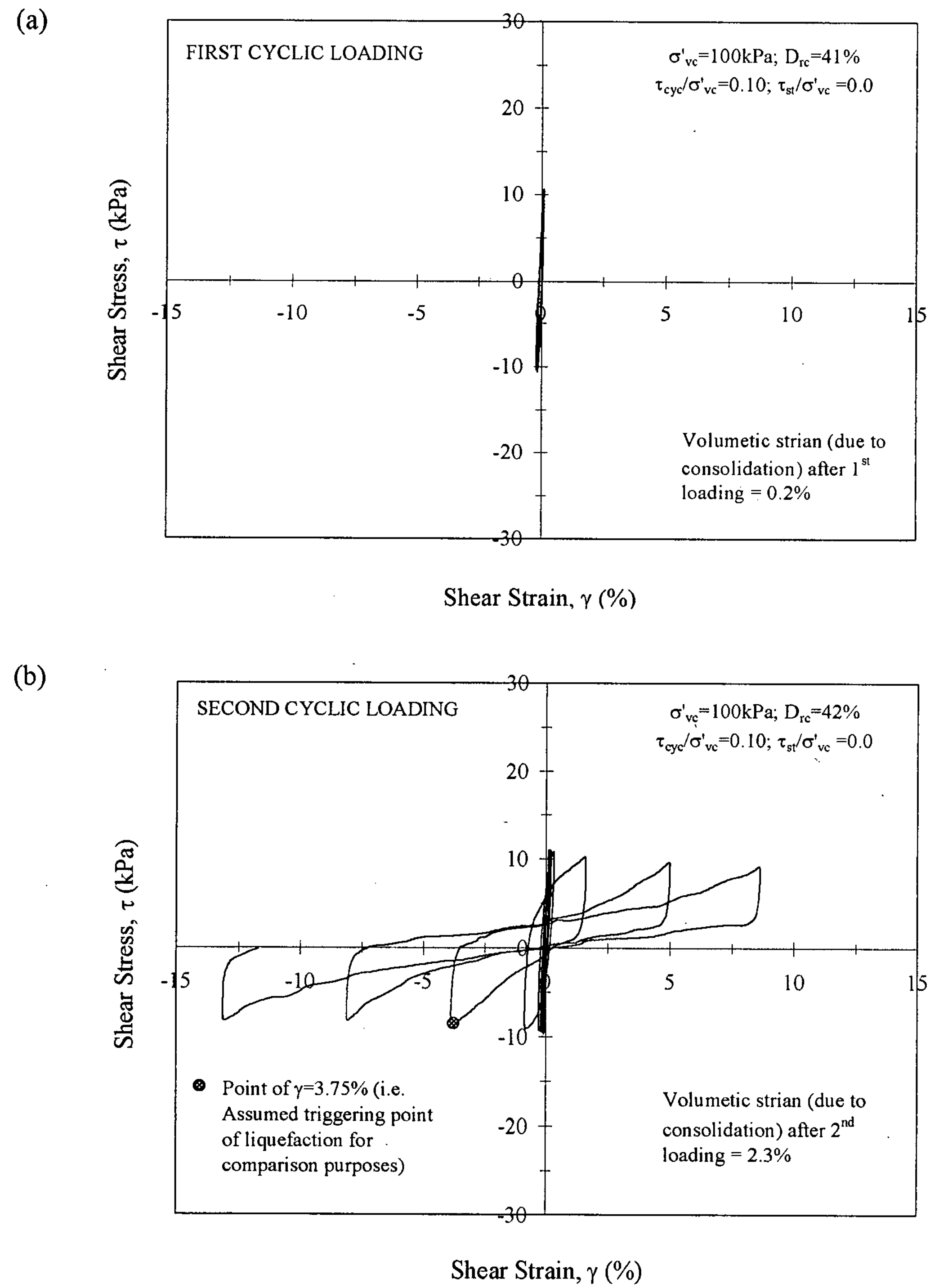

Figure 4.28 Cyclic stress-strain response of initially loose sand during repeated cyclic loading (a) First Cyclic Loading Phase (R21) (b) Second Cyclic Loading Phase (R22) – Sample R2.

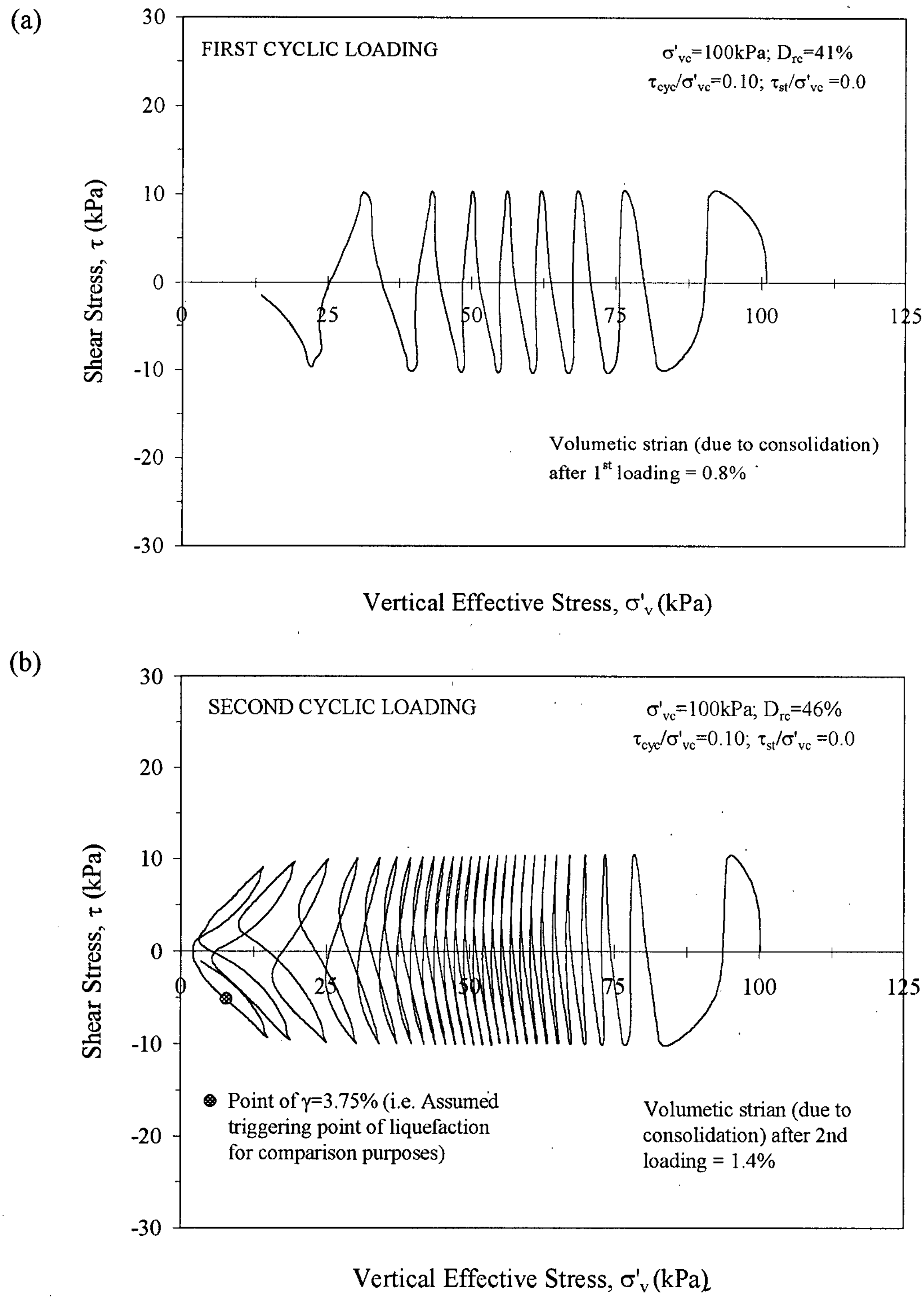

Figure 4.29 Cyclic stress paths of initially loose sand during repeated cyclic loading (a) First Cyclic Loading Phase (R31) (b) Second Cyclic Loading Phase (R32) – Sample R3.

(a)

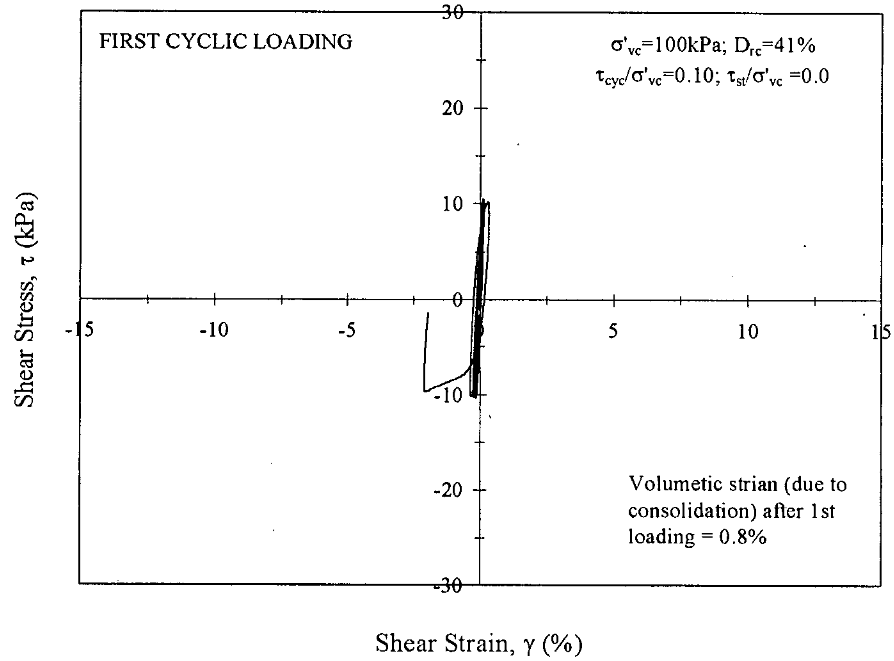

(b)

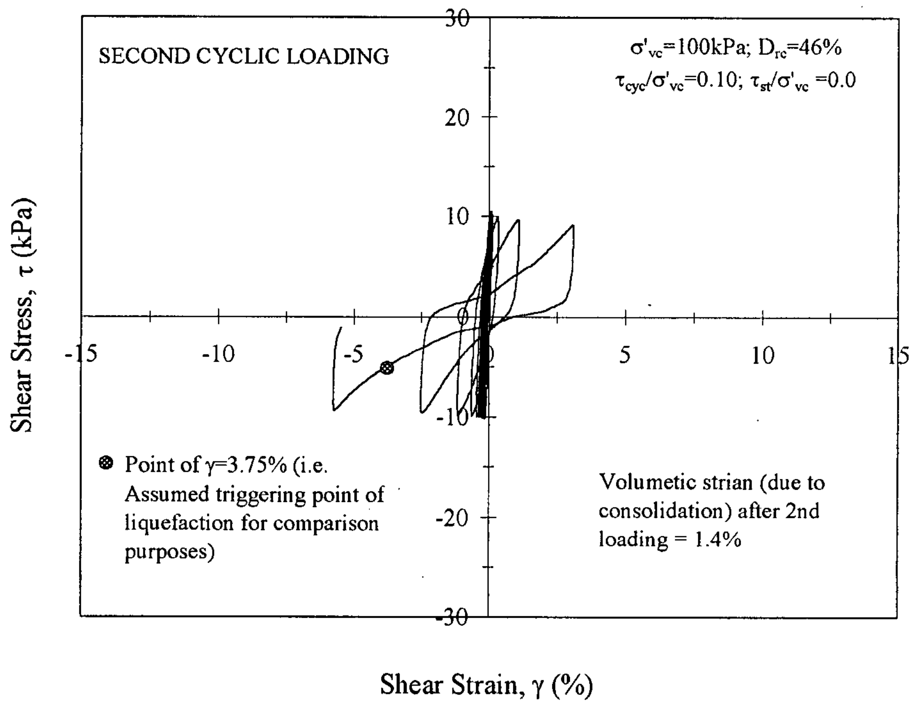

Figure 4.30 Cyclic stress-strain response of initially loose sand during repeated cyclic loading (a) First Cyclic Loading Phase (R31) (b) Second Cyclic Loading Phase (R32) – Sample R3.

likely because of the slightly higher density of Sample R1 than Sample L2. During re-consolidation, the sample experienced a volumetric strain of 1.9%, and this resulted in an increase of the relative density to a value of 52%. As shown in Figures 4.25(b) and 4.26(b), in the second cyclic loading phase (R12), this sample liquefied after reaching lesser number of cycles (6 cycles) than first cyclic loading (R11) despite the increase in the relative density. It appears that the high excess pore water pressures (r_u = 100%) incurred during Phase R11 had resulted in weakening the soil. The observed behaviour is in accord with the previous findings by others on the response of water-pluviated samples subjected to large pre-shearing (Finn et al., 1970; Ishihara and Okada, 1978; Vaid et al., 1989).

Sample R2 was subjected to first cyclic loading phase (R21) until it reached a r_u of 46% (Figure 4.27). This r_u value was reached in 5 cycles of loading and only with very small amplitude of shear strain (γ_{max} = 0.18%). The noted good agreement between the first five cycles of loading in this loading Phase R21 and the Phase R11 of previous sample again confirms the repeatability of the test results. A volumetric strain of 0.2% and a relative density increase to a value of 42% was noted during re-consolidation. As shown in Figures 4.27(b) and 4.28(b), in the second cyclic loading phase (R22), this sample liquefied after reaching significantly larger number of cycles (28 cycles) than first cyclic loading (Phase R11). This noted significant increase in cyclic shear resistance cannot be due to the small increase in the relative density from 41% to 42%. This suggests that some strengthening in the soil fabric that may have taken place during Phase R21 that was terminated before generating larger r_u values (r_u = 46%) and shear strains (γ_{max} = 0.18%). This observed behaviour is in accord with the previous findings by others on the response of water-pluviated samples subjected to small pre-shearing (Finn et al., 1970; Seed et al., 1977; Ishihara and Okada, 1978; Vaid et al., 1989).

Sample R3 was subjected to first cyclic loading (Phase R31) until an r_u of 88% that was reached during the 8^{th} cycle. A maximum shear strain of 2.1% was experienced by the sample during this stage. While this strain level is significantly less than that experienced by the Sample R1 (γ_{max} = 8.0%), it is still lager than that occurred in Phase R21 of Sample R2 (γ_{max} = 0.18%). There is good agreement in the response between this first cyclic loading phase and those observed from R11 and R21, again, confirming the repeatability of the test results. The Sample R3 was then re-consolidated to 100 kPa confining stress level as before. A volumetric strain of 0.8% was noted during re-consolidation and the relative density of the sample was increased to 46% during this process. As shown in Figures 4.29(b) and 4.30(b), in the second cyclic loading phase (R32), this sample liquefied after reaching lager number of cycles (27 cycles) than that required for liquefaction in first cyclic loading phase (R11). It is of interest to note that during second cyclic loading the Sample R3 reached liquefaction after reaching almost the same number of cycles as that observed for Sample R2 despite the difference in the relative densities prior to second loading phase.

Figures 4.31 and 4.33 present the stress paths under first, second and third cyclic loading phases of test numbers R4 and R5, respectively, conducted on loose air-pluviated Fraser River sand specimens {Type (1)}. The stress-strain responses corresponding to these two tests are given in Figures 4.32 and 4.34. As indicated in Table 3.5, the samples had identical conditions (an initial relative density of 40% at a confining stress level of 100 kPa) and the first and second cyclic loadings of a given sample were stopped upon reaching a certain predetermined excess pore water pressure ratio (r_u).

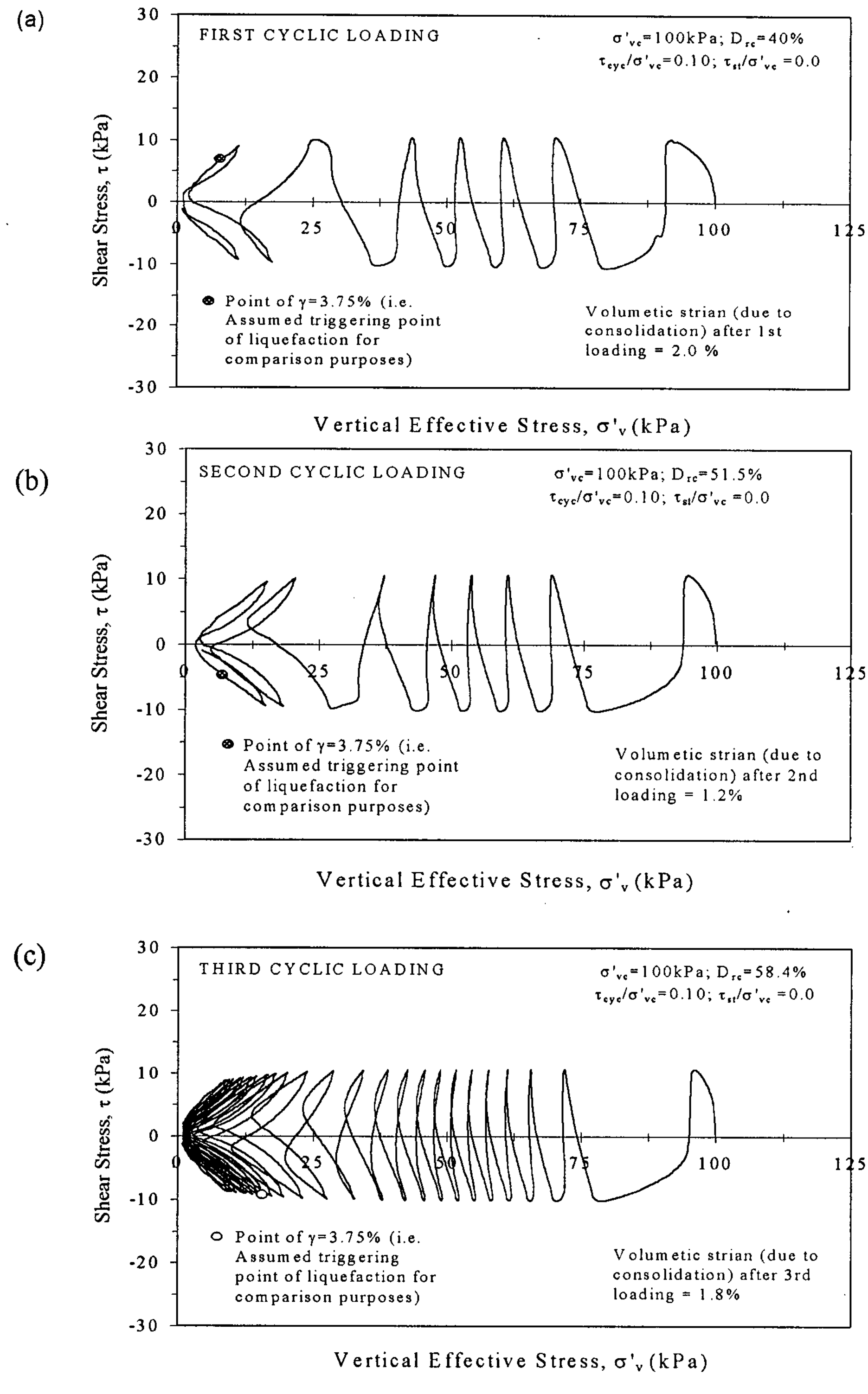

Figure 4.31 Cyclic stress paths of initially loose sand during repeated cyclic loading (a) First Cyclic Loading Phase (R41) (b) Second Cyclic Loading Phase (R42) (c) Third Cyclic Loading Phase (R43)– Sample R4.

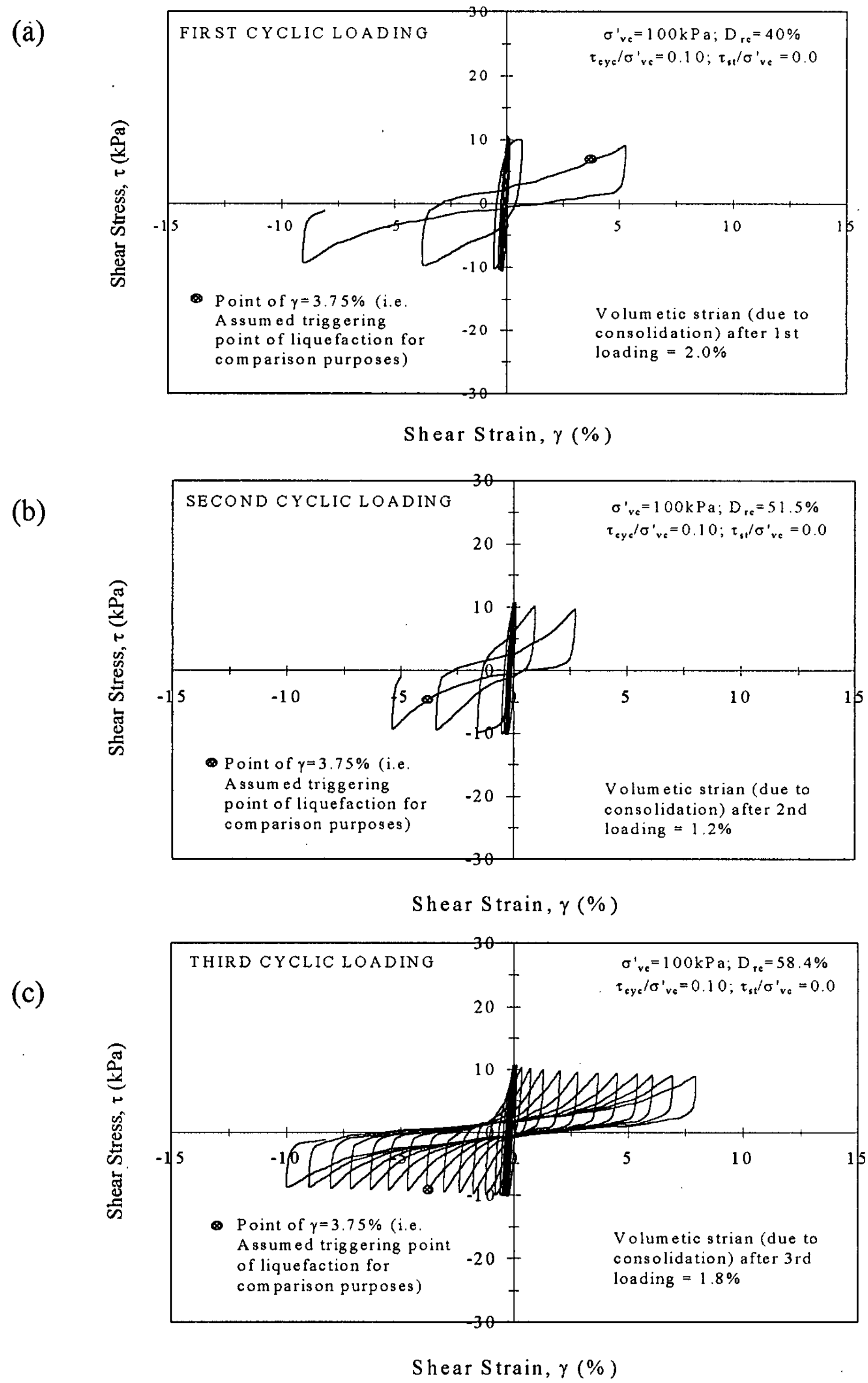

Figure 4.32 Cyclic stress-strain response of initially loose sand during repeated cyclic loading (a) First Cyclic Loading Phase (R41) (b) Second Cyclic Loading Phase (R42) (c) Third Cyclic Loading Phase (R43)– Sample R4.

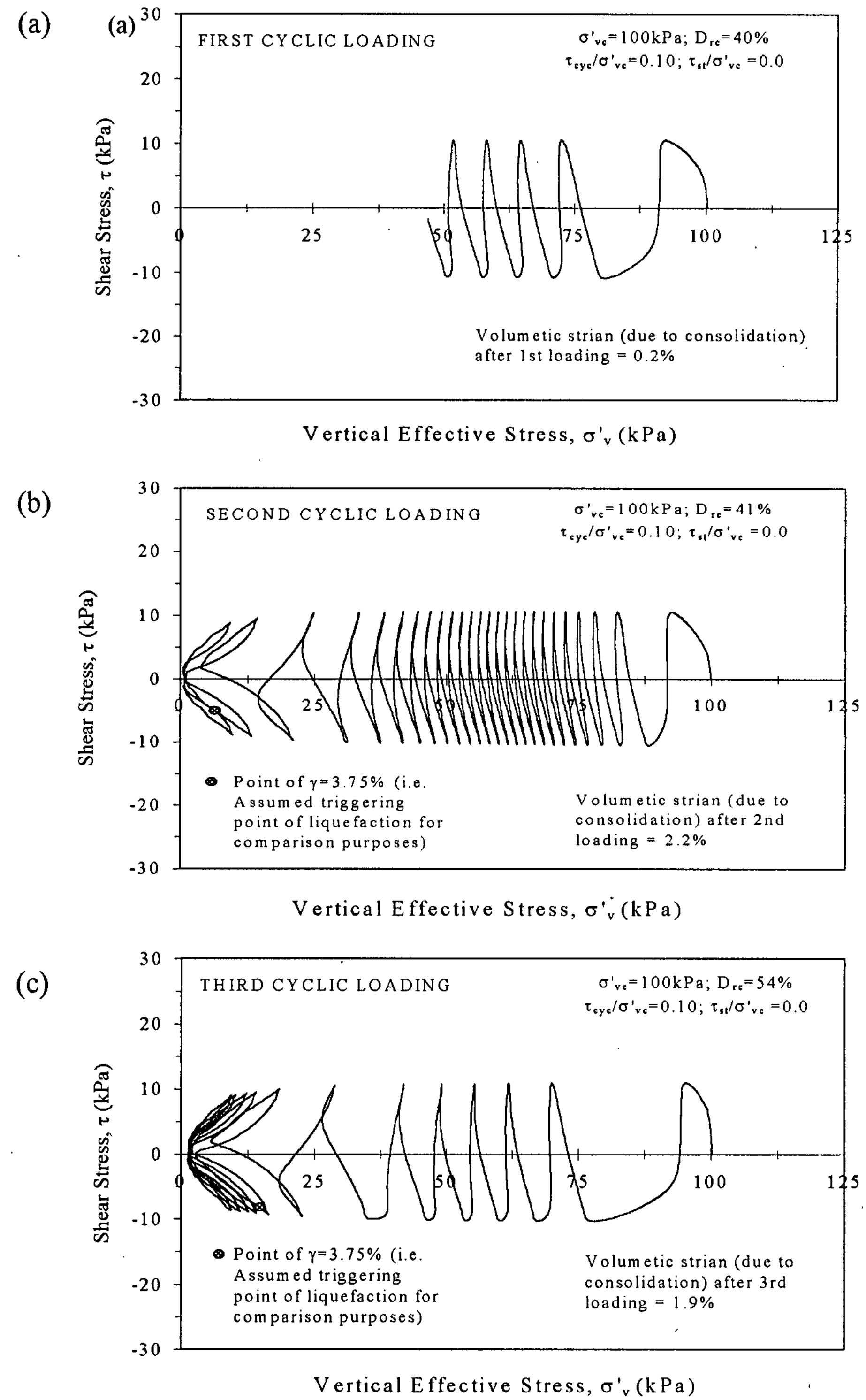

Figure 4.33 Cyclic stress paths of initially loose sand during repeated cyclic loading (a) First Cyclic Loading Phase (R51) (b) Second Cyclic Loading Phase (R52) (c) Third Cyclic Loading Phase (R53)– Sample R5.

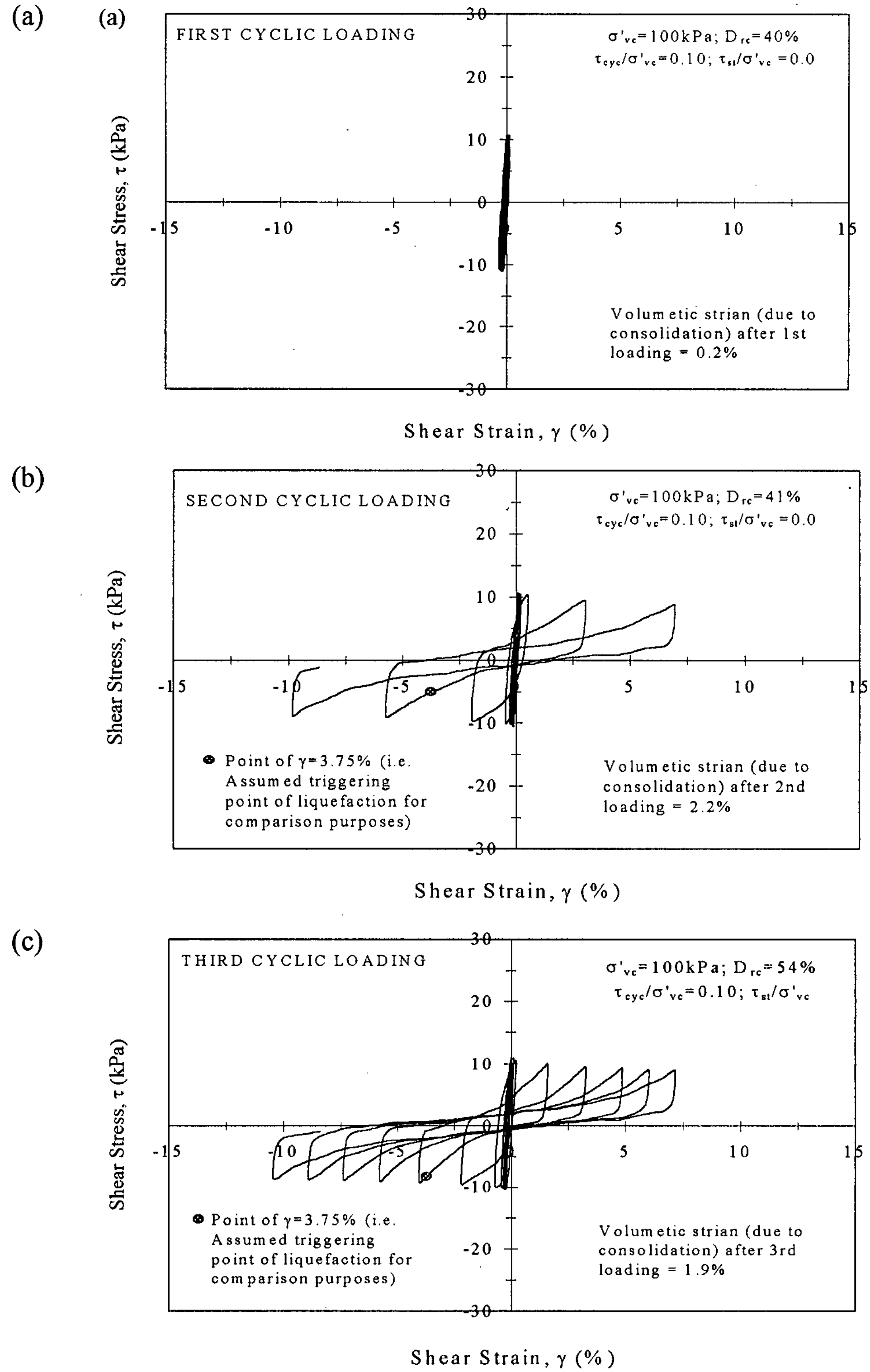

Figure 4.34 Cyclic stress-strain response of initially loose sand during repeated cyclic loading (a) First Cyclic Loading Phase (R51) (b) Second Cyclic Loading Phase (R52) (c) Third Cyclic Loading Phase (R53)– Sample R5.

Sample R4 was subjected to first cyclic loading (phase R41) until it reached a r_u of 100% and reached liquefaction in the 7th cycle. During re-consolidation in preparation for loading Phase R42, the sample experienced a volumetric strain of 2.0 % and a relative density increase to a value of 51.5%. As shown in Figures 4.31(b) and 4.32(b), in the second cyclic loading phase (R42), this sample liquefied after reaching almost same number of cycles (8 cycles) as Phase R41 despite the larger relative density.

It is noted that the Sample R4 and loading Phase R41 are essentially identical to the Sample R1 and its first loading Phase R11. As such, the observed behaviour in second loading phase for both the samples are very similar. Once again, this almost unchanged cyclic shear resistance suggests a clear weakening in the soil fabric due to the first occurrence of liquefaction. When the Phase R42 was terminated the sample reached an r_u = 100%.

The sample was, again re-consolidated to a vertical confining stress of 100 kPa to prepare for the next cyclic loading phase (R43). During this consolidation, the sample suffered an additional volumetric strain of 1.2% and the relative density was increased to 58.4%. As shown in Figures 4.31(c) and 4.32(c), during third cyclic loading Phase (R43), this sample reached liquefaction in the 17th cycle (γ = 3.75%), which is higher than the required number of cycles to cause liquefaction during first two cyclic loading phases (R41 and R42). This increase in the cyclic resistance during third cyclic loading appears to be arising from increase in density that took place during re-consolidation after Phase R42. Based on the previous observed trends, since the sample R4 almost reached r_u = 100% in Phase R42, it should have exhibited significant weakening in Phase R43. It appears that any such possible degradation of cyclic strength has been over-shadowed by the increase in the relative density.

Sample R5 was subjected to loading Phase R51 until it reached a r_u of 54% after 5 cycles of loading. A volumetric strain of 0.2% (with D_r reaching to a value of 41%) was noted during re-consolidation for Phase R52. As shown in Figures 4.33(b) and 4.34(b), the loading Phase R52 required significantly larger number of cycles (25 cycles) to reach liquefaction. This is essentially identical to Phase R22 (see Figures 4.27(b) and 4.28(b)) and the observations can be explained using potential strengthening in the soil fabric due to small pre-shearing as before. During second re-consolidation, the sample experienced a volumetric strain of 2.2% and the relative density was increased to 54%. As shown in Figure 4.33(c) and 4.34(c), in the third cyclic loading Phase R53, this sample reached liquefaction in the 8^{th} cycle, which is almost same as the required number of cycles to cause liquefaction during first cyclic loading Phase R51. Herein, any strengthening in soil fabric associated with small pre-shearing appears to be erased due to fabric alterations due to liquefaction during second loading.

The series of results presented above confirms the effect of pre-shearing on the cyclic response of soils observed by other researchers (Finn et al., 1970; Seed et al., 1977; Ishihara and Okada, 1978; Vaid et al., 1989). It appears that:

- The small pre-shearing improves the soil fabric and, in turn, increases the cyclic resistance of sand to liquefaction during the next cyclic loading phase (e.g. Samples R3 and R5).
- The large pre-shearing weakens the soil fabric and, in turn, decreases the cyclic resistance of sand to liquefaction during next cyclic loading phase (e.g. Samples R1 and R4).

- Sometimes, the reduction in the cyclic resistance of sand to liquefaction arising from the weakening in soil fabric due to large pre-shearing may be overridden by the increase in relative density that take place during re-consolidation process (e.g. Samples R3 and R4).

4.1.5 Shear Strains Due to Cyclic Loading and Post-Cyclic Consolidation Volumetric Strains

The maximum shear strains (γ_{max}) observed during first cyclic loading of samples R1 through R3 are plotted with respect to the maximum excess pore water pressure ratio (r_u) in the Figure 4.35(a). In a similar manner, Figure 4.35(b) shows the volumetric strains incurred during post-cyclic consolidation versus excess pore water pressure ratio (r_u) during cyclic loading for the same tests. As expected, both volumetric and shear strains increase with increasing excess pore water pressure ratio (r_u). The rate of increase of γ_{max} is lower at lower values of r_u and this rate increases at high r_u levels. This type of response for loose sands has been observed by other researchers (Tokimatsu and Seed, 1987; Nagase and Ishihara, 1988). The same data in Figures 4.35(a) and (b) are re-plotted in a γ_{max} versus ε_v graph in Figure 4.36. The post-cyclic consolidation volumetric strains increase with increasing γ_{max} during cyclic loading; for example, it can be seen that a post-cyclic volumetric strain of 1.9% was obtained at a maximum cyclic shear strain level of 8%.

(a)

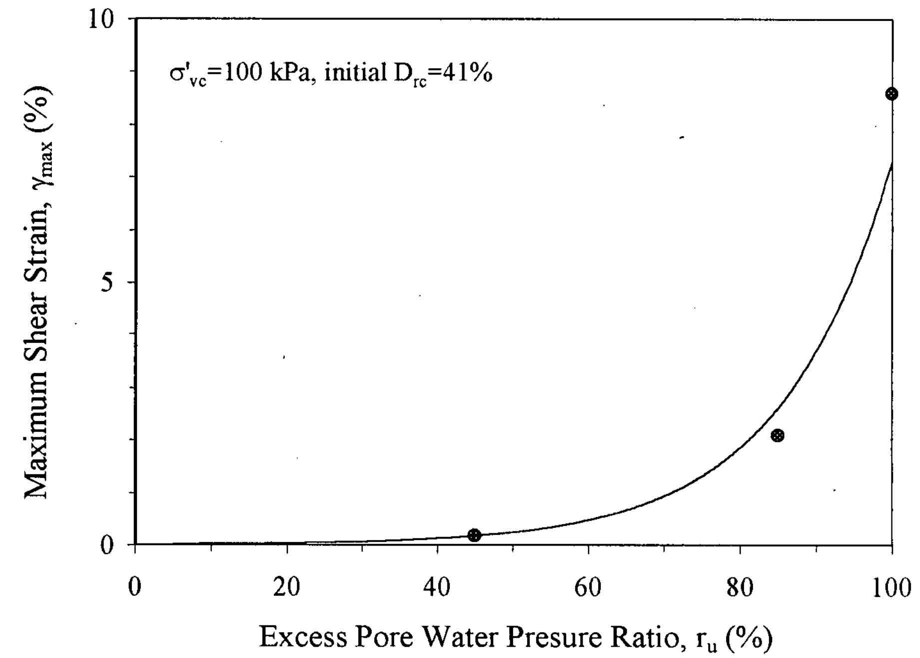

(b)

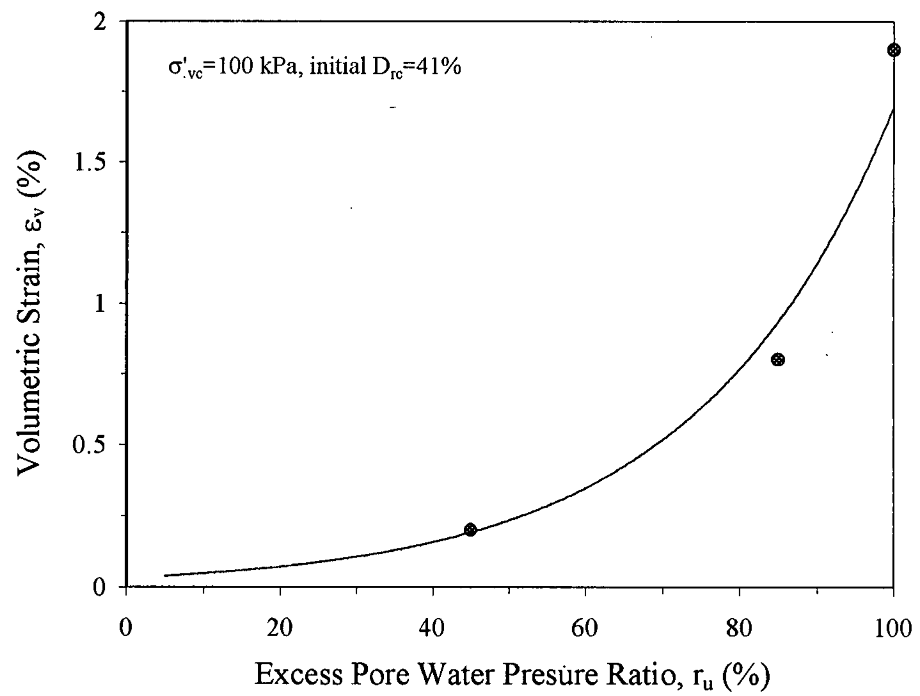

Figure 4.35 Variation of (a) volumetric strain (ε_v) (b) maximum shear strain (γ_{max}) with excess pore water pressure ratio (r_u) during cyclic simple shear loading.

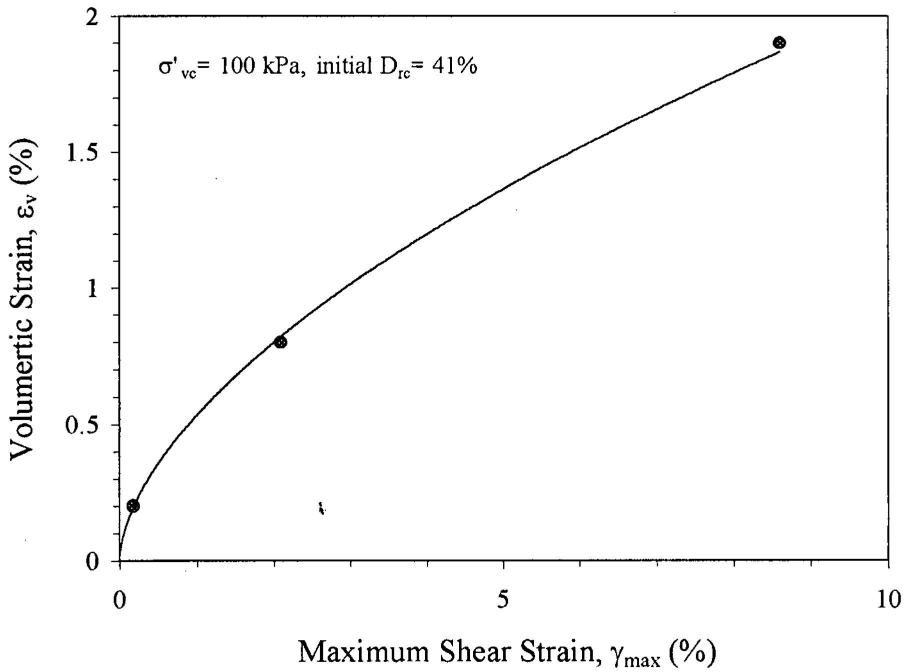

Figure 4.36 Variation of volumetric strain (ε_v) with maximum shear strain (γ_{max}) during cyclic simple shear loading

4.2 UNDRAINED RESPONSE OF DENSE FRASER RIVER SAND

4.2.1 Cyclic Loading Response – Without Initial Static Shear Stress Bias

Figures 4.37 through 4.39 present the response of dense Fraser River sand (Type (2) samples as described in Section 3.5.1.2) during cyclic DSS loading of samples, consolidated to σ'_{vc} = 100 kPa and D_{rc} = 80%, without application of initial static shear stress (i.e. $\tau_{st} = 0$) as per Series E1 (Table 3.3). For example, the test depicted in Figure 4.37 (Sample D1) was loaded with a cyclic stress ratio (τ_{cyc} / σ'_{vc}) of 0.25. Sample D1 exhibited gradual drop in σ'_{vc} (or rise in pore water pressure) with increasing number of cycles, with liquefaction triggering in the 46th cycle [i.e. Point of γ= 3.75%]. There is significant pore water pressure generation during the unloading phase of a cycle in comparison to the counterpart loading phase, even in the first cycle of cyclic loading. This is significant contrast to the response of loose samples. The loose samples did not develop any significant excess pore water pressure during the unloading phase (almost elastic unloading) of initial loading cycles, for loose samples, the excess pore water pressure generation during unloading cycle started to be significant only when stress path reached the line of phase transformation (see Figures 4.2 through 4.5). This relatively large excess pore water pressure generation during unloading in loose samples is a reflection of contractive tendency and "plastic unloading" after the development of phase transformation. This plastic unloading occurs at early stages in the case of dense sample perhaps due to the early development of phase transformation. Similar responses can be noted for test results obtained for other dense samples as presented in Figures 4.38 and 4.39. The observed trends of stress-strain and pore water pressure development under cyclic loading discussed above are generally similar to those noted by

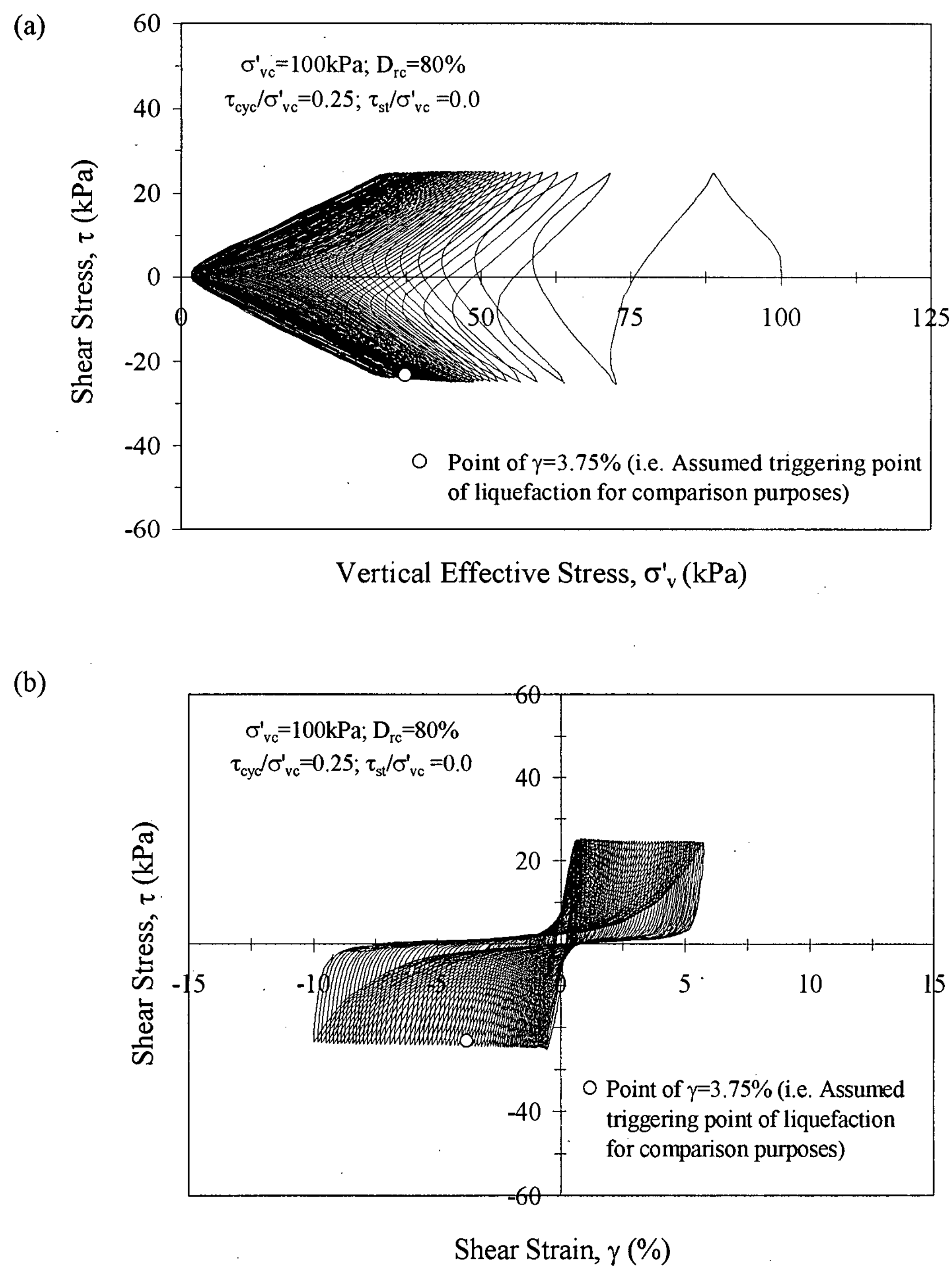

Figure 4.37 Cyclic (a) stress path and (b) stress-strain response of dense sand without initial static shear stress – Sample D1.

(a)

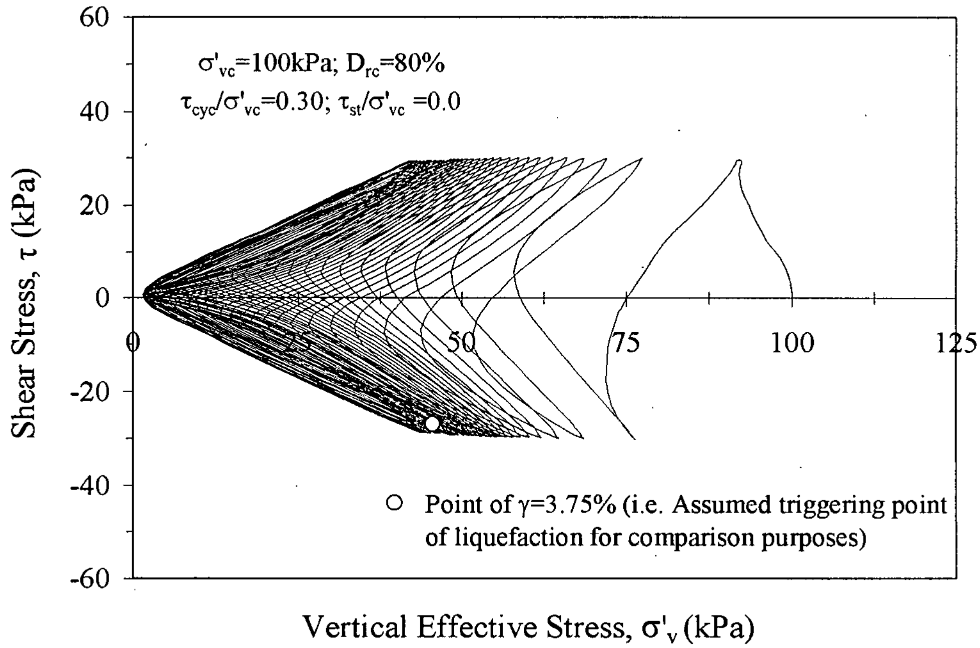

(b)

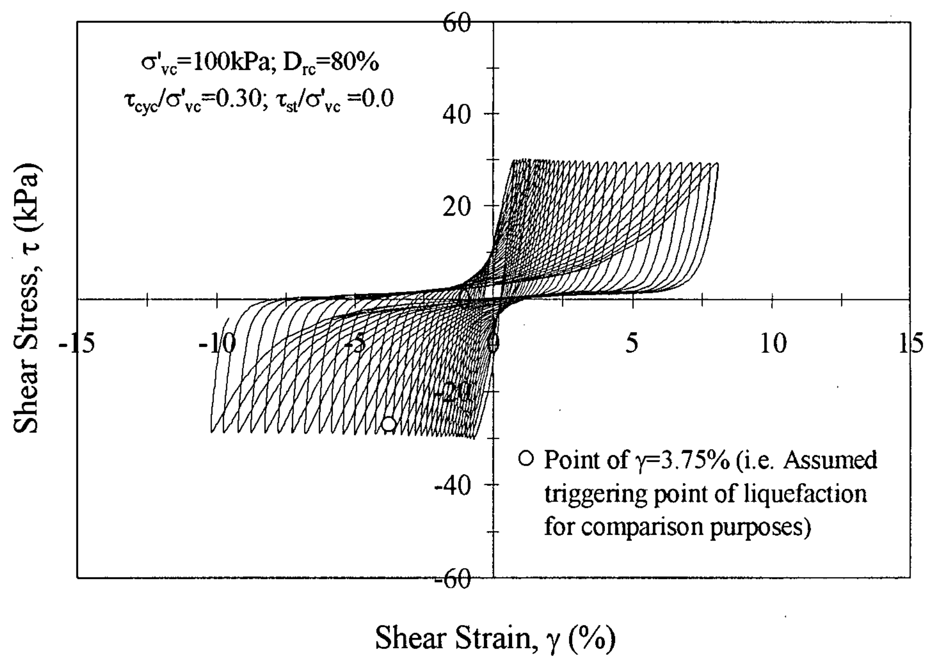

Figure 4.38 Cyclic (a) stress path and (b) stress-strain response of dense sand without initial static shear stress – Sample D2.

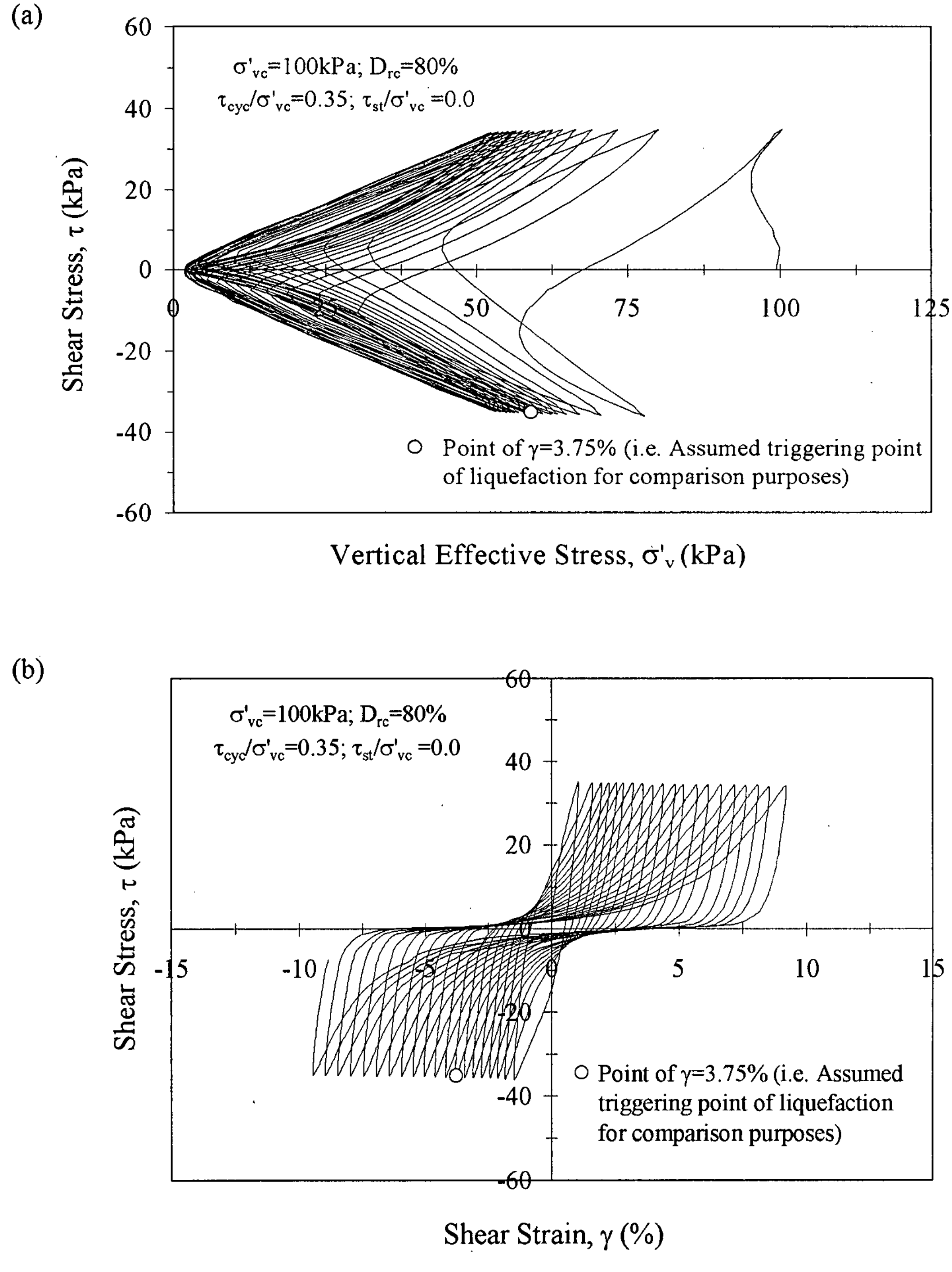

Figure 4.39 Cyclic (a) stress path and (b) stress-strain response of dense sand without initial static shear stress – Sample D3.

others from tests on water-pluviated dense sands (e.g. Kammerer et al., 2001; Seed et al., 2003).

4.2.1.1 Influence of Vertical Confining Stress and Effect of Stress Densification on the Cyclic Loading Response of Dense Sand

Figures 4.40 through 4.42 present the response of dense Fraser River sand (Type (2) samples) during cyclic DSS loading of samples, consolidated to σ'_{vc} = 200 kPa and D_{rc} = 81%, without application of initial static shear stress (i.e τ_{st} = 0) as per Series F1 (Table 3.3). The tests were aimed at assessing the effect of vertical confining stress and any associated stress densification in an integral manner. The stress-strain response is similar to those observed for the Series E1.

The variation of applied cyclic stress ratio versus number of cycles required to liquefaction (N_L) for cyclic shear tests on dense Fraser River sand conducted on samples consolidated to vertical stresses of σ'_{vc} = 100 kPa (D_{rc} = 80%) and 200 kPa (D_{rc} = 81%) are shown in Figure 4.43. The results obtained from the loose samples (from Figure 4.14) are also included in the figure for comparison. For dense samples, the number of cycles to liquefaction under a given cyclic stress ratio level decreases with the increase in initial vertical confining stress. The results are illustrated in another format in Figure 4.44, where values of CRR corresponding to N_L = 15 cycles from DSS tests on dense samples are extracted from Figure 4.43 and re-plotted with respect to σ'_v, again, along with data for loose sand. The observations are in accord with the findings regarding the effect of K_σ on cyclic resistance of sand. It appears that, in contrast to loose sand as discussed Section 4.1.2.2, the effect of stress densification is insignificant in dense sand. This is likely since the relative

(a)

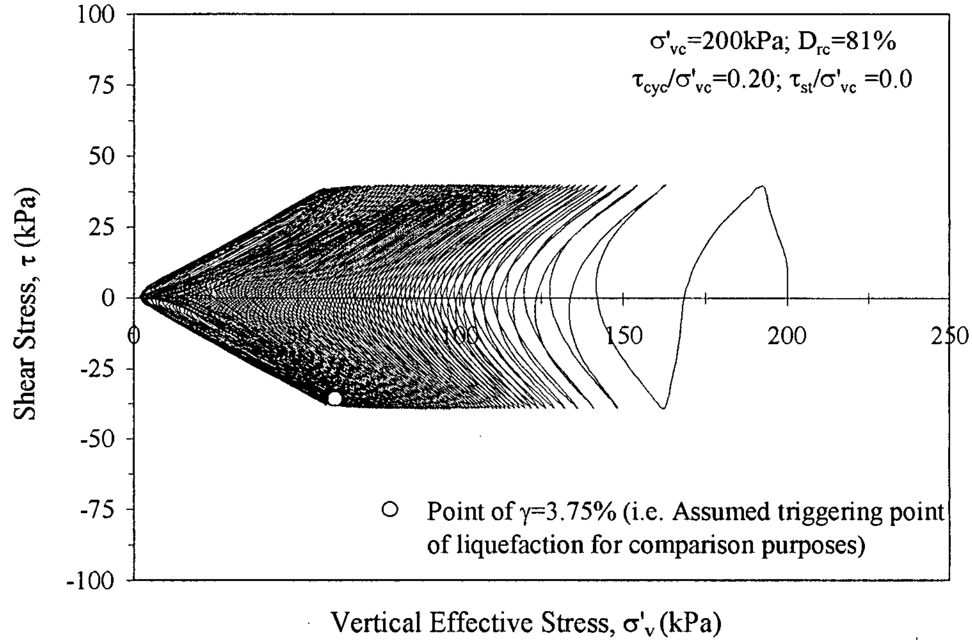

(b)

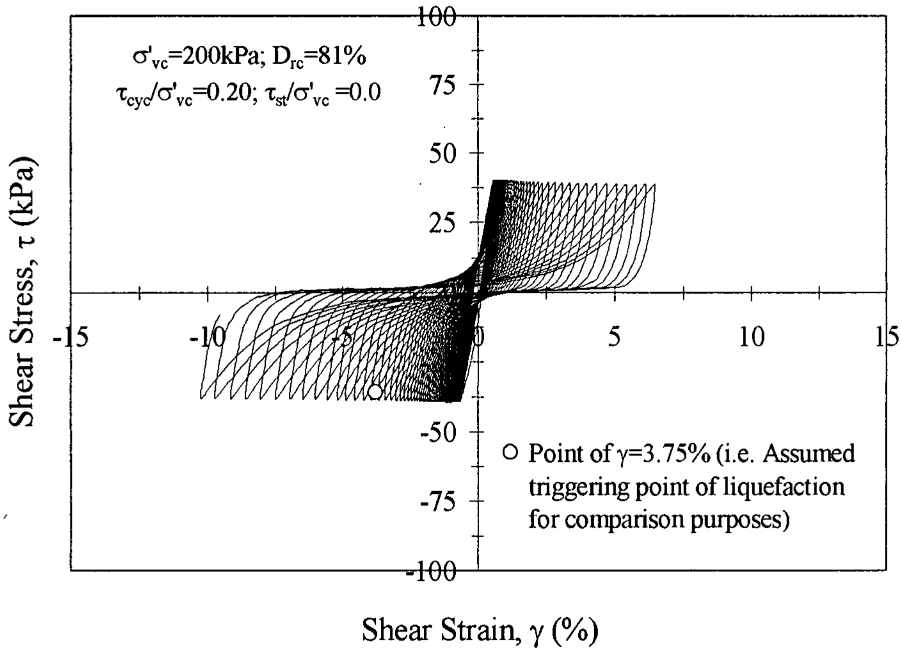

Figure 4.40 Cyclic (a) stress path and (b) stress-strain response of dense sand without initial static shear stress – Sample D4.

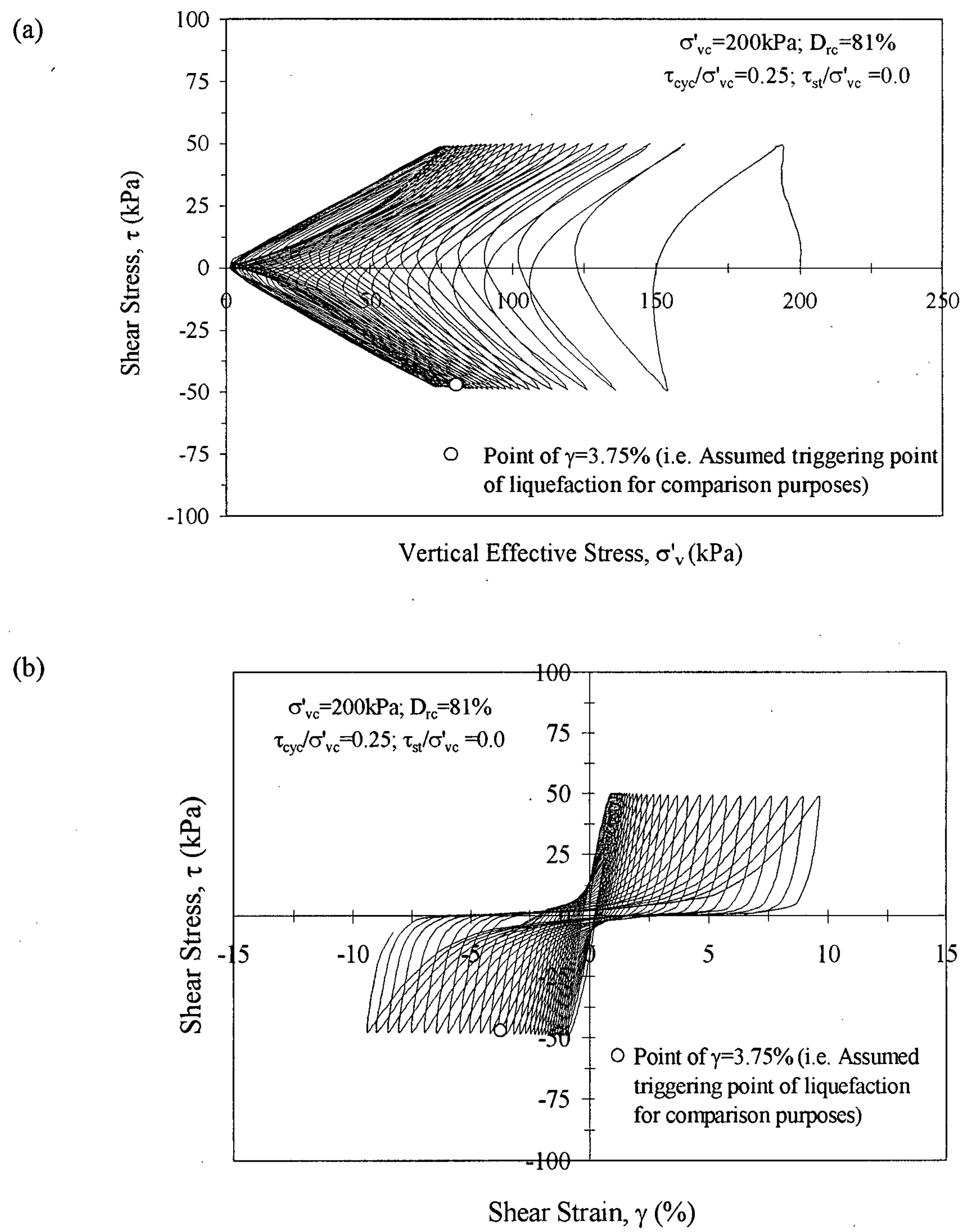

Figure 4.41 Cyclic (a) stress path and (b) stress-strain response of dense sand without initial static shear stress – Sample D5.

(a)

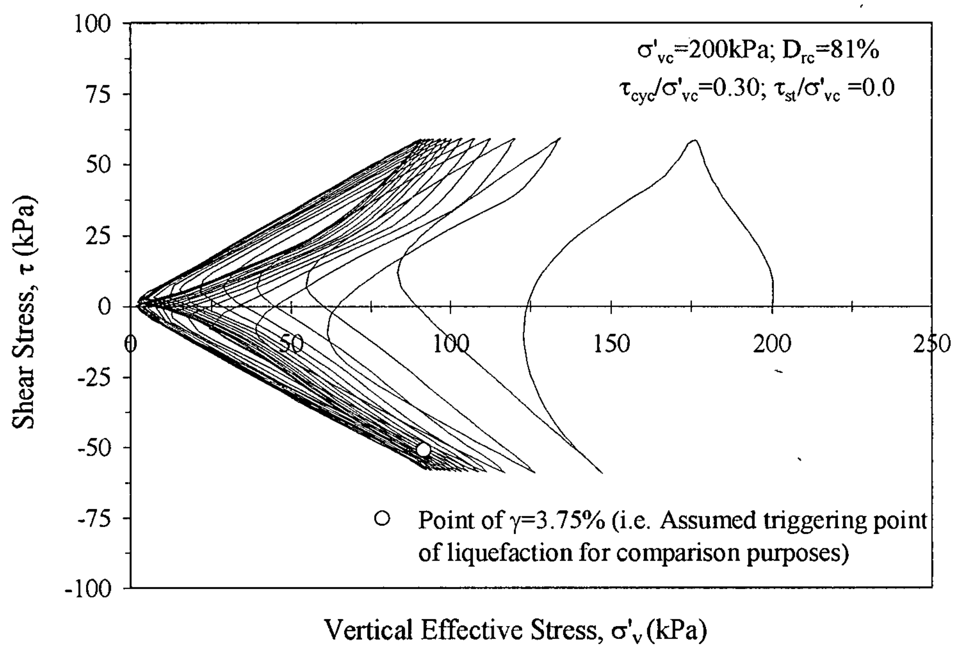

(b)

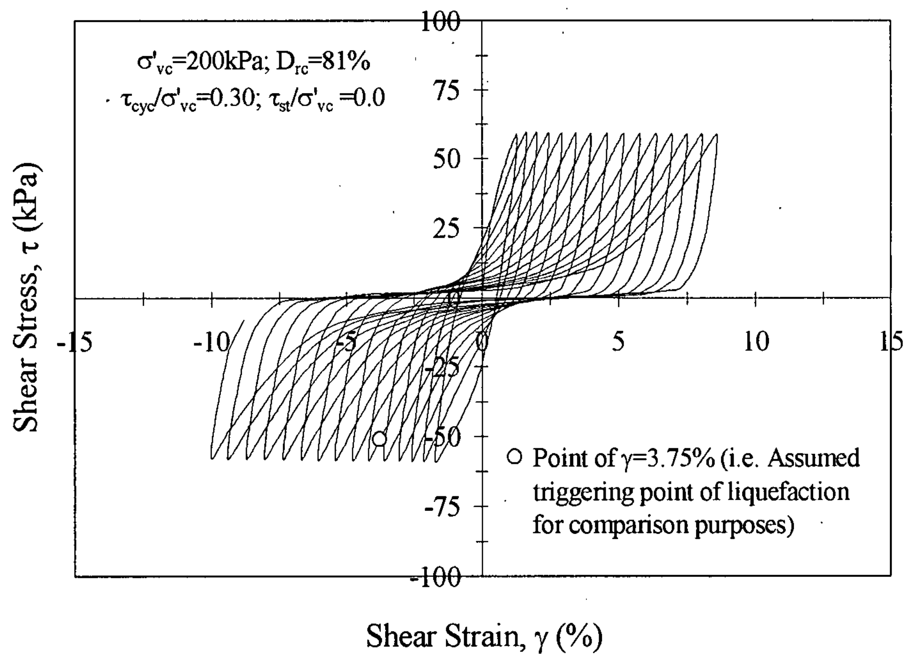

Figure 4.42 Cyclic (a) stress path and (b) stress-strain response of dense sand without initial static shear stress – Sample D6.

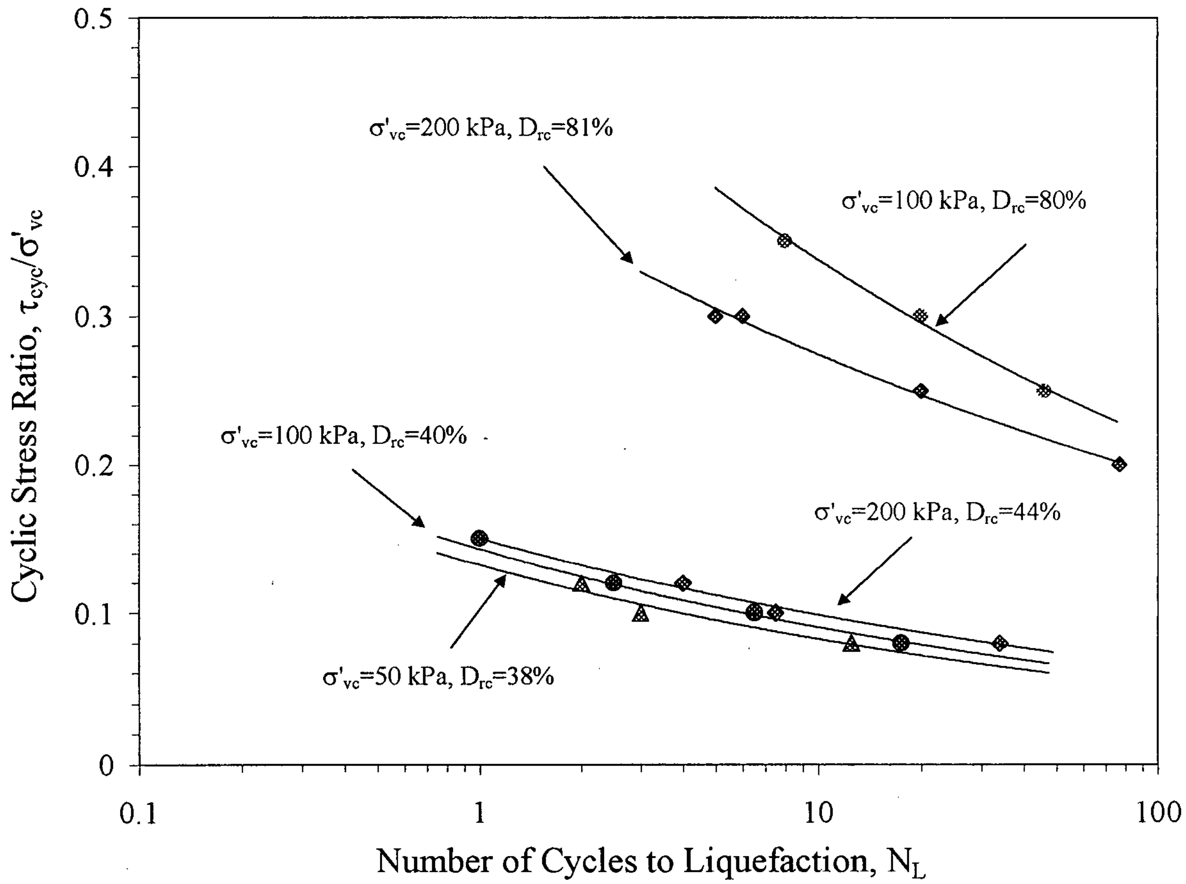

Figure 4.43 Comparison of the effect of stress densification on the cyclic resistance of dense sand with that of loose sand.

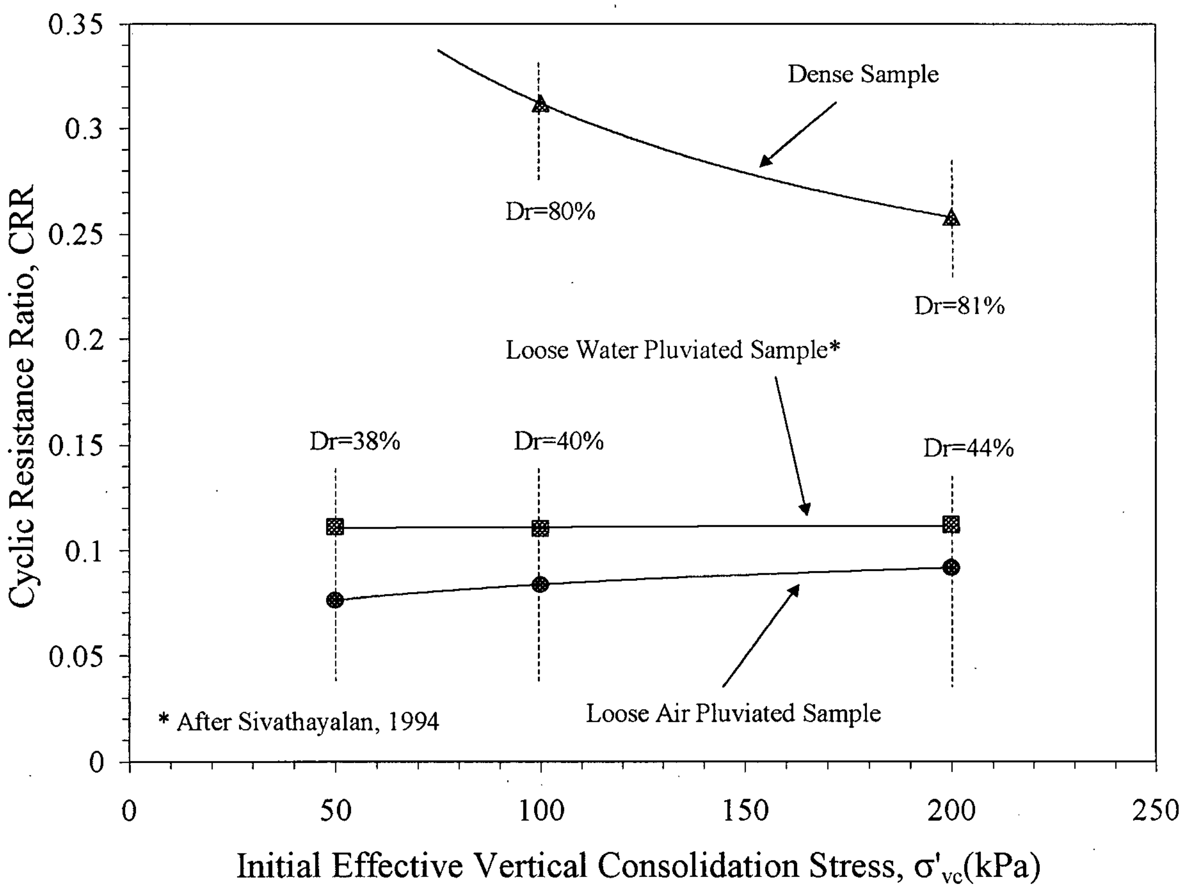

Figure 4.44 Comparison of cyclic resistance curve for dense sand with those obtained for loose sands at identical stress conditions.

density change due to the increase in confining stress from 100 kPa to 200 kPa is very little (~ 1%) and only the effect of K_σ (increasing contractive tendency with increasing confining pressure) is dominant.

4.2.2 Cyclic Loading Response – With initial Static Shear Stress Bias

Figures 4.45 through 4.47 present the cyclic response of dense Fraser River sand specimen that was initially consolidated to σ'_{vc} = 100 kPa (D_{rc} = 80%) with an initial static shear stress bias (i.e. normalized static shear stress level = $\alpha = \tau_{st}/\sigma'_{vc}$), and then subjected to cyclic loading as per Series E2 (Table 3.3). For example, the test depicted in Figure 4.45 is for a sample (D7) subjected to cyclic loading with shear stress reversal. Similar to the observed response of loose samples with shear stress reversal (Samples L15 and L19), Sample D7 finally reached zero effective confining stress level after certain number of cycles. The responses observed for the Samples D8 and D9 are also similar (Figures 4.46 and 4.47).

As may be noted from the Figures 4.45 through 4.47, all the samples exhibited reduction in effective stress (or rise in pore water pressure) with increasing number of cycles with lager dilation spikes. The results are, again, similar to the observations from the DSS tests on dense samples without initial static shear stress (Section 4.2.1), where samples exhibited lager pore water pressure generation during unloading even at the early cycles of cyclic loading.

(a)

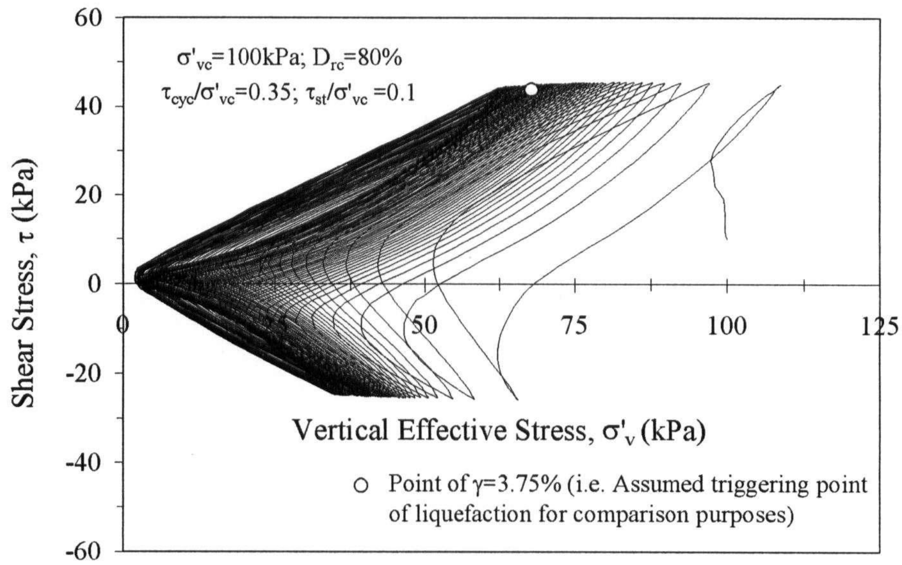

(b)

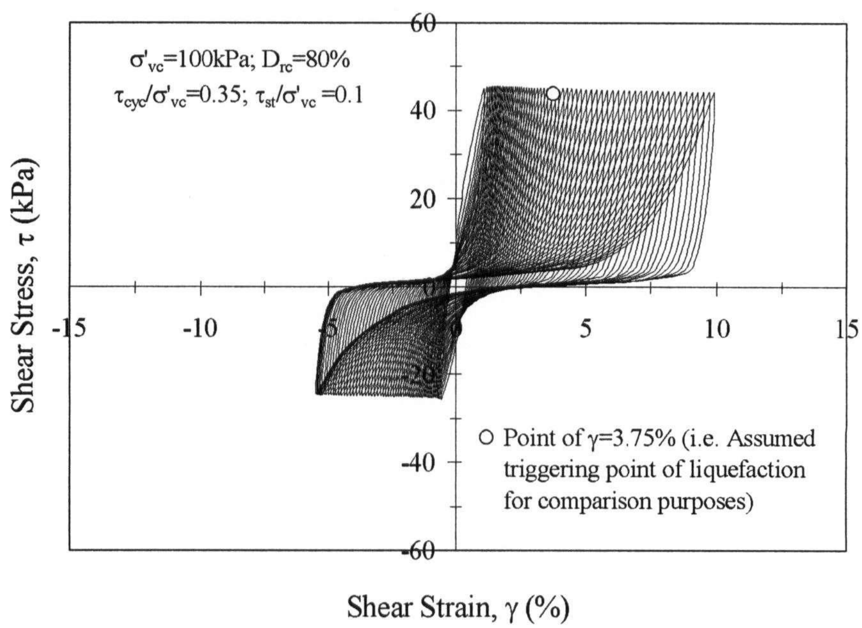

Figure 4.45 Cyclic (a) stress path and (b) stress-strain response of dense sand with initial static shear stress – Sample D7.

(a)

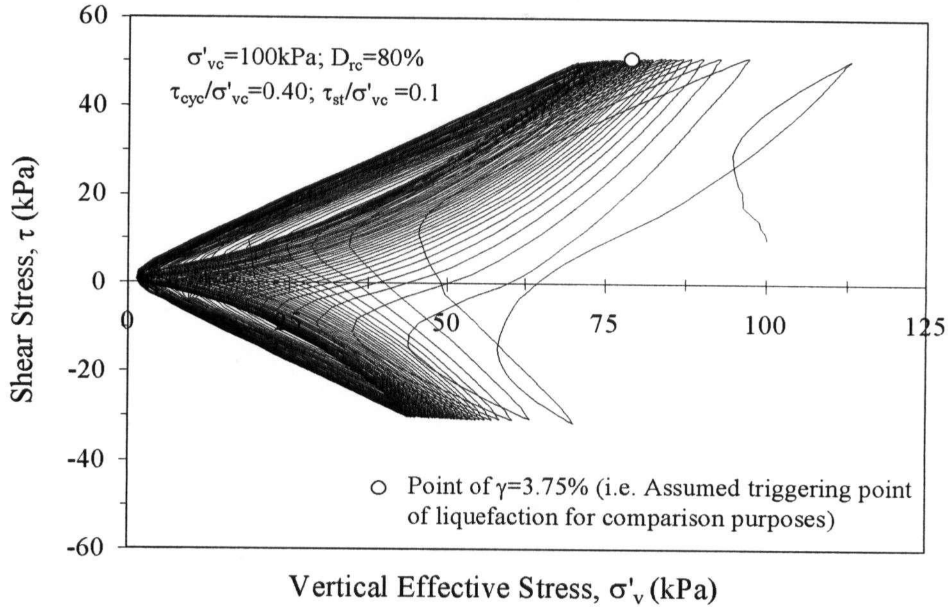

(b)

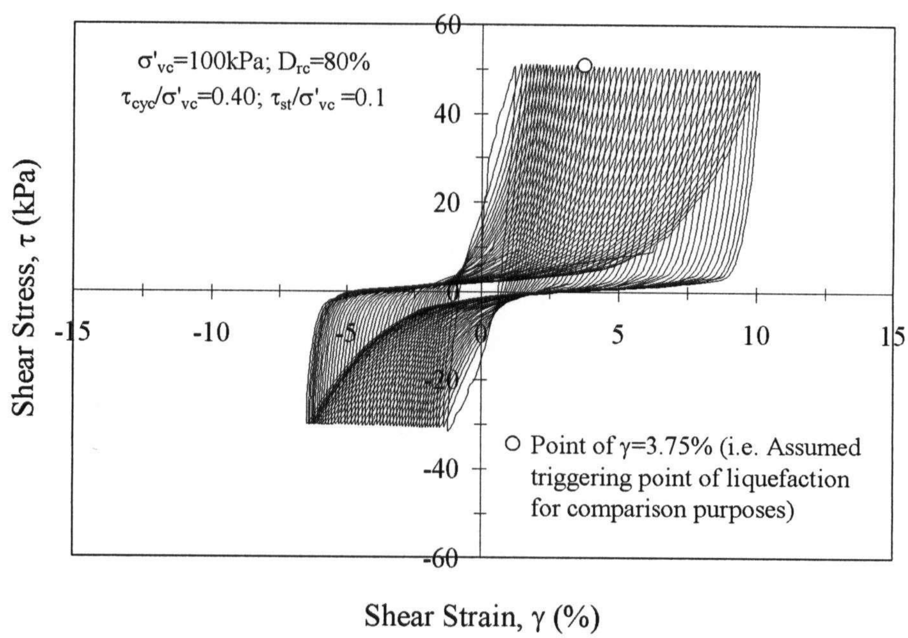

Figure 4.46 Cyclic (a) stress path and (b) stress-strain response of dense sand with initial static shear stress – Sample D8.

(a)

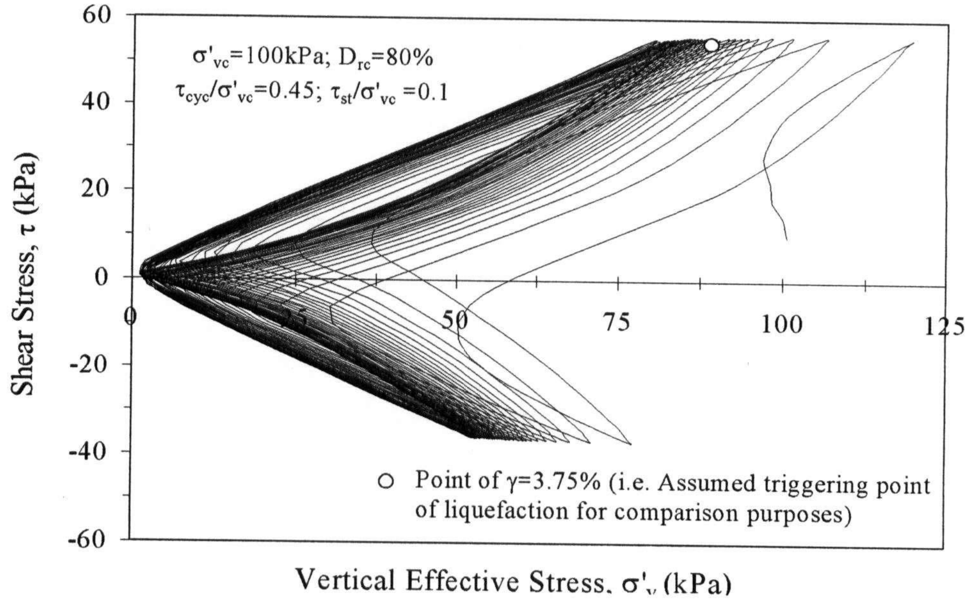

(b)

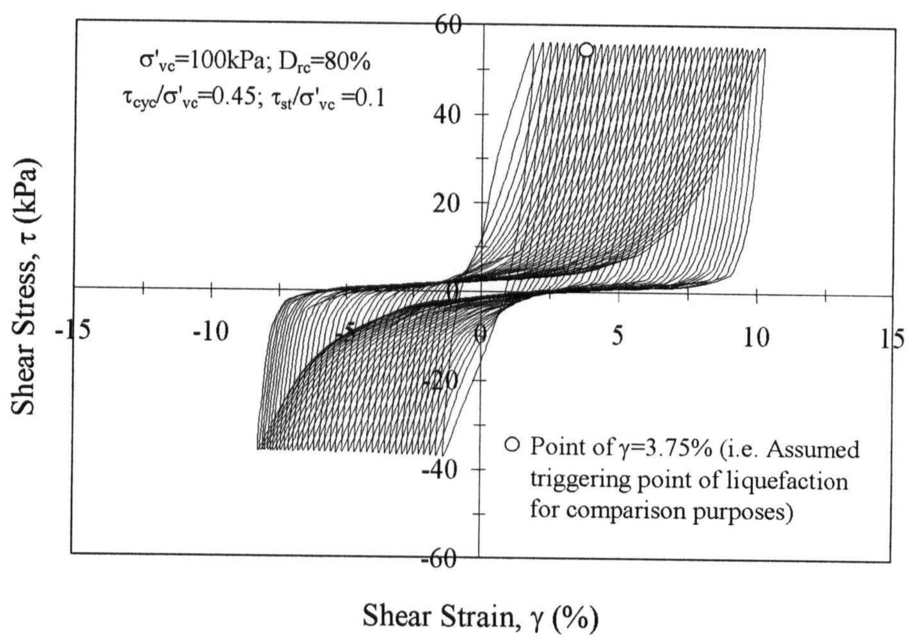

Figure 4.47 Cyclic (a) stress path and (b) stress-strain response of dense sand with initial static shear stress – Sample D9.

4.2.2.1 Cyclic Resistance (Number of Cycles to Liquefaction)

Figure 4.48 shows the variation of applied cyclic stress ratio (CSR) level versus number of cycles required to liquefaction (N_L) derived from DSS tests conducted on dense Fraser River sand with an initial static shear stress $\alpha = \tau_{st} / \sigma'_{vc} = 0.1$ plotted along with the results obtained from DSS tests on loose sand (from Figure 4.24). The dense samples were consolidated to vertical stresses of: $\sigma'_{vc} = 100$ kPa ($D_{rc} = 80\%$) and, the results are compared with those obtained from DSS tests without static bias. In contrast to loose sand, dense sand shows an increase in cyclic resistance to liquefaction in the present of initial static shear. A K_α value of 1.3 is obtained for the vertical normal effective stresses of 100 kPa (D_{rc}= 80%). This value is slightly higher than the upper bound of the K_α values for sands suggested by Harder and Boulanger (1997) for $\alpha = 0.1$ and σ'_{vc} values less than 300 kPa, but for a smaller relative density (D_{rc}) condition of 70%. As mentioned earlier, since Harder and Boulanger (1997) relations are understood to be weighted more heavily towards data obtained from direct simple shear and torsional simple shear tests, they are compatible with the loading mode used in the present study.

4.3 DRAINED SIMPLE SHEAR RESPONSE OF FRASER RIVER SAND

4.3.1 Response of Loose Sand (Type (1) Samples)

Figure 4.49 and 4.50 present the drained cyclic loading response of several samples of loose air-pluviated Fraser River sand {Type (1)} samples, consolidated to $\sigma'_{vc} = 100$ kPa and $D_{rc} = 40\%$, loaded in a strain-controlled manner to different shear strain amplitudes as per Series G1 and G2 (Table 3.4), respectively. The samples in Series G2 were sheared with a larger rate of shear strain (20% strain/hour) than those in Series G1 (10% strain/hour). This

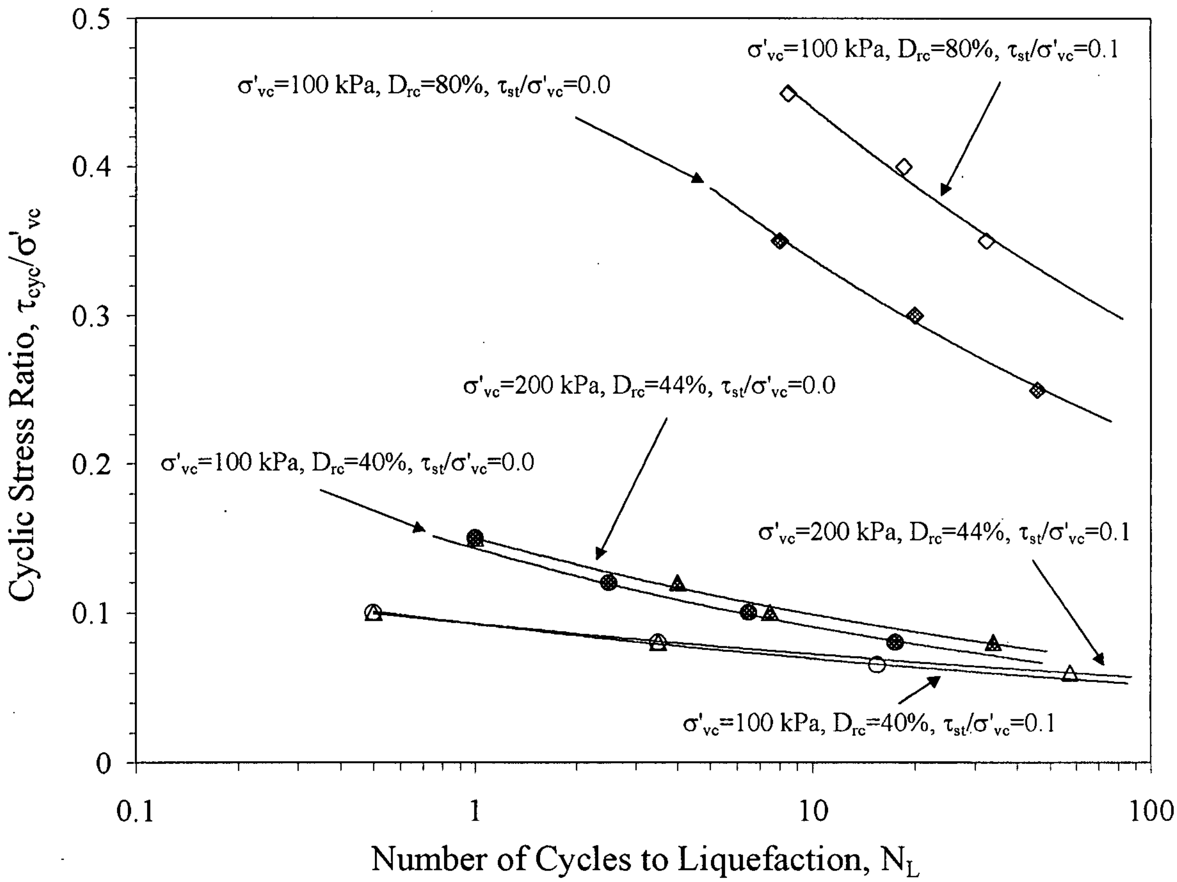

Figure 4.48 Comparison of cyclic resistance curves for dense and loose sand with and without initial static shear stress.

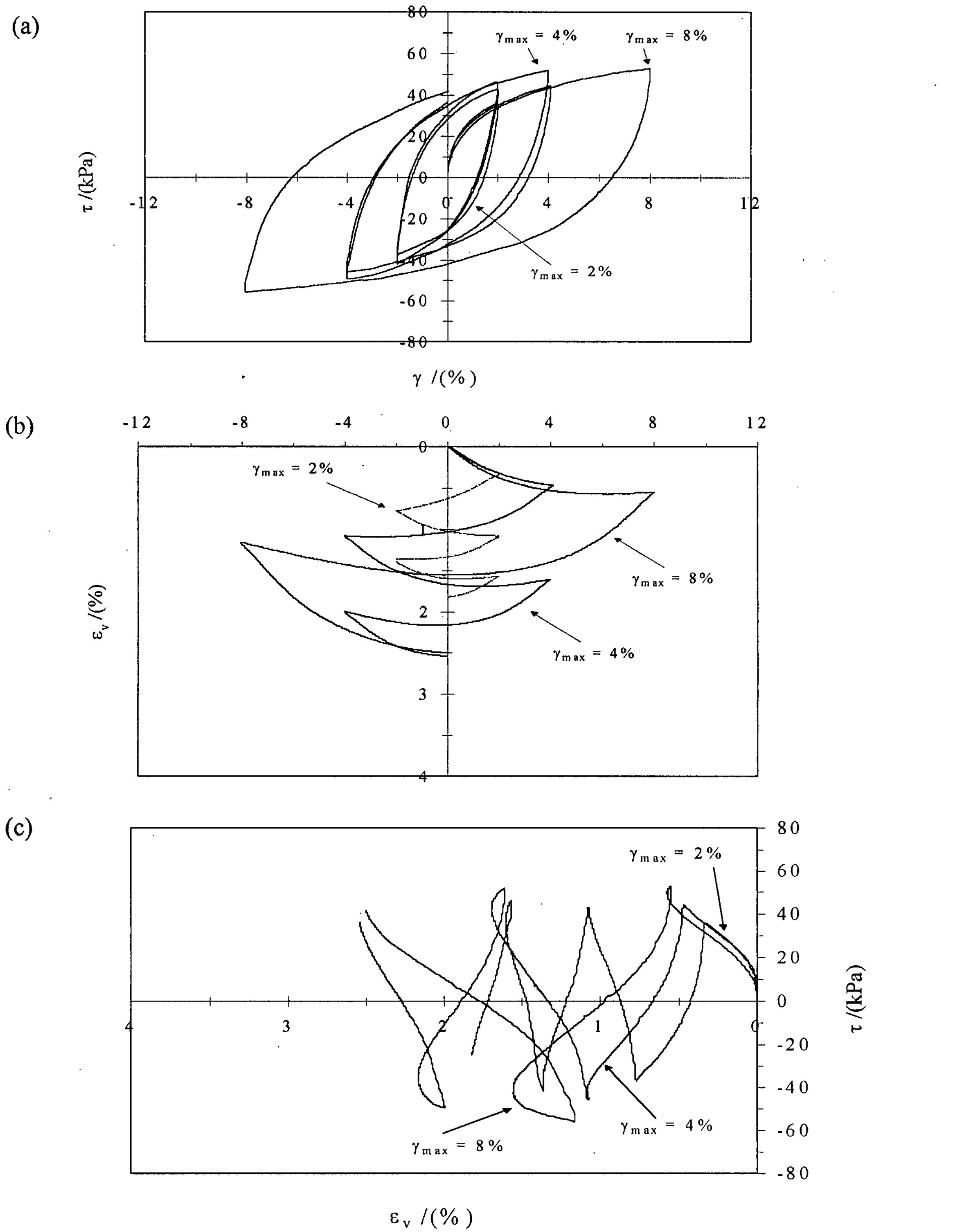

Figure 4.49 Cyclic drained simple shear response of loose air-pluviated Fraser River sand (Rate of Strain 10% per hour).

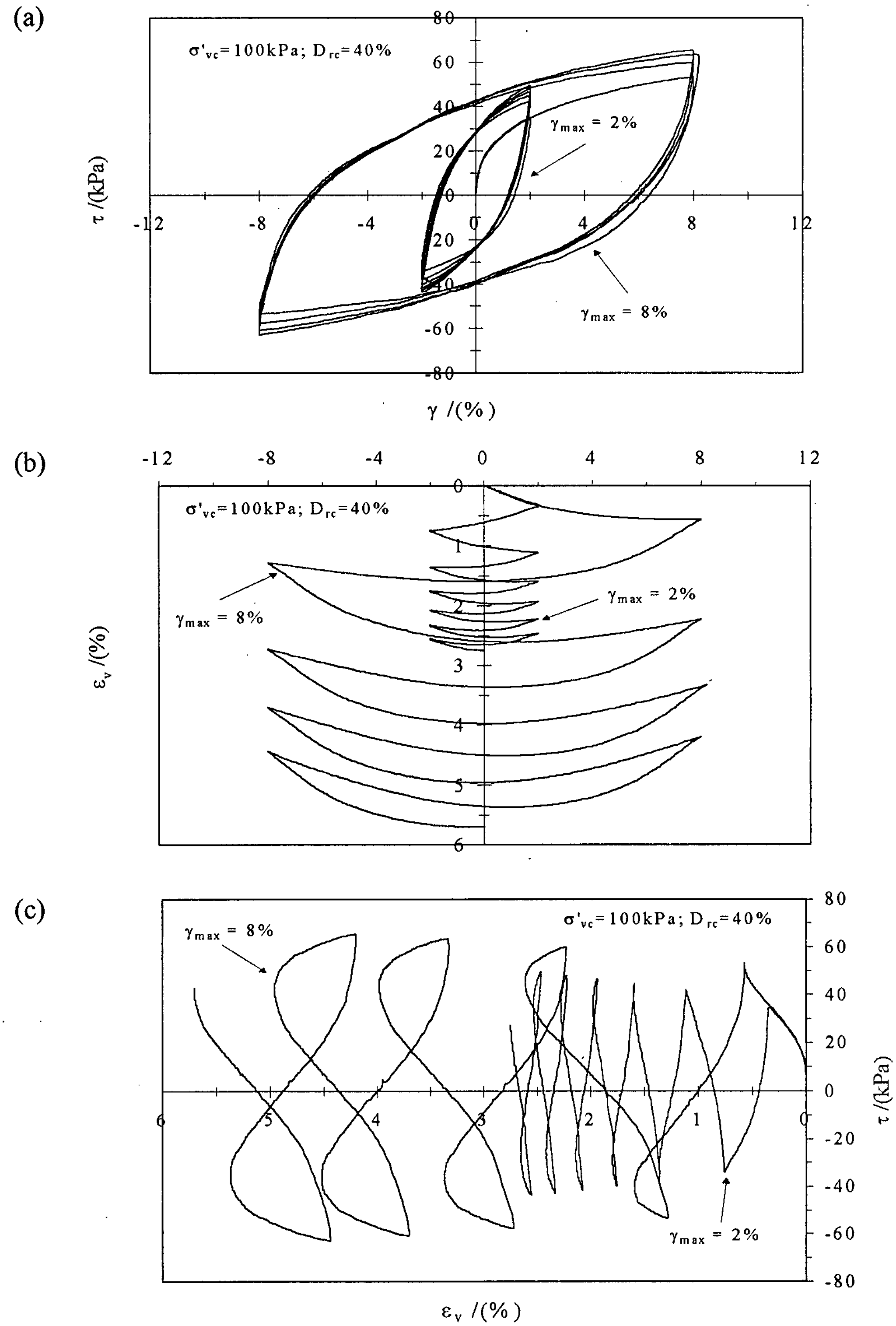

Figure 4.50 Cyclic drained simple shear response of loose air-pluviated Fraser River sand (Rate of Strain 20% per hour).

rate change was made in order to reduce the total time required for testing since the samples in Series G2 were sheared to a lager number of cycles than those Series G2. As can be seen in Figures 4.49(b) and 4.50(b), shear-induced volumetric strain accrues with increasing number of cycles and amplitude of shear strain. The shear-induced volumetric strain during both loading and unloading phases of the first half cycle increases with increasing shear strain amplitude. It is also of interest to note that this volumetric strain during the unloading phase is significantly greater for the sample, which had been sheared to a shear strain amplitude of 8% compared to those for the samples with 2% and 4%. It was observed that the sample that was strained to 8% dilated during the first loading. The effect of dilation during the loading phase is to induce a large plastic contraction upon unloading. This is consistent with the large reduction in effective stress in undrained tests upon unloading after phase transformation has occurred.

4.3.1.1 Volumetric Strain Vs Number of Cycles

Figure 4.51(a) presents the variation of shear-induced volumetric strain with number of cycles plotted in values corresponding to every half cycle. As may be noted, the development of net volumetric strain with number of cycles appears to be independent of the time rate of shear strain used for the tests. This is in agreement with the already noted strain rate/frequency independent behaviour of sand by Youd (1972).

It can also be seen that the volumetric strain increases with increasing shear strain amplitude (γ_{max}), but it is not directly proportional to γ_{max}. This is in contrast to the noted proportionality of ε_v to γ_{max} by Martin et al. (1975) based on data from cyclic shear tests conducted using only small amplitudes of cyclic shear strain. As such, the discrepancy between the observations from the present study and those from Martin et al. may be mainly due to difference in level of shear strain amplitude. Since the samples in the present study have been sheared to larger strain levels, they experienced dilation during the loading phase and this, in turn would have contributed to the volumetric strains non-proportional to γ_{max}.

In seeking the possibility of a regular pattern for the development of ε_v with number of cycles, the volumetric strain curves in Figure 4.51(a) were normalized with respect to the value of volumetric strain corresponding to a certain number of cycles (say after 1 or 2 cycles). Such normalized results are plotted in Figure 4.51(b). When normalized, the results seem to fall on a single curve, indicating that the similarity of the shape of the volumetric strain development characteristics for different amplitudes of strain. This suggests that it may be possible to predict the shear-induced volumetric strain with number of cycles for any γ_{max} by knowing the relationship between the volumetric strain after first cycle (ε_{v1}) and γ_{max}. Based on the results for Fraser River sand from this study, ε_{v1} versus γ_{max} is presented in Figure 4.52, and this relationship can be expressed using an equation as below

$$\varepsilon_{v1} = A_1 \gamma^{A2} \qquad [4.3]$$

where $A_1 = 0.66$ and $A_2 = 0.65$ (for air-pluviated Fraser River sand with a $D_r = 40\%$).

The shear-volume coupling model for sand presented by Byrne (1991) for cyclic shear loading has been based on tests conducted with small strain amplitudes. In tests with

(a)

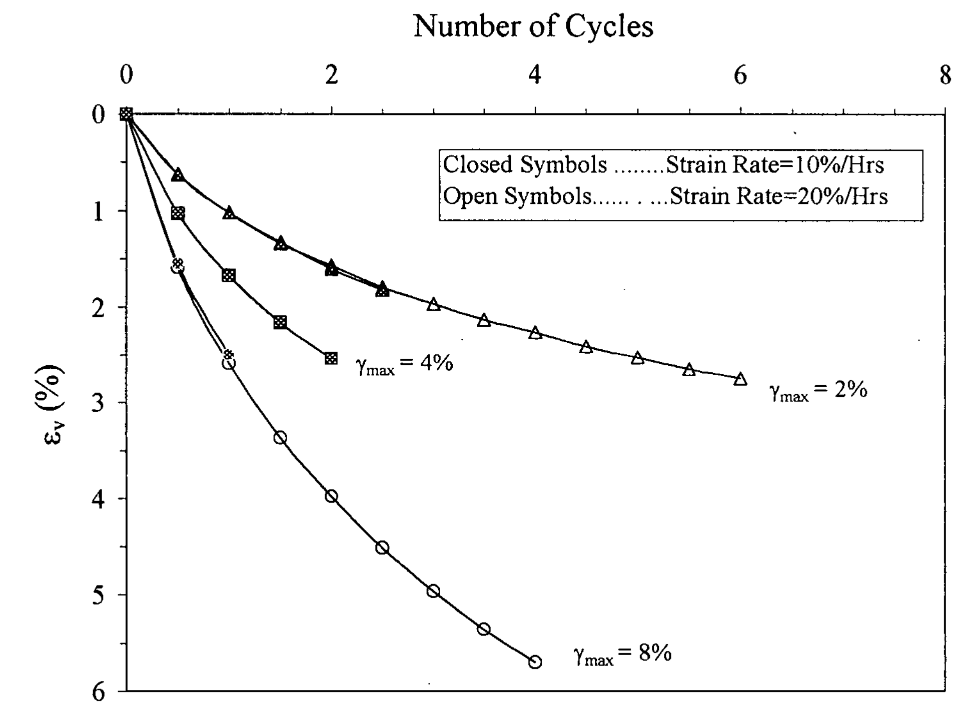

(b)

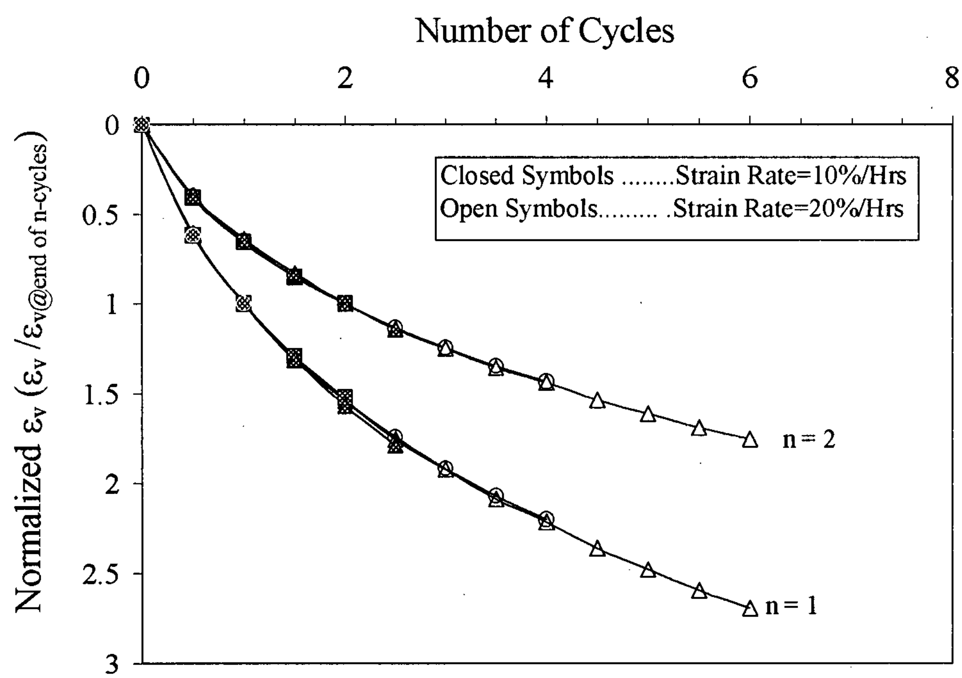

Figure 4.51 Variation of (a) absolute and (b) normalised volumetric strain with number of cycles in drained cyclic simple shear tests.

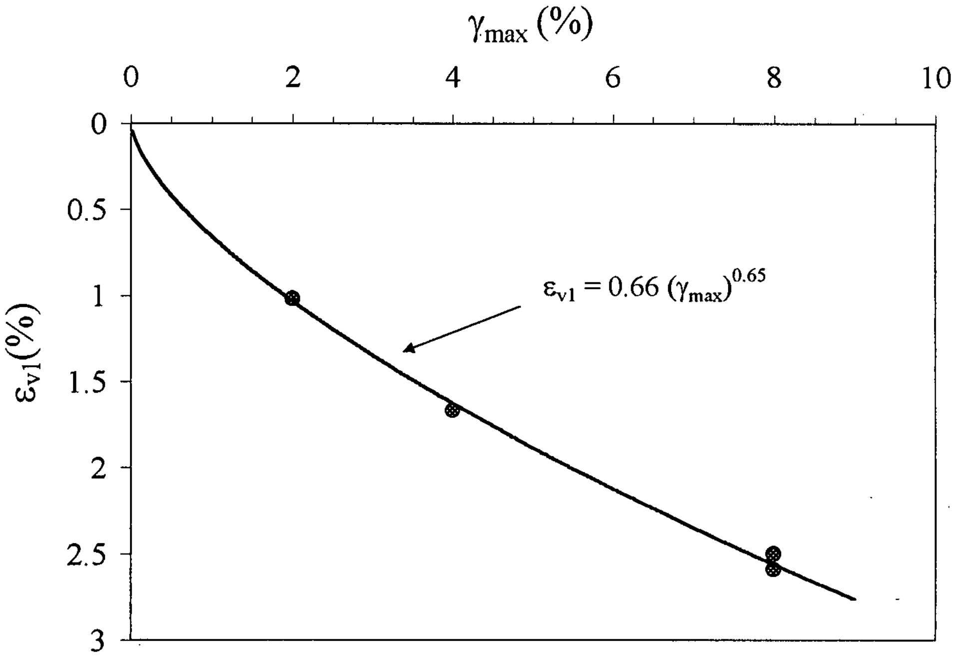

Figure 4.52 Variation of volumetric strain at the end of first cycle (ε_{v1}) with the amplitude of cyclic shear strain (γ_{max}) in drained cyclic simple shear tests.

small strain amplitudes, the volumetric strain is proportional to the shear strain as per Martin et al. (1975). Since the volumetric strain is not proportional to the shear strain at large strains as shown in Figure 4.51, the shear-strain coupling relation proposed by Byrne (1991) cannot be extrapolated to large strains. If a fictitious volumetric strain ε_v^* as in Equation [4.4] below is introduced, ε_v^* would be proportional to γ_{max}.

$$\varepsilon_v^* = (\varepsilon_v.\gamma)/\varepsilon_{v1} \qquad [4.4]$$

Now, examination of a plot of $(\Delta\varepsilon_v^*/\gamma)$ versus (ε_v^*/γ) reveals that all the data would collapse to a unique relationship as shown in Figure 4.53. As may be noted in the figure, this relationship can be expressed as:

$$(\Delta\varepsilon_v^*/\gamma) = C_1 \mathrm{Exp}\{-C_2(\varepsilon_v^*/\gamma)\} \qquad [4.5]$$

where $C_1 = 0.60$ and $C_2 = 0.70$ for the air-pluviated Fraser River sand with a $D_r = 40\%$, and this equation has the same format as the 2-parameter model proposed by Byrne (1991). Now the new shear-volume coupling can be obtained from the above-obtained relationships as follows:

From Eq. [4.4] and [4.5]: $$\{\Delta(\varepsilon_v)/\varepsilon_{v1}\} = C_1 \mathrm{Exp}\{-C_2((\varepsilon_v)/\varepsilon_{v1})\} \qquad [4.6]$$

From Eq. [4.3] and [4.6]: $$\Delta\varepsilon_v = C_1 A_1 \gamma^{A2} \mathrm{Exp}\{-C_2[\varepsilon_v/(A1\ \gamma^{A2})]\} \qquad [4.7]$$

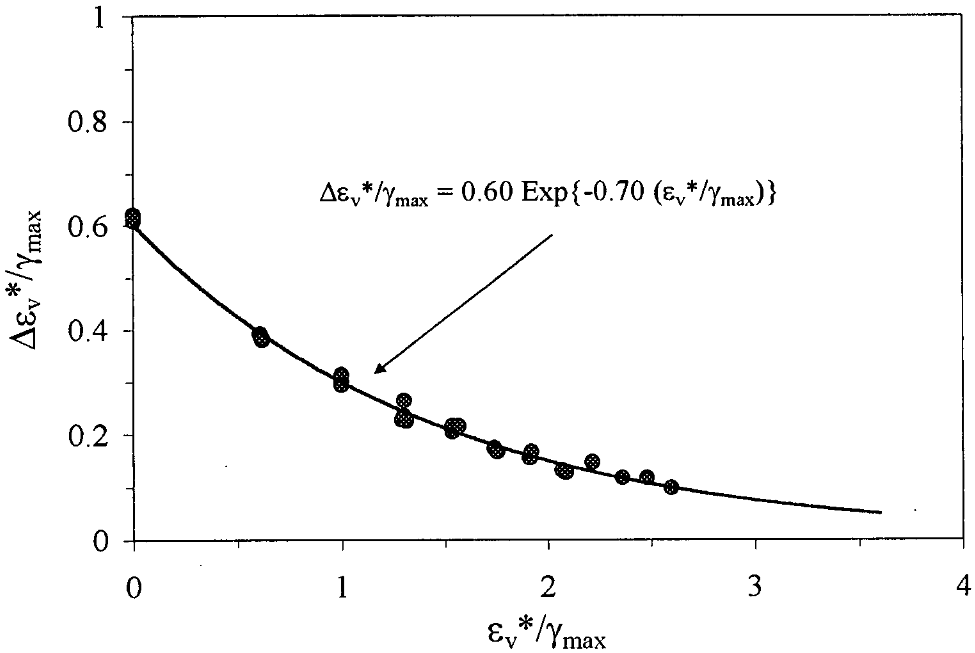

Figure 4.53 Relationship between $\Delta\varepsilon_v^*/\gamma_{max}$ and $\varepsilon_v^*/\gamma_{max}$ for air-pluviated Fraser River sand with D_r= 40%.

$$\Delta\varepsilon_v = A\gamma^C \mathrm{Exp}\{-B\varepsilon_v / \gamma^C\} \qquad [4.8]$$

where $A = C_1A_1$, $B = C_2/A_1$, and $C = A2$; for air-pluviated Fraser River sand with $D_r = 40\%$ $A = 0.4$, $B = 1.1$, and $C = 0.65$.

The Equation [4.8] was developed based on data from tests with $\gamma_{max} = 2$, 4, and 8%. The obtained relationship was verified against the experimental dada obtained for test with $\gamma_{max} = 5\%$. As can be seen in Figure 4.54 the predicted values are in good agreement with the experimental results for $\gamma_{max} = 5\%$ confirming the suitability of the new shear-volume coupling relationship.

4.3.2 Response of Dense Sand (Type (2) Sample)

Figure 4.55 presents the drained cyclic loading response of dense Fraser River sand {Type (2)} for a test conducted with a cyclic loading amplitude $\gamma_{max} = 4\%$. The results from a loose {Type (1)} sample is also presented in the same figure for comparison. In contrast to the loose sample, the dense sample shows significant dilation during loading cycles and relatively small cumulative volumetric strains. As can be seen in Figures 4.55(b), the dense sample shows progressive increase in cumulative volumetric strain with number of shear cycles in a trend similar to loose samples. This observation is also in accord with the undrained cyclic shear response of dense sand observed in Section 4.2.1, where the excess pore water pressure gradually increased with increasing number of cycles despite the lager dilation spikes in the loading cycles. It can also be noted that there is a significantly large shear-induced volumetric strain during unloading phases of cyclic loading.

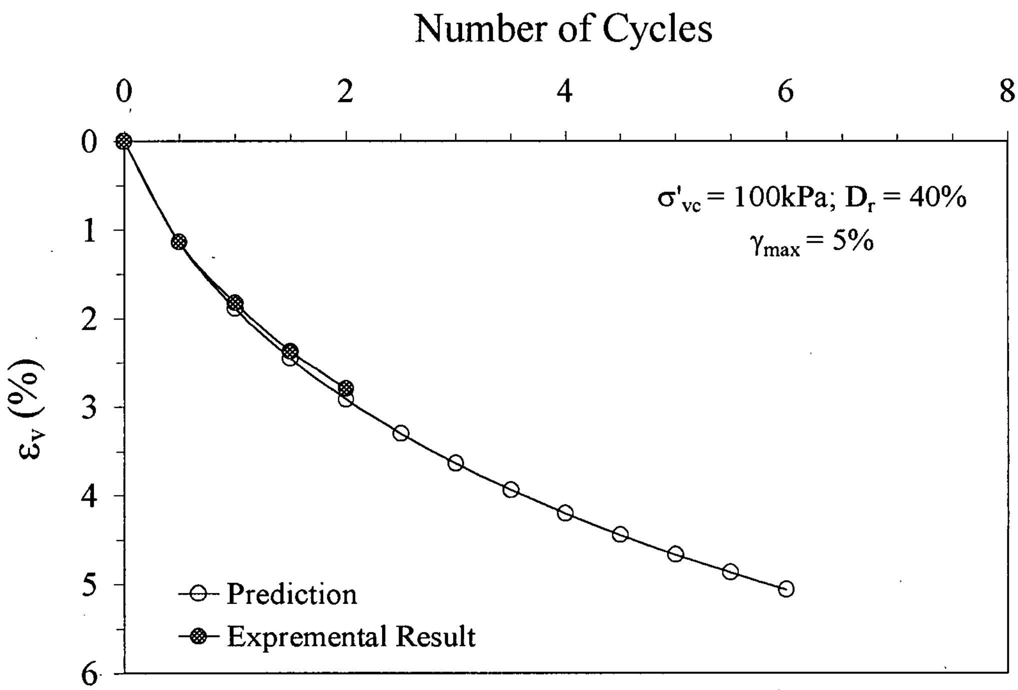

Figure 4.54 Comparison of predicted and measured volumetric strain with number of cycles for γ_{max} =5%.

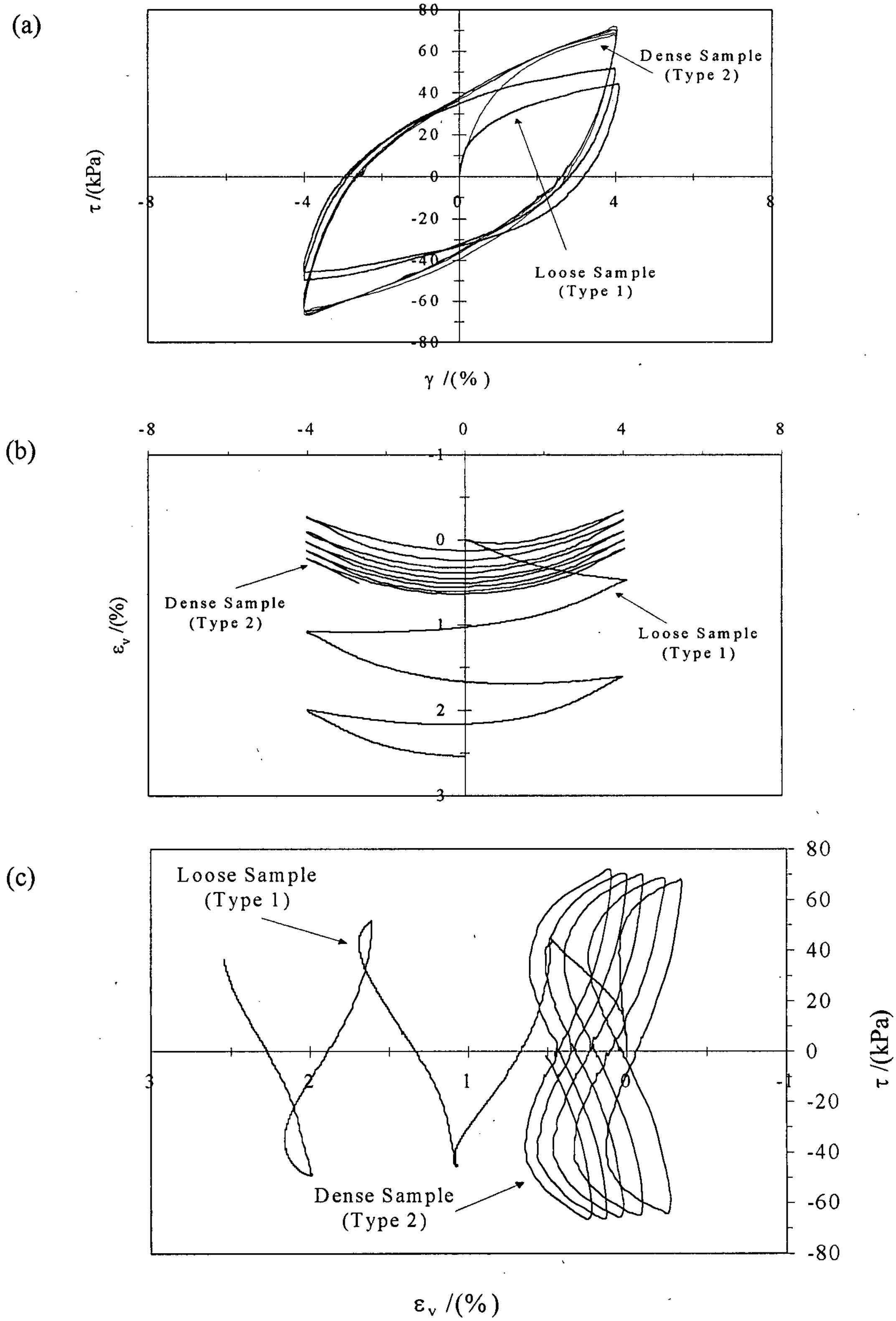

Figure 4.55 Comparison of Cyclic drained simple shear response of loose and dense Fraser River sand (γ_{max} = 4%).

4.3.2.1 Volumetric Strain Vs Number of Cycles

Figure 4.56 (a) presents the variation of shear-induced volumetric strain with number of cycles for the dense sand test along with those observed the loose sands. Similar to the approach used for loose sands, the volumetric strain for the dense sand test was normalized with respect to the volumetric strain that was observed at the end of 1st and 2nd cycles, and plotted in Figure 4.56(b). The normalized results for the dense sample is different for those developed for the loose samples (see Figure 4.55(b)). This may be due the differences in the density as well as the sample fabric. (Note: Type (1) and Type (2) samples are judged to have significantly different fabric, even when their densities are same, because of the difference in the sample reconstitution as described in Section 3.5.1).

Similar to the case of loose sand, a relationship between ($\Delta\varepsilon_v^*/\gamma$) and ($\varepsilon_v^*/\gamma$) was attempted for the results from dense sand. As shown in Figure 4.57, the normalized curve for the dense sample lies above that obtained for the loose sample. The derived value of the coefficient C1 is 0.6, which is essentially same as that for both loose sand. However, the derived value of the coefficient C2 for the dense sample is 0.54 is smaller than the value of 0.7 that was derived for loose sand.

It is, however, noted that the above observations have been made using limited data from 4.75 cycles of shear loading on a single specimen of dense sand. As such, detailed assessments such as those undertaken to investigate the shear-volume coupling of sand (Section 4.3.1.1) is not warranted herein.

(a)

(b)

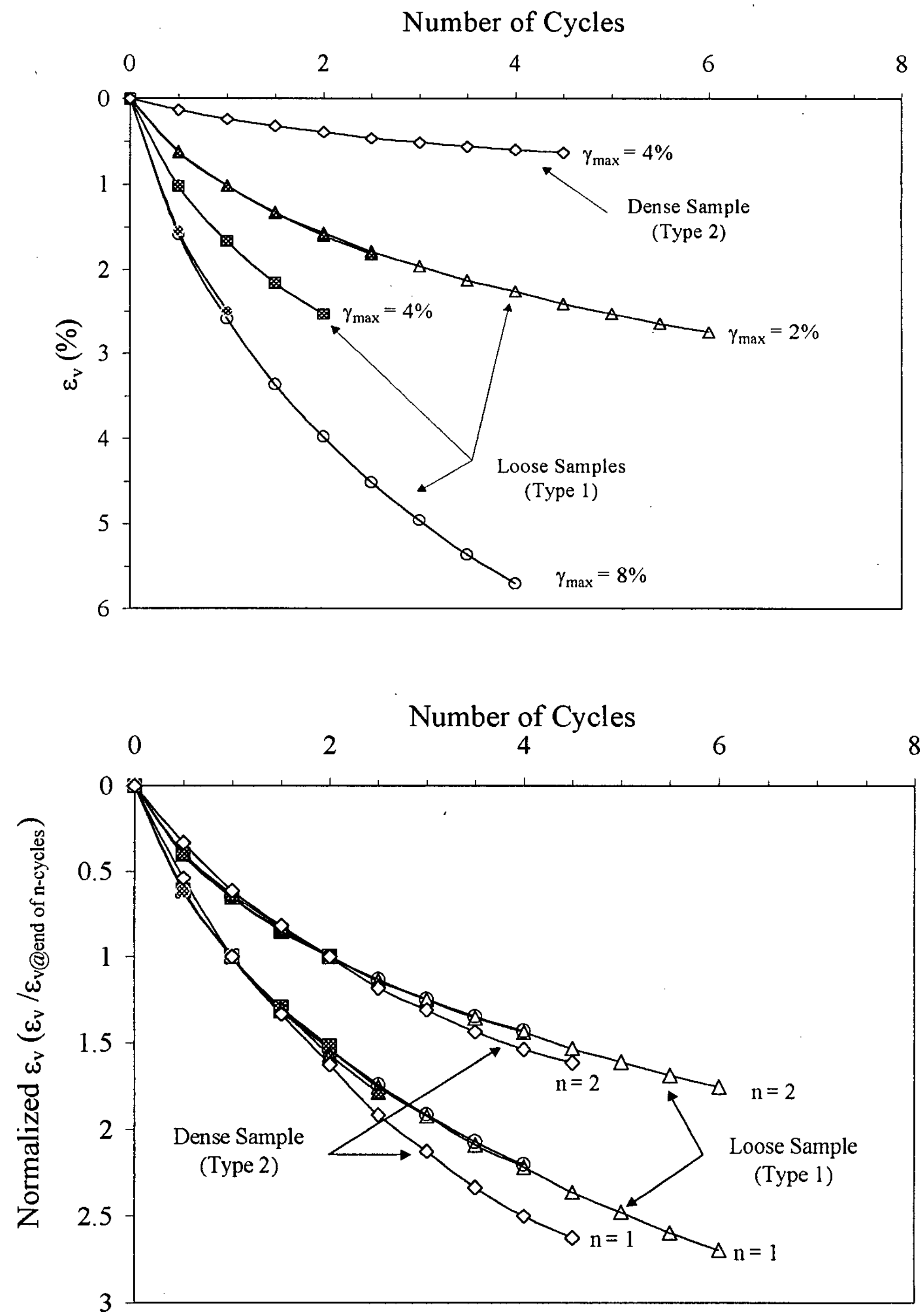

Figure 4.56 Comparison of the Variation of (a) absolute and (b) normalised volumetric strain with number of cycles for loose and dense Fraser River sand in drained cyclic simple shear tests.

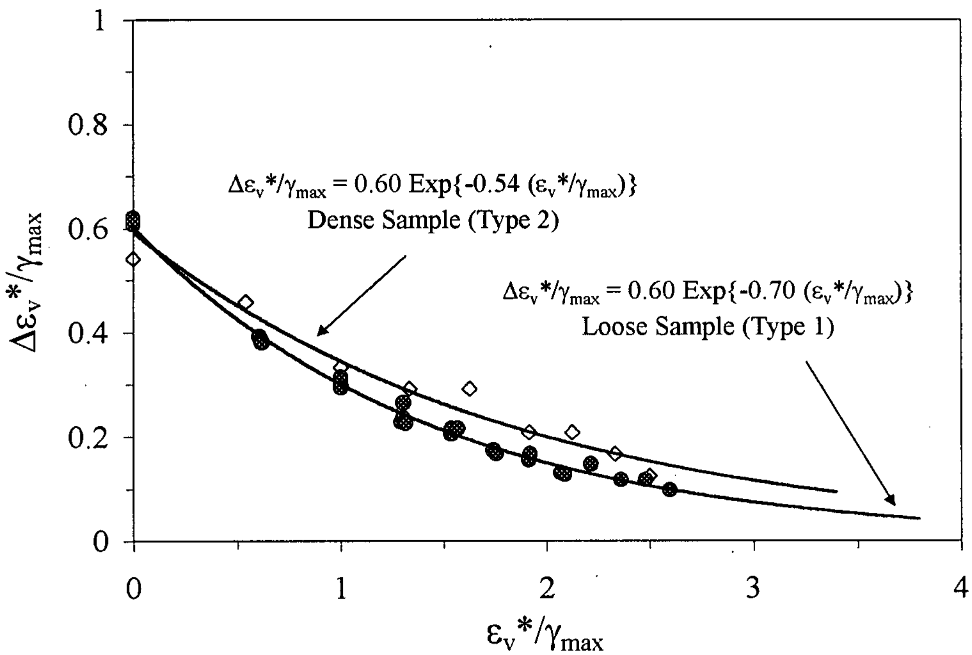

Figure 4.57 Relationship between $\Delta\varepsilon_v^*/\gamma_{max}$ and $\varepsilon_v^*/\gamma_{max}$ for loose and dense Fraser River sand.

4.4 EFFECT OF IMPARTED VIBRATIONS DURING SAMPLE PREPARATION ON STRESS-STRAIN RESPONSE OF FRASER RIVE SAND

Figure 4.58 shows stress paths and stress-strain responses of two loose Fraser River sand samples with identical initial conditions (Dr = 40%, σ'_{vc} = 100 kPa) but reconstituted using different approaches, subjected to monotonic constant volume simple shear loading. In the first approach, the sample is of Type (1) (see Section 3.5.1.1) that reached the target relative density of 40% when consolidated to a vertical stress of 100 kPa. The second sample is of Type (3) (see Section 3.5.1.3), and it reached the same target relative density of 40% upon consolidation to a 100 kPa vertical stress. Essentially, the samples prepared using the two approaches are identical with regard to the method of placement, density, and the confining stress, except for the vibration imparted during the preparation of the latter. The responses of the two samples under monotonic shear loading are presented in Figure 4.58. The sample prepared without vibration showed a limited-liquefaction type of a stress-strain response. In contrast, the sample that was subjected to vibration clearly exhibited a dilative, strain-hardening response. These observations suggest that particle fabric is influenced not only by the mode of deposition, but also by other actions such as external vibrations. A greater part of previous studies conducted on re-constituted sands has been based on tests conducted on samples prepared using water-pluviation followed by vibration, with the implicit assumption that vibration is not a major contributor to the changes in fabric. However, the limited results presented herein demonstrate that this assumption may not be always valid, and that particle fabric is an important consideration in the re-constitution of soil samples.

(a)

(b)

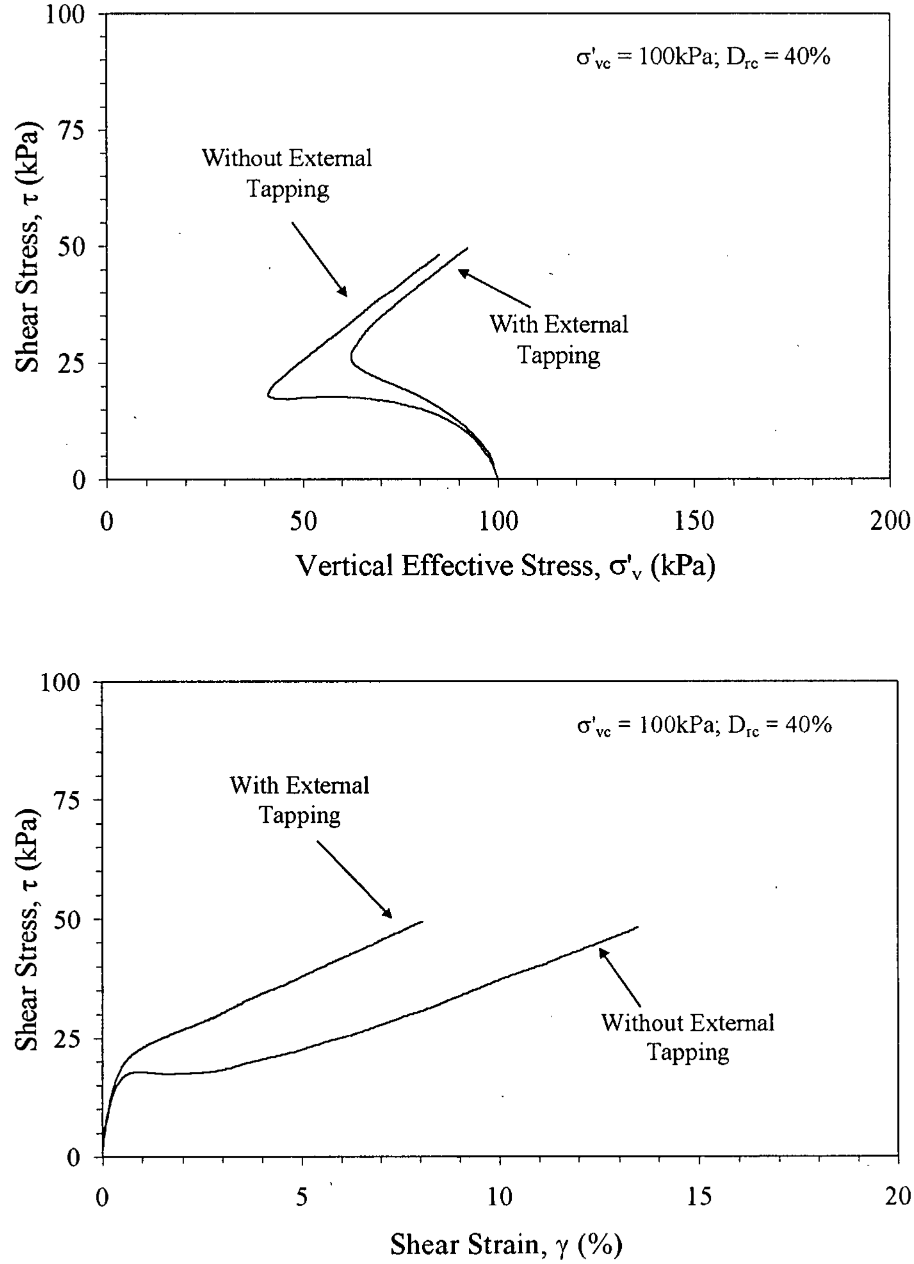

Figure 4.58 Comparison of (a) stress paths and (b) stress-strain response of air-pluviated samples prepared with and without external tapping.

CHAPTER 5

SUMMARY AND CONCLUSIONS

A detailed laboratory element testing research program was undertaken to investigate the cyclic undrained shear response of Fraser River sand. The element response of the sand was observed in constant-volume direct simple shear (DSS) tests conducted with and without initial static shear stress conditions.

This chapter presents the summary and conclusions drawn from the contents of this thesis. Since the information is arising from several key areas of research (as described in detail in Chapters 4.1 through 4.5), the infornation below is also presented as separate subsections, for maintaining clarity and orderliness.

5.1 Undrained Cyclic Loading Response of Loose Fraser River sand

While the trends of stress-strain and effective stress change (or pore water pressure development) under cyclic loading are generally similar to those noted previously for loose water-pluviated sand, the loose samples of Fraser River sand prepared using air-pluviation were identified to be more susceptible to liquefaction than their water-pluviated counterparts. Since the comparisons between the responses arising from the two sample re-constitution methods were made at the same relative density (void ratio) and confining stress levels, the difference in liquefaction susceptibility can be attributed to differences in the particle structure resulting from the two placement methods. This further corroborates the importance of incorporating particle structure in the assessment of mechanical response of sands including liquefaction susceptibility.

In the case of loose air-pluviated sands, increase in relative density due to increase in confining stress (stress densification) can cause a significant increase in cyclic shear resistance. This has broad implications, particularly in the interpretation of observations from centrifuge testing. Since stress gradients arising from centrifugal accelerations could lead to significant density non-uniformities in sand specimens that initially had uniform densities, it is important that the effect of stress densification is duly accounted for in the interpretation of centrifuge observations as well as in the laboratory element tests that are undertaken to provide input for numerical modelling. The noticeable effect of stress densification on the cyclic resistance observed with respect to air-pluviated samples does not appear to be present for the case of water-pluviated samples. This contrast can possibly be attributed to the difference in the fabric between the air-pluviated and water-pluviated sands.

The effect of initial static shear stress reduces the cyclic shear resistance of loose air-pluviated Fraser River sand. While the assessed K_α values (~ 0.8), for loose air-pluviated sand, are in reasonable agreement with those previously suggested for loose sands based on data mainly derived from DSS and torsional simple shear tests, they are not in line with K_α > 1 obtained from triaxial tests for loose water-pluviated sand. The difference in loading mode between the triaxial and simple shear loading, as well as the particle fabric effects, may be responsible for this discrepancy.

The significance of the above findings from the viewpoints of understanding earthquake-induced performance of sands is several-fold. In particular, the results indicate the need to consider the effect of particle fabric, in addition to the commonly considered parameters such as density (void ratio) and stress level, in adequately characterizing the mechanical response of sands. They confirm the need to use data from laboratory element tests on samples that are re-constituted using the same techniques as those used for preparing centrifuge specimens, if the numerical models are to be validated in a meaningful manner.

5.2 Undrained Multiple Cyclic Loading Response of Loose Fraser River sand

Undrained cyclic shear tests conducted on samples that had been previously subjected to cyclic loading indicated that the response of sand depends on the degree of excess pore water pressure (or maximum shear strain) that was reached during previous cyclic loading, as well as the densification that occurred during re-consolidation after previous cyclic loading. The following were noted in particular:

- Cyclic shearing that did not impart significant excess pore water pressure or shear strains increases the resistance of sand against liquefaction in future cyclic loadings;
- Relatively large levels of excess pore water pressure or shear strains during cyclic loading weaken the soil fabric and, in turn, decrease the resistance of sand against liquefaction in future cyclic loadings.
- However, the reduction in the cyclic resistance of a given sand to liquefaction due to large cyclic pre-shearing may be overridden by the increase in relative density that take place during the reconsolidation process.

5.3 Undrained Cyclic Loading Response of Dense Fraser River sand

In the case of dense sands (D_{rc}= 80%), increase in relative density due to increase in confining stress (stress densification) is very small. Therefore, in contrast to the observations made for loose air-pluviated sands, the effect of stress consolidation on the cyclic shear resistance is essentially absent in the case of dense samples.

It is observed that dense sand shows an increase in cyclic resistance to liquefaction in the present of initial static shear. A K_α value of 1.3 is obtained for the vertical normal effective stresses of 100 kPa (D_{rc}= 80%). This is a significant departure from the observations on loose sand where the effect of initial static shear stress reduced the cyclic shear resistance.

The dense sand exhibited significant excess pore water pressure generation during the unloading phase (plastic unloading) of a given cycle of loading in comparison to the counterpart loading phase, even during the initial loading cycle. This is in significant contrast to the response of loose sand, where the initial unloading cycles are almost elastic (i.e. very small pore water pressure generation during unloading phase of a cycle).

5.4 Drained cyclic Loading Response of Fraser River Sand

Drained cyclic shear tests conducted on air-pluviated samples of Fraser River sand indicated the following:

- The development of net volumetric strain with increasing number of cycles was noted to be independent of the time rate of shear strain;
- The shear-induced volumetric strain increases with increasing shear strain amplitude and number of cycles. The proportionality of shear-induced volumetric strain to the cyclic

shear-strain amplitude, observed by other researchers based on drained cyclic shear tests with small shear strain amplitudes, is not applicable when the material is subjected to relatively large amplitudes of cyclic strain.

- The 2-parameter shear-volume coupling model (equation) proposed by Byrne (1991), based on the noted proportionality of the shear-induced volumetric strain to shear strain, was modified so that it could be extended to the larger strain response. The modified shear-volume coupling relation for large strains is of the form:

$$\Delta\varepsilon_v = A\gamma^C \mathrm{Exp}\{-B\varepsilon_v / \gamma^C\}$$

The validity of the above equation for large strains was demonstrated for loose air pluviated sand by initially calibrating the equation using data from several tests, and then predicting the response for a test that was not included in the calibration.

5.5 Development of Specimen Preparation Methods

In addition to investigating the fundamental characteristic response, the research work was targeted towards developing critically needed element testing data as input to numerical modelling of centrifuge physical models. The research undertaken resulted in developing a simple air-pluviation method to reconstitute laboratory sand samples replicating the soil fabric anticipated in centrifuge soil models. The characteristic variation of as-placed density of air-pluviated Fraser River sand with respect to the rate of flow, and height of deposition, was established to provide directions for sample preparation. It was also demonstrated that the new method would lead to samples having relatively uniform density that are suitable for element testing.

Limited monotonic loading tests indicated that the imparted vibrations during sample preparation could significantly influence in the shear response of a given sand. Essentially, the pluviated samples that were prepared without any vibrations exhibited a weaker response than those prepared with vibration.

REFERENCES

Anderson, D.G., and Stokoe, K.H. 1978. Shear modulus: a time dependent soil property. Dynamic Soil Testing, ASTM STP654, American Society for testing and Materials, pp. 66-90.

Arulanandan, K. 1993. Why VELACS? (VErification of Liquefaction Analysis using Centrifuge Studies). *In* Proceedings of the International Conference on the Verification of Numerical Procedures for the Analysis of Soil Liquefaction Problems, Davis, California, USA, 17-20 October 1993. *Edited by* K. Arulanandan and R.F. Scott. A.A. Balkema/Rotterdam/Brookfield. pp. 277-294.

Arulanandan, K., and Scott, R.F. 1993. Proceedings of the International Conference on the Verification of Numerical Procedures for the Analysis of Soil Liquefaction Problems, Davis, California, USA, 17-20 October 1993. A.A. Balkema/Rotterdam/Brookfield.

Atkinson, J.H., and Bransby, P.L. 1978. The mechanics of soils. An Introduction to Critical State Soil Mechanics. McGraw Hill Book Company Ltd., U.K.

Beaty, M. 2001. A synthesized approach for estimating liquefaction-induced displacements of Geotechnical structures. Ph.D. thesis, Department of Civil Engineering, University of British Columbia, Vancouver, BC, Canada.

Beaty, M., and Byrne, P.M. 1998. An effective stress model for predicting liquefaction behaviour of sand. Geotechnical Earthquake Engineering and Soil Dynamics III, ASCE Geotechnical special publication, No.75, Vol. 1, *In* Proceedings of a Specialty Conference, Seattle, pp. 766-777.

Beaty, M., and Byrne, P.M. 1999. A simulation of the Upper San Fernando dam using a synthesized approach. *In* proceedings of the 13th Annual Vancouver Geotechnical Society Symposium, Slope Stability and Landslides, May 28, 1999, Vancouver, British Columbia, pp. 63-72.

Bishop, A.W. 1971. Shear strength parameters for undrained and remolded soil specimens. *In* Roscoe Memorial Symposium, Cambridge University, pp. 3-58.

Bjerrum, L., and Landva, A. 1966. Direct simple shear testing on Norwegian quick clay. Geotechnique, **16**(1): 1-20.

Boulanger, R.W., Curras, C.J., Kutter, B.L., Wilson, D.W., and Abghari, A. 1999. Seismic soil-pile structure interaction experiments and analysis, Journal of Geotechnical and Geoenvironmental Engineering, ASCE, **125**(9): 750-759.

Byrne, P.M. 1991. A cyclic shear-volume coupling and pore pressure model for sand. *In* Proceedings of 2nd International Conference on Resent Advances in Geotechnical Earthquake Engineering and Soil Dynamics, St. Louis, Missouri, pp. 47-55.

Byrne, P.M., Park, S.S., and Beaty, M. 2003. Seismic liquefaction: centrifuge and numerical modeling. *In* Proceedings of the 3rd International FLAC Symposium, FLAC and Numerical Modeling in Geomechanics, 21-24 October 2003, Sudbury, Ontario, Canada. *Edited by* R. Brummer, P. Andrieux, C. Detournay, and R. Hart. A.A. Balkema Publishers. pp. 321-331.

Byrne, P.M., Park, S.S., Beaty, M., Sharp, M., Gonzalez, L., and Abdoun, T. 2004. Numerical modeling of liquefaction and comparison with centrifuge tests. Canadian Geotechnical Journal, **41**(2): 20p.

Casagrande, A. 1936. Characteristics of cohesionless soils affecting the stability of slopes and earth fills. Journal of the Boston Society of Civil Engineers, pp. 257-276.

Casagrande, A. 1975. Liquefaction and cyclic deformation of sands: A critical review. *In* proceedings of the 5th American Conference on Soil Mechanics and Foundation Engineering, Buenos Aires, Vol. 5, pp. 79-133.

Castro, G. 1969. Liquefaction of sands. Ph.D. thesis, Harvard University, Cambridge, Mass.

Castro, G. 1975. Liquefaction and cyclic mobility of saturated sands. Journal of the Geotechnical Engineering Division, **101**(GT6): 551-569.

Castro, G., and Poulos, S.J. 1977. Factors affecting the liquefaction and cyclic mobility. Journal of the Geotechnical Engineering Division, ASCE, **103**(GT6): 501-516.

Castro, G., Poulos, S.J., France, J.W., and Enos, J.L. 1982. Liquefaction induced by cyclic mobility. Report by Geotechnical Engineers Inc., Winchester, Mass., to the National science Foundation, Washington, D.C., Department of Commerce, Access number PB 82-235508.

Chern, J.C. 1985. Undrained response of saturated sands with emphasis on liquefaction and cyclic mobility. Ph.D. thesis, Department of Civil Engineering, University of British Columbia, Vancouver, BC, Canada.

Chung, E.K.F. 1985. Effects of stress path and pre strain history on the undrained monotonic and cyclic loading behaviour of saturated sand. M.A.Sc. thesis, Department of Civil Engineering, University of British Columbia, Vancouver, BC, Canada.

Cole, E.R.L., 1967. The behaviour of soils in the simple shear apparatus. Ph.D. thesis, University of Cambridge, U.K.

Cresswell, A., Barton, M. E., and Brown, R. 1999. Determining the maximum density of sands by pluviation. Geotechnical Testing Journal, GTJODJ, **22**(4): 324-328.

DeGregoria, V.B. 1990. Loading systems, sample preparation, and liquefaction. Journal of Geotechnical Engineering, ASCE, **116**(5): 805-821.

Dyvik, R., Berre, T., Lacasse, S., and Raddim, B. 1987. Comparison of truly undrained and constant volume direct simple shear tests. Geotechnique, **33**(1): 3-10.

Emery, J.J., Finn, W.D.L., and Lee, K.W. 1973. Uniformity of saturated sand specimens. ASTM STP 523, pp. 182-194.

Finn, W.D.L., and Vaid, Y.P. 1977. Liquefaction potential from drained constant volume cyclic simple shear tests. *In* Proceedings of the 6th World Conference on Earthquake Engineering. Sarita Prakashan Publishers, Meerut, India. Vol. III, pp. 2157-2162.

Finn, W.D.L., Bhatia, S.K., and Pickering, D.J. 1982. The cyclic simple shear test. Soil Mechanics – Transient and Cyclic Loads. *Edited by* G.N. Pande and O.C. Zienkiewicz, pp. 583-605.

Finn, W.D.L., Bransby, P.L., and Pickering, D.J. 1970. Effect of strain history on liquefaction of sand. Journal of the Soil Mechanics and Foundations Division, ASCE, **96**(SM6): 1917-1934.

Finn, W.D.L., Pickering, D.J., and Bransby, P.L. 1971. Sand liquefaction on triaxial and simple shear tests. Journal of the Soil Mechanics and Foundations Division, ASCE, **97**(SM4): 639-659.

Finn, W.D.L., Vaid, Y.P., and Bhatia, S.K. 1978. Constant volume simple shear testing. *In* Proceedings of the 2nd International Conference on Microzonation for Safer Construction, Research and Application, San Francisco, U.S.A., Vol. II, pp. 839-851.

Finn, W.D.L., Yogendrakumar, M., Yoshida, N., and Yoshida, H. 1986. TARA-3: A program to compute the seismic response of 2-D embankments and soil-structure interaction systems to seismic loadings, Department of Civil Engineering, University of British Columbia, Vancouver, Canada.

Gananathan, N. 2002. Partially drained response of sands. M.A.Sc. thesis, Department of Civil Engineering, University of British Columbia, Vancouver, BC, Canada.

Garrison, R.E., Luternauer, J.L., Grill, E.V., MacDonald, R.D., and Murray, J.W. 1969. Early diagenetic cementation of recent sands, Fraser River Delta, British Columbia. Sedimentology, **12**: 27-46.

Harder, L.F. Jr., and Boulanger, R. 1997. Application of K_α and K_σ correction factors. *In* Proceedings of the NCEER Workshop on Liquefaction Resistance of Soils, Technical Report NCEER-97-0022, National Center for Earthquake Engineering Research, State University of New York at Buffalo, N.Y. *Edited by* T.L. Youd and I.M. Idriss, pp. 167-190.

Howie, J.A., Shozen, T., and Vaid, Y.P. 2001. Effect of aging stiffness of loose Fraser River sand. Advance Laboratory Stress-Strain Testing of Geomaterials. *Edited by* F.Tatsuoka, S.Shibuya, and R. Kuwano. A.A. Balkema Publishers. pp. 235-243.

Hynes, M.E., and Olsen, R.S. 1999. Influence of confining stress on liquefaction resistance. *In* Proceedings of the International Workshop on Physics and Mechanics of Soil Liquefaction. Balkema, Rotterdam, The Netherlands. pp. 145-152.

Idriss, I.M., and Boulanger, R.W. 2004. Semi-empirical procedure for evaluating liquefaction potential during earthquakes. *In* Proceedings of 11th International Conference on Soil Dynamics and Earthquake Engineering and 3rd International Conference on Earthquake Geotechnical Engineering, University of California, Berkeley, CA, January, 2004, pp. 32-56.

Ishihara, K. 1993. Liquefaction and flow failure during earthquakes. Geotechnique, **43**(3): 351-415.

Ishihara, K., and Okada, S. 1978. Effects of stress history on cyclic behaviour of sand. Soils and Foundations, **18**(4): 31-45.

Ishihara, K., and Okada, S. 1982. Effects of large pre-shearing on cyclic behaviour of sand. Soils and Foundations, **22**(3): 109-125.

Ishihara, K., and Yoshimine, M. 1992. Evaluation of settlement in sand deposits following liquefaction during earthquake. Soils and Foundations, **32**(1): 173-188.

Ishihara, K., Tatsuoka, F., and Yasuda, S. 1975. Undrained deformation and liquefaction under cyclic stresses. Soils and Foundations, **15**(1): 29-44.

Kammerer, A., Wu, J., Pestana, J., Riemer, M., and Seed, R. 2002. Undrained response of Monterey 0/30 sand under multidirectional cyclic simple shear loading conditions: Electronic Data Files, Geotechnical Engineering Research Report No. UCB/GT/02-02, University of California, Berkeley.

Kuerbis, R.H. 1989. Effect of gradation and fine content on the undrained response of sands. M.A.Sc. thesis, Department of Civil Engineering, University of British Columbia, Vancouver, BC, Canada.

Ladd, R.S. 1974. Specimen Preparation and Liquefaction of Sands. Journal of the Geotechnical Engineering Division, ASCE, **100**(GT10): 1180-1184.

Ladd, R.S. 1977. Specimen Preparation and cyclic stability of Sands. Journal of the Geotechnical Engineering Division, ASCE, **103**(GT6): 535-547.

Lade, P.V., Bopp, P.A., and Peters, J.F. 1993. Instability of dilating sands. Mechanics of Materials, **16**: 249-264.

Lam, C.K.K. 2003. Effects of aging duration, stress ratio during aging and stress path on stress-strain behaviour of loose Fraser River sand. M.A.Sc. thesis, Department of Civil Engineering, University of British Columbia, Vancouver, BC, Canada.

Lambe, T.W. 1967. Stress Path Method, Journal of the Soil Mechanics and Foundation Division, ASCE, **93**(SM6): 309-331.

Lee, C.J., 1991. Deformation of sand under cyclic simple shear loading. *In* Proceedings of 2nd International Conference on Resent Advances in Geotechnical Earthquake Engineering and Soil Dynamics, St. Louis, Missouri, pp. 47-55.

Lee, K.L., and Seed, H.B. 1967a. Dynamic strength of anisotropically consolidated sand. Journal of the Soil Mechanics and Foundations Division, ASCE, **93**(SM5): 169-190.

Lee, K.L., and Seed, H.B. 1967b. Drained strength characteristics of sands. Journal of the Soil Mechanics and Foundations Division, ASCE, **93**(SM6): 117-141.

Lee, K.L., Makdisi, F.L., Idriss, I.M., and Seed, H.B. 1975. Properties of soil in the San Fernando hydraulic fill dams. Journal of the Geotechnical Engineering Division, ASCE, **101**(8): 801-821.

Leroueil, S., and Hight, D.W. 2003. Behaviour and properties of natural soils and soft rocks. Characterization and Engineering Properties of Natural Soils. *Edited by* T.S. Tan, K.K. Phoon, D.W. Hight, and S. Leroueil. A.A. Balkema Publishers. Vol. 1, pp. 29-254.

Martin, G.R., Finn, W.D.L., and Seed, H.B. 1975. Fundamentals of liquefaction under cyclic loading. Journal of the Goetechnical Engineering Division, ASCE, **101**(GT5): 423-437.

Miura, S., and Toki, S. 1982. A sample preparation method and its effects on static and cyclic deformation strength properties of sands. Soils and Foundations, **22**(1): 61-77.

Mulilis, J.P., Seed, H.B., Chan, C.K., Mitchell, J.K., and Arulanandan, K. 1977. Effect of sample preparation on sand liquefaction. Journal of the Goetechnical Engineering Division, ASCE, **103**(GT2): 91-108.

Negussey, D., Wijewickreme, D., and Vaid, Y.P. 1988, "Constant Volume Friction Angle of Granular Materials", Canadian Geotechnical Journal, **25**(1): 50-55.

NRC 1985. Liquefaction of soils during earthquakes. National Research Council Report CETS-EE-001, National Academic Press, Washington, D.C.

Oda, M. 1972. Initial fabric and their relations to mechanical properties of granular material. Soils and Foundations, **12**(1): 17-36.

Oda, M., Koishikawa, I., and Higuehi, T. 1978. Experimental study of anisotropic shear strength of sand by plane strain tests. Soils and Foundations, **18**(1): 25-38.

Park, S.S. 2003. Earthquake Induced Damage Mitigation from Soil Liquefaction, http://www.civil.ubc.ca/liquefaction/.

Park, S.S., and Byrne, P.M. 2004. Stress densification and its evaluation. Canadian Geotechnical Journal, **41**(1): 181-186.

Peacock, W.H., and Seed H.B 1968. Sand liquefaction under cyclic loading simple shear conditions. Journal of the Soil Mechanics and Foundations Division, ASCE, **94**(SM3): 689-708.

Phillips, R. 2003. Personal communication.

Phillips, R., Guo, P.J., and Popescu, R. 2002. Proceedings of the International Conference on Physical Modeling, John's, Newfoundland, Canada, 10-12 July 2002. A.A. Balkema Publishers.

Pillai, V.S., and Byrne, P.M. 1994. Effect of overburden pressure on liquefaction resistance of sand. Canadian Geotechnical Journal, **31**: 53-60.

Polito, C. P., and Martin, J. R. 2001. Effect of nonplastic fines on the liquefaction resistance of sands. Journal of Geotechnical and Geoenvironmental Engineering, ASCE, **127**(5): 408-415.

Rad, N.S., and Tumay, M.T. 1987. Factors affecting sand specimen preparation by raining. Geotechnical Testing Journal, GTJODJ, **10**(1): 31-37.

Riemer, M.F., and Seed R.B. 1997. Factors affecting apparent position of the steady state line. Journal of the Geotechnical Engineering, ASCE, **123**(3): 281-288.

Robertson, P.K., Wride (Fear), C.E., List, B.R., Atukorala, U., Biggar, K.W., Byrne, P.M., Campanella, R.G., Cathro, D.C., Chan, D.H., Czajewski, K., Finn, W.D.L., Gu, W.H., Hammamji, Y., Hofmann, B.A., Howie, J.A., Hughes, J., Imrie, A.S., Konrad, J.-M., Küpper, A., Law, T., Lord, E.R.F., Monahan, P.A., Morgenstern, N.R., Phillips, R., Piché, R., Plewes, H.D., Scott, D., Sego, D.C., Sobkowicz, J., Stewart, R.A., Watts, B.D., Woeller, D.J., Youd, T.L., and Zavodni, Z. 2000. The CANLEX project: summary and conclusions. Canadian Geotechnical Journal, **37**(3): 563-591.

Roscoe, K.H., Schofield, A.N., and Thurairajah, A. 1963. An evaluation of test data for selecting a yield criterion for soils. ASTM special technical publication. No. 361, pp. 111-128.

Rowe, P.W. 1962. The stress dilatancy relation static equilibrium of an assembly of particles in contact. *In* Proceedings of the Royal Society, A269, pp. 500-527.

Schofield, A.N., and Steedman, R.S. 1988. Recent development on dynamic model testing in Geotechnical Engineering. State of the Art Report. *In* Proceedings of the 9th World Conference on Earthquake Engineering, Japan, August, Vol. 8, pp. 813-824.

Seed, H.B. 1979. Soil liquefaction and cyclic mobility evaluation for level ground during earthquakes. Journal of the Geotechnical Engineering Division, ASCE, **105**(GT2): 201-255.

Seed, H.B., and Peacock, W.H. 1971. Test procedures for measuring soil liquefaction characteristics. Journal of the Soil Mechanics and Foundations Division, ASCE, **97**(SM8): 1099-1119.

Seed, H.B., and Silver, M.L. 1972. Settlement of dry sands during earthquakes. Journal of the Soil Mechanics and Foundations Division, ASCE, **98**(SM4): 381-397.

Seed, H.B., Mori, K., and Chan, C.D. 1975. Influences of seismic history on the liquefaction characteristics of sands. Report EERC 75-25, Earthquake Engineering Research Center, University of California, Berkeley, Calif.

Seed, H.B., Mori, K., and Chan, C.D. 1977. Influence of seismic history on liquefaction of sands. Journal of the Geotechnical Engineering Division, ASCE, **103**(GT4): 257-270.

Seed, R.B., and Harder, L.F. 1990. SPT based analysis of cyclic pore pressure generation and undrained residual strength. *In* Proceedings of the Seed Memorial Symposium, Vancouver, BC, Canada. *Edited by* J.M. Duncan. BiTech Publishers. pp. 351-376.

Silver, M.L., and Seed, H.B. 1971. Volume Changes in sands during cyclic loading. Journal of the Soil Mechanics and Foundations Division, ASCE, **97**(SM9): 1171-1182.

Sivathayalan, S. 1994. Static, Cyclic and Post liquefaction Simple Shear Response of Sand. M.A.Sc. thesis, Department of Civil Engineering, University of British Columbia, Vancouver, BC, Canada.

Sivathayalan, S., and Vaid, Y.P. 2002. Influence of generalized initial state and principle stress rotation on the undrained response of sands. Canadian Geotechnical Journal, **39**: 63-76.

Sladen, J.A., D'Hollander, R.D., and Krahn, J. 1985. The liquefaction of sands, a collapse surface approach. Canadian Geotechnical Journal, **22**(3): 564-578.

Stedman, J.D. 1994. Effects of confining pressure and static shear on liquefaction resistance of Fraser River sand. M.A.Sc. thesis, Department of Civil Engineering, University of British Columbia, Vancouver, BC, Canada.

Suzuki, T., and Toki, S. 1984. Effect of pre-shearing on liquefaction characteristics of saturated sand subjected to cyclic loading. Soils and Foundations, **24**(2): 16-28.

Taboada, V.M., and Dobry, R. 1993. Experimental results of Model No 2 at RPI. *In* Proceedings of the International Conference on the Verification of Numerical Procedures for the Analysis of Soil Liquefaction Problems, Davis, California, USA, 17-20 October 1993. *Edited by* K. Arulanandan and R.F. Scott, A.A. Balkema/Rotterdam/Brookfield. pp. 277-294.

Thomas, J. 1992. Static, Cyclic and Post Liquefaction Behaviour of Fraser River Sand, M.A.Sc. thesis, Department of Civil Engineering, University of British Columbia, Vancouver, BC, Canada.

Uthayakumar, M., and Vaid, Y.P. 1998. Liquefaction of sand under multiaxial stresses. Canadian Geotechnical Journal, **35**: 273-283.

Vaid, Y.P., and Chern, J.C. 1983. Effect of static shear on resistance to liquefaction. Soils and Foundations, **23**(1): 47-60.

Vaid, Y.P., and Chern, J.C. 1985. Cyclic and monotonic undrained response of sands. *In* Advances in the Art of Testing Soils under Cyclic Loading Conditions, Proceedings of the ASCE Convention, Detroit, pp. 171-176.

Vaid, Y.P. and Finn, W.D.L. 1979. Static shear and liquefaction potential. Journal of the Geotechnical Engineering Division, ASCE, **105**(GT10): 1233-1246.

Vaid, Y.P., and Negussey, D. 1986. Preparation of reconstituted sand specimens. Soil Mechanics Series No. 98, Department of Civil Engineering, University of British Columbia, Vancouver, BC, Canada.

Vaid, Y.P., and Sivathayalan, S. 1996. Static and cyclic liquefaction potential of Fraser River sand in simple shear and triaxial tests. Canadian Geotechnical Journal, **33**: 281-289.

Vaid, Y.P., and Sivathayalan, S. 2000. Fundamental factors affecting liquefaction susceptibility of sands. Canadian Geotechnical Journal, **37**(3): 592-606.

Vaid, Y.P., and Thomas, J. 1995. Liquefaction and post-liquefaction behaviour of sand. Journal of Geotechnical Engineering, ASCE, **121**(2): 163-173.

Vaid, Y.P., Chern, J.C., and Tumi, H. 1985. Confining pressure, grain angularity, and liquefaction. Journal of the Geotechnical Engineering Division, ASCE, **111**(10): 1229-1235.

Vaid, Y.P., and Chung, E.K.F., and Kuerbis, R.H. 1989. Pre-shearing and undrained response of sand. Soils and Foundations, **29**(4): 49-61.

Vaid, Y.P., and Chung, E.K.F., and Kuerbis, R.H. 1990. Stress path and steady state. Canadian Geotechnical journal, **27**: 1-7.

Vaid, Y.P., Sivathayalan, S., and Stedman, J.D. 1999. Influence of specimen reconstitution method on the undrained response of sand. Geotechnical Testing Journal, GTJODJ, **22**(3): 187-195.

Vaid, Y.P., Stedman, J.D., and Sivathayalan, S. 2001. Confining stress and static shear effects in cyclic liquefaction. Canadian Geotechnical Journal, **38**(3): 580-591.

Vaid, Y.P., Uthayakumar, M., Sivathayalan, S., Robertson, P.K., and Hofmann, B. 1995. Laboratory testing of Syncrude sand. *In* proceedings of the 48th Canadian Geotechnical Conference, Vancouver, British Columbia, Vol. 1, pp. 223-232.

Vesic A.S., and Clough, G.W. 1968. Behaviour of granular material under high stresses. Journal of the Soil Mechanics and Foundation Engineering Division, ASCE, **94**(SM3): 661-688.

Wijewickreme, D. 2004. Effective stress paths in laboratory cyclic shear testing and earthquake field loadings from a general stress space viewpoint. Submitted to Canadian Geotechnical Journal.

Yoshimi, Y., and Oh-Oka, H. 1975. Influence of degree of shear stress reversal on the liquefaction potential of saturated sand. Soils and Foundation, **15**(3): 27-40.

Youd, T.L 1972. Compaction of sands by repeated shear straining. Journal of the Soil Mechanics and Foundations Division, ASCE, **98**(SM7): 709-725.

Youd, T.L, Idriss, I.M., Andrus, R.D., Arango, I., Castro, G., Christian, J.T., Dobry, R., Finn, W.D.L., Harder Jr., L.F., Hynes, M.E., Ishihara, K., Koester, J.P., Liao, S.S.C., Marcuson III, W.F., Martin, G.R., Mitchell, J.K., Moriwaki, Y., Power, M.S., Robertson, P.K., Seed, R.B., and Stokoe II, K.H. 2001. Liquefaction resistance of soils: summary report from the 1996 NCEER and 1998 NCEER/NSF workshops on evaluation of liquefaction resistance of soils. Journal of Geotechnical and Geoenvironmental Engineering, ASCE, **127**(10): 817-833.

Zienkiewicz, O. C., Pastor, M., Xie, Y. M. 1991. Constitutive modelling of soils and computation of earthquake damage and liquefaction (state of the art paper). *In* Proceedings of 2nd International Conference on Resent Advances in Geotechnical Earthquake Engineering and Soil Dynamics, St. Louis, Missouri, vol. II, pp. 1743-1752.